DIEGO CORREA RAMOS

QUALITY OF EUCALYPTUS CHARCOAL FOR USE IN SILICON PRODUCTION

Thesis presented to the Universidade Federal de Viçosa, as part of the specifications of the Graduate Program in Forest Science, to obtain the title of *Doctor Scientiae*.

VIÇOSA
MINAS GERAIS – BRASIL
2018

Ficha catalográfica preparada pela Biblioteca Central da Universidade Federal de Viçosa - Câmpus Viçosa

T
R175q
2018

Ramos, Diego Correa, 1987-
Quality of *Eucalyptus* charcoal for use in silicon production / Diego Correa Ramos. – Viçosa, MG, 2018.
viii, 137 f. : il. ; 29 cm.

Texto em inglês.
Orientador: Angélica de Cássia Oliveira Carneiro.
Tese (doutorado) - Universidade Federal de Viçosa.
Inclui bibliografia.

1. Carvão vegetal - Propriedades. 2. Carvão vegetal - Qualidade. 3. Carboneto de silício. 4. Carbonização.
I. Universidade Federal de Viçosa. Departamento de Engenharia Florestal. Programa de Pós-Graduação em Ciência Florestal.
II. Título.

CDO adapt. CDD 22. ed. 634.98675

DIEGO CORREA RAMOS

QUALITY OF EUCALYPTUS CHARCOAL FOR USE IN SILICON PRODUCTION

Thesis presented to the Universidade Federal de Viçosa, as part of the specifications of the Graduate Program in Forest Science, to obtain the title of *Doctor Scientiae*.

APPROVED: August 16, 2018.

Marcio Arêdes Martins

Benedito Rocha Vital

Adriana de Oliveira Vilela

Bárbara Luísa Corradi Pereira

Angélica de Cassia Oliveira Carneiro
(Adviser)

ACKNOWLEDGEMENTS

To God.

To my parents, Zilma and José, and to my brother Junior, for the unconditional support at all times.

To my girlfriend, Carolina, for always being at my side.

To my advisor Angelica de Cassia for the attention and patience that was dedicated to me, in addition to the valuable teachings.

To my co-advisor Merete Tangstad for the NTNU University research opportunity, confidence, and teachings.

To Professors, Benedito Rocha Vital, Paulo Fernando Trugilho, Raghed Saadieh, and Paulo Von Kruger, for the collaboration in development of research.

To NTNU employees and friends for friendship and contributions in the research.

To the company Minasligas, for allowing the use of research data developed in the SFGM charcoal production unit.

To the friends and employees of Minasligas for the companionship, collaboration, and sharing of experiences.

To the Federal University of Viçosa, to the Forestry Engineering Department, to the Coordination for the Improvement of Higher Education Personnel (Capes), to the Foundation for Research Support of the State of Minas Gerais (Fapemig), to the Center of Research-based Innovation of Norway (SFI), to the Research Company SINTEF and to the National Council for Scientific and Technological Development (CNPq) for the opportunity and financial support.

To my friends at LAPEM Lab and LPM, for help, companionship, and for making the work routine more fun.

To the friends of Viçosa and Ouro Preto for the countless good moments and the companionship.

To all who, in some way, contributed to the accomplishment of this work.

BIOGRAPHY

DIEGO CORREA RAMOS, son of Zilma Correa Ramos and José Souza Ramos, was born in Pirapora, Minas Gerais, on May 21, 1987.

In July 2009, he graduated in Forestry Engineering from the Federal University of Viçosa, Minas Gerais.

In August 2011, he obtained the title of Magister Scientiae in Forestry Science, specializing in Silviculture and Agroforestry Systems, from the Graduate Program in Forestry Science of the Federal University of Viçosa.

In the period from 2010 to 2014, he worked as a Forest Engineer at the company Minasligas.

In August of 2015, he completed an MBA in Project Management at Fundação Getúlio Vargas.

In March of 2015, he began the doctoral program in Forestry Science at the Federal University of Viçosa, specializing in Forest Product Technology.

In August of 2018, he completed a thesis defense.

TABLE OF CONTENTS

ABSTRACT

RAMOS, Diego Correa, D.Sc., Universidade Federal de Viçosa, August, 2018. **Quality of Eucalyptus charcoal for use in silicon production.** Adviser: Angélica de Cássia Oliveira Carneiro.

Replacing the use of fossil reductants with charcoal in silicon production has a great potential with respect to reducing CO_2 emissions, increasing silicon quality and yield. Nevertheless, charcoals can be produced from different raw materials and under various process conditions, and have different properties influencing further applications. This study aimed to evaluate the charcoal properties of three *Eucalyptus spp*. produced under different carbonization parameters for use in silicon production. In carbonization, the final temperature of carbonization (380 and 460 °C) and residence time (2 and 8 hours) were evaluated. A metallurgical coke was used for comparison purpose. Basic density, chemical composition and anatomy of wood were determined. Carbonizations in a laboratory kiln were done and the proximate and elemental analysis, porosity, apparent density, elemental composition, morphological characterization of pores and fibers, BET surface area, functional chemical groups and reactivity towards SiO gas of the charcoal were determined. The reactivity test was performed in an electric furnace with vertical reactor, at 1650 °C, in an inert atmosphere for 120 minutes. In the reactor, agglomerates made of a mixture of quartz (SiO_2) and silicon carbide (SiC) and charcoal sample were used. The results reveal that there is wood variability between the clones evaluated and strong correlations among wood and charcoal properties. The SiO reactivity test developed in this study was a useful tool to classify charcoal for silicon use. All charcoals had significantly higher SiO-reactivity than coke. The charcoal reactivity was influenced mainly by the apparent density and functional chemical groups on charcoal. Based on the parameters investigated and under the experimental conditions, the charcoal CL-3, the 380 °C final temperature of carbonization and the 8 h residence are most suitable to produce charcoal for use in silicon production process.

RESUMO

RAMOS, Diego Correa, D.Sc., Universidade Federal de Viçosa, agosto de 2018. **Qualidade do carvão vegetal de Eucalyptus para uso na produção de silício.** Orientadora: Angélica de Cássia Oliveira Carneiro.

A substituição de redutores fósseis pelo carvão vegetal na produção de silício tem grande importância no que diz respeito a redução de emissões de CO_2, aumento da qualidade do silício e rendimento. Carvões, no entanto, podem ser produzidos a partir de diferentes matérias-primas e sob várias condições de pirólise e ter diferentes propriedades que influenciam distintas aplicações. O objetivo deste estudo foi avaliar as propriedades do carvão vegetal de três clones de *Eucalyptus spp*. produzidos sob diferentes condições de carbonização para uso na produção de silício. Na carbonização, foram avaliados a temperatura final de carbonização (380 e 460 °C) e o tempo de residência (2 e 8 horas). Um coque metalúrgico foi utilizado para fins de comparação. O estudo das propriedades da madeira foi realizado a partir da densidade básica, relação cerne/alburno, análise morfológica de fibras e poros, análise química estrutural e análise elementar. A carbonização foi realizada em um forno de laboratório, e então determinados a composição elementar e imediata, densidade aparente, caracterização morfológica dos poros e fibras, área superficial BET, grupos químicos funcionais e reatividade do carvão vegetal ao gás SiO. O teste de reatividade foi realizado em um forno elétrico com reator vertical, a 1650° C, sob atmosfera inerte por 120 min. No reator, utilizou-se aglomerados feito de uma mistura de quartzo (SiO_2) e carbeto de silício (SiC) e o carvão vegetal. Os resultados mostram que há variabilidade da madeira entre os clones avaliados e fortes correlações entre as propriedades de madeira e carvão. O teste de reatividade desenvolvido no presente estudo foi uma ferramenta útil para classificar o carvão vegetal para uso na produção de silício. Todos os carvões tiveram reatividade significativamente maior do que o coque. A reatividade do carvão vegetal foi influenciada principalmente pela densidade aparente e grupos químicos funcionais do carvão vegetal. Com base nos dados investigados e sob condições experimentais, o clone 3, a temperatura final de carbonização de 380 °C e o tempo de residência de 8 h são mais adequados para produzir carvão vegetal para uso na produção de silício.

1. GENERAL INTRODUCTION

Brazil is the only country that produces large-scale charcoal for use in industry, being used, mainly, for the pig iron and steel sectors that consume approximately 70.5%, followed by ferro-alloys and metal silicon with 11.1% (Ben, 2017). In 2016, charcoal production in Brazil was approximately 5.4 million tons (Ben, 2017), 84% of which came from planted forests (Ibá, 2017). The vast territorial area of the country, capable of supporting large forest masses, together with the peculiar characteristics of climate and soil, are promising for the growth and development of forest species. This is especially true for the use of species with relatively short cutting cycle and high productivity, mainly of the genus *Eucalyptus*.

The silicon production in Brazil uses exclusively charcoal as a reducing agent. In other countries, charcoal is also used but to a lesser expressive. In 2016, world production of silicon was approximately 2.5 million tons (Usgs, 2017), and Brazil produced approximately 100 thousand tons (Sgm, 2017), consuming about 160 thousand tons of charcoal.

Charcoal is one of the best reducing agents for the production of silicon because its low content of impurities results in higher purity of the metal. In addition, the porous structure of the charcoal guarantees a significant chemical reactivity and, as a consequence, there is a better yield in silicon (Kim *et al*., 2013). Moreover, the use of charcoal, a bio-reducer of renewable origin, compared to fossil-based reducers, dramatically reduces SO_2 emissions and mitigates the environmental impact of CO_2 (Lindstad *et al.* 2010), which is decisive in the context of the Paris Agreement (Unfccc, 2016). On the other hand, the use of charcoal presents some challenges to be overcome, for example, the low mechanical resistance and, usually, the high price and low availability in the international market.

It is known that charcoal can be produced from various raw materials and carbonization parameters (Assis *et al.*, 2016; Kan *et al.*, 2016), resulting in different properties that may influence the production of silicon. Among these properties, the reactivity towards SiO gas, that is, the ability of the reducing material to react with the SiO gas and to produce silicon carbide (SiC) and CO, is one of the most important

parameters in the performance of the silicon production process. According to Myrvågnes and Lindstad (2007), the reaction of carbon with SiO, a high calorific gas, determines the Si yield, in addition to energy consumption in the process.

Therefore, the evaluation of the properties of charcoal along with the knowledge of the industrial process, where it will be used, is the first step to ensure the proper and efficient use of charcoal. In this work, a better understanding of eucalypt wood performance as raw material and the influence of carbonization on charcoal properties was sought in order to select genetic materials and carbonization process parameters more suitable for the production of charcoal for use in the manufacture of silicon.

2. OBJECTIVES

2.1. General objective

To evaluate the charcoal properties of Eucalyptus clones produced under different carbonization parameters for use in silicon production.

2.2. Specific Objectives

- Determine the anatomical structure, chemical properties and basic density of wood;
- Determine the chemical, anatomical and mechanical properties of charcoal;
- Evaluate the influence of the clone and the carbonization parameters on the porosity, BET specific surface area, microstructure and fixed carbon stock of charcoal.
- Evaluate the influence of the clone and the carbonization parameters on the friability of charcoal.
- Develop a test to evaluate the charcoal reactivity towards SiO gas.
- Evaluate the influence of the clone and the carbonization parameters on the charcoal reactivity.
- Identify the *Eucalyptus* clones and carbonization parameters that are most ideal for charcoal production for use in silicon production.

3. REFERENCES

ASSIS, M. R. et al. Factors affecting the mechanics of carbonized wood: literature review. **Wood Sci Technol,** v. 50, p. 519-536, 2016.

BEN. **Brazilian Energy Balance**. ENERGY, M. O. M. A. Rio de Janeiro**:** 296 p. 2017.

SGM. **Brazilian Metallurgy Statistical Yearbook**. ENERGY, D. O. M. A. Brasília**:** 95 p. 2017.

IBÁ. **Brazilian Tree Industry**. Pöyry Consultoria em Gestão e Negócios Ltda. Brasília, p.80. 2017

KAN, T.; STREZOV, V.; EVANS, T. J. Lignocellulosic biomass pyrolysis: A review of product properties and effects of pyrolysis parameters. **Renewable and Sustainable Energy Reviews,** v. 57, p. 1126-1140, 2016. ISSN 1364-0321.

KIM, V.; TOLYMBEKOV, M.; KIM S.; ULYEVA, G.; KUDARINOV, S. Carbon reductant for silicon metal production. The thirteenth International Ferroalloys, Congress, Almaty, Kazakhstan, 2013. 9 - 13 June. p. 519-526.

LINDSTAD, T., MONSEN, B.; OLSEN, K. S. How the ferroalloys industry can meet greenhouse gas regulations. INFACON XII, Helsinki, Finland, 2010. 6-9 June. p. 63-70.

TANGSTAD, M. **Metal Production in Norway**. Trondheim: Akademika forlag, 2013. 240.

USGS. **Silicon Statistics and Information**. Reston, USA: 2017, p.150-151. 2017.

UNFCCC. **Paris Agreement** NATIONS, U. Paris: 27 p. 2015.

MYRVÅGNES, V.; LINDSTAD, T. The importance of coal and coke properties in the production of high silicon alloys. INFACON XI, 2007, New Delhi, India. 18-21 February. p.402-413.

CHAPTER I

1. THEORETICAL REFERENCE

1.1. Charcoal production in Brazil

In 2016, the area occupied by forest plantations in Brazil totaled 7.4 million hectares, in which 75.6% were plantations of eucalyptus species. The pulp and paper sector accounts for 34% of the country's total wood production, followed by the firewood and charcoal (16%), wood panels (6%) and sawnwood (4%), and the rest is investors and independent producers (Ibá, 2017).

Brazil is the only country that produces large-scale charcoal for industrial use, and stands out, therefore, as the largest producer and consumer of charcoal (Fao, 2017). In 2016, charcoal production in Brazil was approximately 5.4 million tons, with 84% of the wood coming from planted forests, especially of species of the genus *Eucalyptus* (Ibá, 2017). According to the literature, its fast growth and density characteristics guarantee a high productivity of wood, and an easily renewable and good quality charcoal (Santos *et al.*, 2011; Trugilho *et al.*, 2011; Pereira *et al.*, 2012; Protásio *et al.*, 2012; Pereira *et al.*, 2013).

The industrial activities that consumed the most charcoal in Brazil were the production of pig iron and steel (3.7 million tons), followed by the ferro-alloys and silicon (0.6 million tons) (Ben, 2017). According to Rezende and Santos (2010), it is estimated that, in Brazil, approximately one-third of pig iron production and more than half of ferro-alloy production use charcoal. It is worth mentioning that when analyzing the national ferro-alloys sector, metallic silicon (Si-met.) is also included. This, although not an alloy, is a semi-metal classified in the ferro-alloys group, due to having an industrial process and similar applications (Kruger, 2009). It is noteworthy that the production of silicon metal in Brazil is exclusively made with the use of charcoal as a reducing agent, while in other countries, the use of coal is predominant.

The production of charcoal in Brazil, until the middle of 1990, was carried out in rudimentary furnaces, where the operational procedures for the control and standardization of the carbonization were carried out subjectively, resulting in low

charcoal gravimetric yield and lower quality charcoal, such as high friability and chemical heterogeneity (Morello, 2009). Since then and the increase in the cost of production of firewood that was imposed by the substitution of native forest for forest plantations, companies producing charcoal have started to invest in research to improve the technology of production of charcoal, increase gravimetric yield, and improved training to qualify the workforce. That is, the activity of charcoal production began to gain importance among other activities developed by companies that consume charcoal (Morello, 2009).

A great deal has evolved in the charcoal production chain in Brazil. Production of charcoal began in tradicional kilns (rudimentary) that have low gravimetric yield, goes through the JG kiln, surface kilns, and this has helped achieve technology of industrial rectangular kilns with supervisory systems. There is still the industrial continuous retort that find difficulty in becoming economically competitive, since they require sums of investments above the capacity of most producers (Valverde and Carneiro, 2016). Ongoing efforts have been made in the sector in search of technological alternatives to ensure the competitiveness of charcoal instead using reducing materials of fossil origin, thus strengthening the industry and contributing to sustainability. Among the technological alternatives, highlight researches in the context of the origin and quality of the raw material, development of furnaces and supervisory systems for charcoal production, artificial cooling in furnaces, synchronization of productive systems coupled to furnaces for the burning of carbonization gases, and use of carbonization gases for drying of the wood and generation of electric energy (Pereira *et al.*, 2013; Vilela *et al.*, 2014; Cardoso, 2015; Damásio *et al.*, 2015; Oliveira *et al.*, 2015; Pereira *et al.*, 2017; Donato, 2018; Ramos *et al.*, 2018; Vanegas *et al.*, 2018).

1.2. Charcoal Quality

The yield and the quality of the charcoal are influenced by the properties of the wood and parameters of the carbonization process. A charcoal considered to be of good quality, for industrial use, must have physical, chemicalm and mechanical parameters that aid or are even necessary to the processing steps.

Within the physical parameters, the charcoal density is one of the most cited quality indices. This parameter directly reflects the reactivity of charcoal in the production of silicon, influencing the yield and the energy consumption of the process (Myrhaug *et al.*, 2004; Myrvågnes and Lindstad, 2007). According to Ramos *et al*. (2018), considering similar carbonization conditions, the lower the apparent density of charcoal results in a greater range of SiO gas at reactive sites within the solid and, consequently, the higher the reactivity. However, the authors stated that using less dense, i.e. more porous charcoal, results in less carbon stock per unit volume of this bioreductant and higher for transportation of charcoal. In addition, it is emphasized that the less dense charcoal presents less mechanical resistance and, usually, higher friability (Assis *et al*., 2016).

In addition to density, a characteristic factor of charcoal is its fixed carbon content. In the production of silicon, via a carbothermic reduction process, the higher the fixed carbon content in charcoal results in greater the amount of carbon to react in the furnace. In addition to the amount of fixed carbon, it is also important to consider the carbon structure in the carbonaceous matrix of charcoal, because the aromatic carbon is less reactive than the aliphatic carbon (Asadullah *et al.*, 2010; Yip *et al.*, 2010; Wang *et al.*, 2017). The determination of the fixed carbon content in charcoal should be based on economic reasons. This is because the gravimetric charcoal yield has a negative correlation with the fixed carbon content and technological parameters, such as changes in porosity and mechanical resistance, as well as modifications of the charcoal carbon chains.

Also, it is known that fixed carbon content and volatile materials are inversely proportional. Gładysz and Karbowniczek (2008) stated that exaggerated content of volatile materials can generate a kind of pyrolytic carbon film that burns on the surface of the charge, damaging the permeability of gases in the furnace. This, in turn, will reflect negatively on the operation of electric furnaces producing ferro-alloys and silicon.

Charcoal moisture is another chemical parameter that interferes with the quality of charcoal for use in silicon production. The increased moisture content in the charcoal damages the thermal balance of the process, due to the thermal losses that occur during evaporation and partial dissociation of the water. In addition, an increase in hydrogen content may occur in the alloy (Gładysz and Karbowniczek, 2008).

The concentration of inorganic compounds is also indicative of the quality of charcoal. It is known that higher mineral content results in lower carbon content in the reducing material. In addition, depending on the type of mineral and its amount, it can be transferred to the metal silicon and, thus, disqualifying it. Mineral elements in low concentration, also called trace elements, enter the silicon production process through the electrodes and raw materials and are incorporated into the metal and/or microsilica. There are still some trace elements that can leave the process through the gas leaving the kiln. The behavior of trace elements depends on factors, such as furnace temperature, boiling point of the mineral element in its pure state, relative stability of the mineral in the form of oxides or carbides, and mineral solubility in the metallic silicon (Myrhaug, 2003).

In the production of high purity silicon for application in the solar industry, some trace elements should not exceed the level of 1 ppm (Mitrašinović and Utigard, 2009). Despite the low content of minerals in the wood and therefore in the charcoal, small variations in the amount of the element phosphorus, a macronutrient essential to the growth of plants that is mainly accumulated in the eucalyptus stem (Barros and Novais, 1990), can compromise the quality of the alloy. Phosphorus in charcoal, when present in stable form (FeP), is mainly incorporated into metallic silicon, making it brittle, less malleable, and with fields favorable to the propagation of cracks (Myrhaug, 2003).

The trace elements in the reducing material are not in any case a detrimental factor to the production of silicon. According to Myrvågnes and Lindstad (2007), the presence of Si incrustations in the form of quartz impurities in coke caused a significant increase in the reactivity of this reducer. This was explained by the reaction between quartz and carbon in its surroundings at temperatures above 1400 °C that produce silicon monoxide, which will react with carbon to form SiC. Furthermore, the porosity at the reaction site also increases as the quartz inclusions are consumed. Additionally, Romero *et al.* (1999) observed that the group VIII (Fe and Ni) metals in coke are catalysts during the formation of silicon carbide.

The mechanical strength of charcoal is a parameter of great importance because the charcoal is subjected to numerous handling and transportation operations from its production to the final destination, hence genetic materials of greater strength are desirable. In fact, the mechanical resistance levels of charcoal, because it is a fairly friable

material, has direct implications for its granulometry, medium size, and generation of fines. According to Assis *et al*. (2016), less resistant charcoal will more easily degrade, reflecting the decrease in their average size and increase in fines generation.

The low mechanical strength of the charcoal can also interfere in the reduction of the gas permeability in the furnace load (Gładysz and Karbowniczek, 2008). It should be noted that silicon production is carried out in low-shaft furnaces, which imply moderate requirements in terms of mechanical strength of the load (Grischenko *et al*., 2013). According to Silveira *et al*. (1986), charcoal has a crushing strength in the range of 30-50 kg cm^{-2}, which is often higher than the charge column pressure of an electric submerged arc furnace, reaching about 0.16 to 0.22 kg cm^{-2} at its most critical point.

The granulometry of the reducing material is another factor of relevance in the production of silicon. According to Grischenko *et al*. (2013), choosing the appropriate size of reducing material depends on the alloy melting technology, furnace size, and properties of the reducing material. Myrhaug (2003) recommends reducing the particle size if the reducing material used has low chemical reactivity, because the lower the particle diameter results in higher reactivity. However, according to Schei *et al*. (1998), there is a limit on the granule size of the reducing material because during the production of silicon, there is a need for the process gases to percolate through the load in the kiln. If the charcoal particles are excessively small, the passage of these gases will be impaired, compromising the proper operation of the furnace. In addition, low-grade carbons burn on the top of the furnace and, therefore, do not participate in the quartz reduction steps. This is reflected in the greater generation of slag and lower production of silicon in the furnace (Schei *et al.,* 1998). It is worth noting that fine fractions of charcoal, particles smaller than 9 mm, are relatively controlled by the practice of sifting the charcoal before placement in the silicon furnace.

An important property of the reducing material is the rate at which it reacts with a reactant gas. This property is called "reactivity". In the production of silicon in particular, the important gaseous reagent is silicon monoxide (SiO), which is formed by the reaction of silicon (Si) or silicon carbide (SiC) with SiO_2 in the high temperature region of the furnace. The reaction of the reducing material with the SiO gas has the purpose of forming the SiC intermediate, which will react with SiO in the high

temperature zone of the furnace to produce the silicon (Myrvågnes, 2008). Therefore, the evaluation of this parameter is of crucial importance in the performance of the silicon production process.

1.2.1. Influence of wood on charcoal quality

The properties and productivity of charcoal depend directly on the physical and chemical properties of the wood. Wood intended for charcoal production should have favorable characteristics, such as high values of basic density and calorific value, low mineral content, high lignin content, low heartwood/sapwood ratio (H/S) and low syringing/guaiacil ratio (S/G), which are characteristics that guarantee high yield, low cost, and high quality in the production of charcoal (Santos *et al.*, 2011; Trugilho *et al.*, 2011; Pereira *et al.*, 2012; Protásio *et al.*, 2012; Pereira *et al.*, 2013; Pereira *et al.*, 2013b; Soares *et al.*, 2015; Costa *et al.*, 2017).

The density of wood is one of the most important indices to be considered among the various physical properties of the wood, since, in addition to affecting the other properties, it interferes in the quality of its derivatives in a significant way. In the process of carbonization, the use of denser woods is preferred because of the optimization of the internal volume of the carbonization kilns and, as a result, higher productivity of the charcoal production unit (Pereira *et al*., 2012; Carneiro *et al*. 2014). Additionally, denser woods, when charred, give rise to a denser, more mechanically resistant and generally less friable charcoal (Assis *et al*., 2016).

It is important to note that the basic wood density is influenced by its anatomical properties. Variations in wood density depend on changes in the proportion, distribution and quantity of vessels, radial and axial parenchyma and, mainly, fibers (Panshin and Zeeuw, 1980). Ramos *et al*. (2018) and Pereira *et al*. (2016) verified that the anatomical parameters of the wood of *Eucalyptus* clones correlated significantly with the basic density of the wood and the apparent density of the charcoal, emphasizing the thickness of the fibers wall. The larger the the wall fraction of the fibers results in a tendency for less voids to be found in the wood and, consequently, in the charcoal produced.

From the technological point of view, another important anatomical property is the quantification of the heartwood and sapwood percentages in the wood. This is because there is the either greater percentage presence of heartwood or sapwood, depending on the use of the wood. It is worth noting that the heartwood/sapwood ratio (H/S) in the wood increases with tree age and trunk diameter (Assis *et al.*, 2016).

In the production of charcoal, the H/S ratio affects the initial stage of the carbonization process, characterized by the drying of the wood. Heartwood, mainly due to the obstruction of the vessels by tyloses, is less permeable compared to the sapwood, and this impedes the transport of water from the inside of the wood to the outside (Galvão and Jankowsky, 1985). In these conditions, the vapor pressure of the gases increases within the anatomical elements, resulting mainly in the rupture of the parenchyma cells that have less thick walls. As a result, there is formation of internal cracks and crevices in the coal, which culminates in increased friability and, therefore, producing a greater amount of fines (Ramos *et al.*, 2015; Assis *et al.*, 2016; Donato, 2018). It is common to find cracks in carbonized pieces that are representative of the wood core, while the sapwood does not exhibit such behavior. According to Costa *et al*. (2017), for the production of charcoal, woods with low core / sapwood ratio are suggested because they generate lesser fines.

The lignin content in wood is closely related to the conversion efficiency of wood to charcoal. Among the chemical elements of the wood, lignin is the organic compound with the highest resistance to thermal degradation and, as a result, positively influences the charcoal yield (Raad *et al.*, 2006; Pereira *et al.*, 2013c). It is important to note that lignins have high resistance to thermal degradation when compared to cellulose and hemicelluloses, due to their high aromaticity, high carbon content, size, and the arrangement of their structure (Haykiri-Acma *et al.*, 2010).

Raad *et al.* (2006) studied the thermal decomposition of wood components via thermogravimetry and concluded that both hemicelluloses and cellulose do not contribute much to charcoal yield. In the carbonization carried out at 450 ºC, the hemicelluloses contributed, on average, to 10% of the charcoal yield, while cellulose and lignins accounted for 20 and 70%, respectively. According to Pereira *et al*. (2013), a minimum

28% lignin content is required for the cost-effective production of charcoal for industrial purposes.

The quality of lignin, i.e. the syringyl/guaiacil ratio (S/G), should also be considered for woods used in the production of charcoal. Genetic materials with lower S/G ratios should be selected, since the guaiacil group is more preserved in the pyrolysis process. The aromatic unit of the guaiacil-type (G) can form bonds (C-C) at the C5 position of the aromatic ring with another guaiacil unit, resulting in the condensation of aromatic rings and greater stability of the lignin molecule (Pereira *et al.*, 2013; Soares *et al.*, 2015).

Inorganic compounds, unlike organic compounds, do not change during the carbonization process. With the volatilization of part of the organic fraction of the wood, however, there is an increase in the inorganic concentration in the charcoal. Therefore, wood with higher concentrations of minerals will produce charcoal with higher inorganic content (Reis *et al.*, 2012; Pereira *et al.*, 2013). In addition, it is known that higher ash content results in lower calorific value of the bioreductor, since the ashes do not participate in the combustion process (Brand, 2010).

The moisture of the wood is a parameter considered undesirable in any type of energy process, since the evaporation of the water is an endothermic reaction and reduces the amount of useful energy produced. In the carbonization process, it is not different because besides compromising production and productivity, it directly affects the mechanical properties of charcoal. The water inside the wood tends to evaporate at high temperatures, and the water vapor, in turn, leaves the wood and causes cracks. This generally causes ruptures in the structure of the formed charcoal, increasing its friability (Assis *et al*., 2016).

1.2.2. Influence of carbonization parameters on charcoal quality

The charcoal consists basically of carbon, but its shape and properties are not absolutely fixed but, instead, depend fundamentally on the type of wood and the carbonization process (Assis *et al.*, 2016; Kan *et al.*, 2016). Heating rate, final carbonization temperature, residence time, and pressure are parameters used in the

carbonization process of the wood. Such parameters affect the production, productivity, and physical and chemical characteristics of charcoal.

The final carbonization temperature differentially affects each chemical element of the wood. The carbon content rises rapidly with the increase of the carbonization temperature, while decreasing the levels of hydrogen and oxygen. The increase of the carbon content in the charcoal with the increase of the final carbonization temperature is accompanied by the concomitant reduction of the content of volatile materials and increase of the gravimetric yield in charcoal (Kan *et al.*, 2016). In addition, the increase in the release of volatile compounds with an increase in the final carbonization temperature reflects the increase of inorganic compounds and fixed carbon in charcoal (Titiladunayo *et al.*, 2012; Protásio *et al.*, 2014).

The carbonization temperature also exerts an effect on the apparent density and mechanical properties of charcoal. There is a tendency of reduction of apparent density and considerable decline of the mechanical properties of the charcoal with the increase of the final carbonization temperatures up to approximately 600 °C, and thereafter, it increases with increasing temperature up to 900 °C (Manabe *et al.*, 2007; Couto *et al.*, 2015; Assis *et al*., 2016). This behavior is mainly attributed to two factors: effects of contraction and loss of mass and rearrangements of carbonaceous structure of charcoal (Manabe *et al.*, 2007; Couto *et al.*, 2015; Assis *et al*., 2016).

It is important to consider the rate of heating in the carbonization process. The rate at which the temperature increases directly influences the process throughput. Gentle heating rates favor a higher yield of the solid fraction produced by the carbonization process, whereas swift heating favors the production of condensable and non-condensable gases (Protásio *et al.*, 2015). Oliveira *et al.* (2010) observed a decrease in the content of volatile materials and apparent density of the coal with the increase of the heating rate. In addition, Monsen *et al.* (2000) reported the reduction of the compressive strength of the coal and the fixed carbon yield with the increase of the carbonization heating rate. Siebeneichler *et al.* (2017) observed a tendency of increase of the friability and reduction in the wall thickness of the charcoal fiber with the increase of the heating rate.

Residence time is another parameter that reflects on the quality of charcoal. As observed by Peng *et al.* (2011) and Kumar *et al.* (1992), the increase in residence time at

the peak temperature of carbonization caused a reduction in the content of volatile materials, increase in the carbon content and ash in the coal, and drop in the gravimetric yield in charcoal. Moreover, according to Peng *et al*. (2011), there was a reduction of aliphatic groups and the development of aromatic carbon with the increase of residence time.

The pressure also influences the yield of the carbonization process. Carbonizing the wood at high pressures limits the output of the volatile compounds from the internal wood/charcoal cavities. Therefore, the increase in the residence time of the volatile compounds inside the solid favors the condensation and re-polymerization into more stable structures (secondary reactions) of these compounds in the internal cavities, thus increasing the mass of the solid fraction produced (Rousset *et al.*, 2011; Noumia *et al.*, 2016).

1.3. Silicon production process

Metallurgical grade silicon, as well as other ferro-silicon alloys, is produced in furnaces heated with graphite electrodes by means of an electric arc submerged to the charge. Quartz (SiO_2) is used as a raw material, and coal, charcoal, and wood chips are used as reducing agents (Tangstad, 2013). The products resulting from the process are silicon ($Si \geq 98\%$), silica powder (SiO_2), and heat. Figure 1.1 shows a silicon production plant.

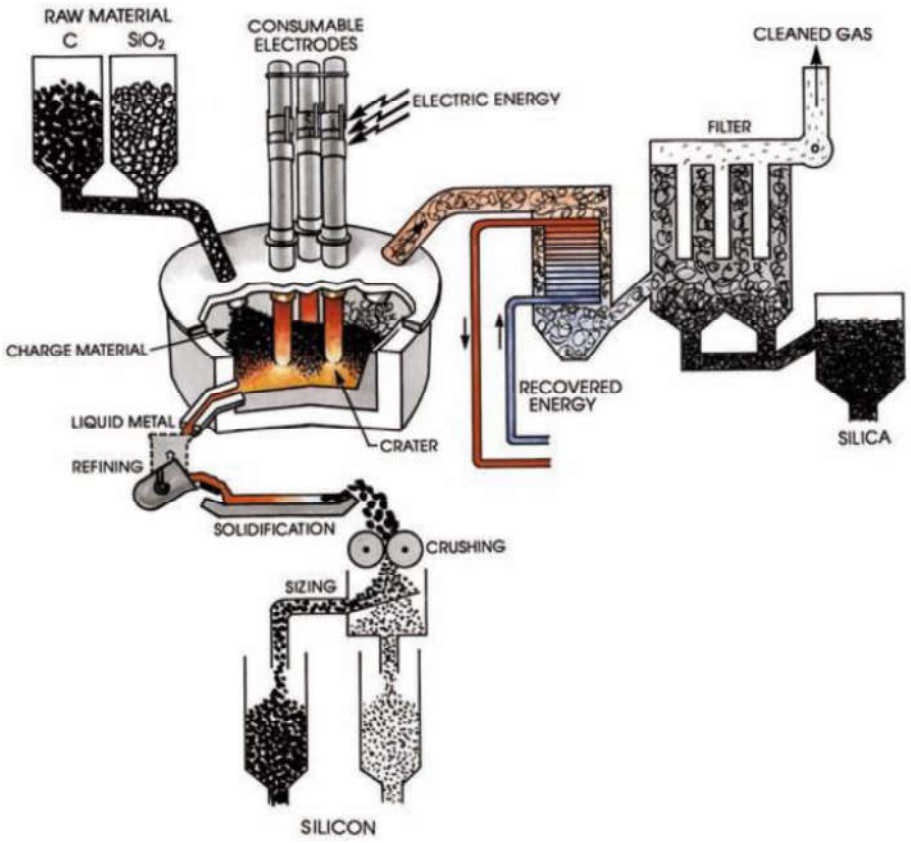

Figura 1.1 - Overview of a silicon plant. Source: (SCHEI *et al.*, 1998).

Quartz (SiO_2), used as the source of Si, is the second most abundant element in the earth's crust (~28% by mass), surpassed only by oxygen. For this reason, SiO_2 is considered a virtually unlimited source of silicon (Schei *et al*., 1998). In order to produce a high purity silicon and to have good operation of the furnace, the chemical composition of the quartz, as well as its mechanical resistance and thermal stability, are quite controlled.

The quality of the reducing material for use in the silicon production process is dependent on characteristics such as high SiO reactivity, high fixed carbon content, and homogeneity in particle size, and these are required as these are essential to achieve the high silicon yield (Myrvågnes and Lindstad, 2007). Wood chips are also used for providing permeability and preventing segregation of the charge. However, the wood chips also contributes as a carbon source because when it comes in contact with the hot

gases from the top of the kiln, the process of wood degradation begins, resulting in the drive off of the volatiles and their conversion to charcoal (Myrhaug *et al.,* 2004).

During the production of silicon, the raw materials are mixed and added to the charge from the top of the furnace, and the silicon is drained into the bottom of the furnace, either continuously or in batches. After the Si flow is acheived, the refining stage occurs, i.e. the oxidation of the metal with oxygen or air, and this is done with the aim of separating the undesirable elements, mainly Ca and Al, into the fused slag supernatant. Finally, the solidification step occurs, followed by the breaking of the ingots into silicon particles, and the grain size of the material meets the specifications desired by the customer (Tangstad, 2013).

The residual gas from the silicon production exits the furnace at temperatures between 1000-1700 °C and contains approximately 0.3 tons of silica powder for each ton of Si produced (Li, 2017). Silica powder, also refered as microsilica, consists of a quasi-spherical particle with a mean diameter of 0.15 μm and a high specific surface area of ~20 m^2 g^{-1}, being mainly sold to the cement industry (Tangstad, 2013). Microsilica is used as a filler element in concrete, promoting the increase of the resistance and the lifetime of this material. While the heat from the waste gas, which accounts for 51 % of the energy input into the system, can be used in a power recovery plant (Tangstad, 2013).

The electrical energy is transformed into thermal energy by establishing an electric arc between the graphite electrodes and the region of the liquid silicon, used to provide the furnace heating and provide energy for the reactions to occur. In most submerged arc furnaces, three pre-cooked graphite electrodes are used, which are consumed and reused during the production process (Tangstad, 2013).

Typically, the mass yield in Si relative to the mass of quartz used in the kiln is about 80 to 90% (Tangstad, 2013). According to Andresen (2016), a silicon furnace with an energy demand of 35 MWh per ton of silicon consumes about 7.5 tons of quartz and 2.5 tons of "C", producing 3 tons of Si and 1 ton of microsilica.

Silicon metal is used in various industrial processes. Approximately 50 % of the world's silicon production is for the purpose of alloying, mainly for the production of aluminum. The remainder is used in the chemical and electronics industry, in addition to the demand for silicon for manufacturing of solar panels (Tangstad, 2013). In the

chemical industry, silicon is used for the production of silicone compounds, the main raw material for a large and growing number of industrial products, including silicone rubbers, urethane foam, sealants, adhesives, lubricants, food additives, coatings, and cosmetics. It is worth noting that silicones are replacing many applications of petroleum-based compounds (Li, 2018).

1.3.1. Chemical Reactions in Silicon Production

The general reaction of the silicon production process can be described, in a simplified way, by Equation 1. It should be noted, however, that there are dozens of intermediate reactions occurring simultaneously inside the furnace, as can be seen in Figure 2.1.

$$SiO_{2(s)} + 2C_{(s)} \longrightarrow Si_{(l)} + 2CO_{(g)} \quad \Delta H°_{1500°C} = -75 \text{ kJ/mol} \qquad (1)$$

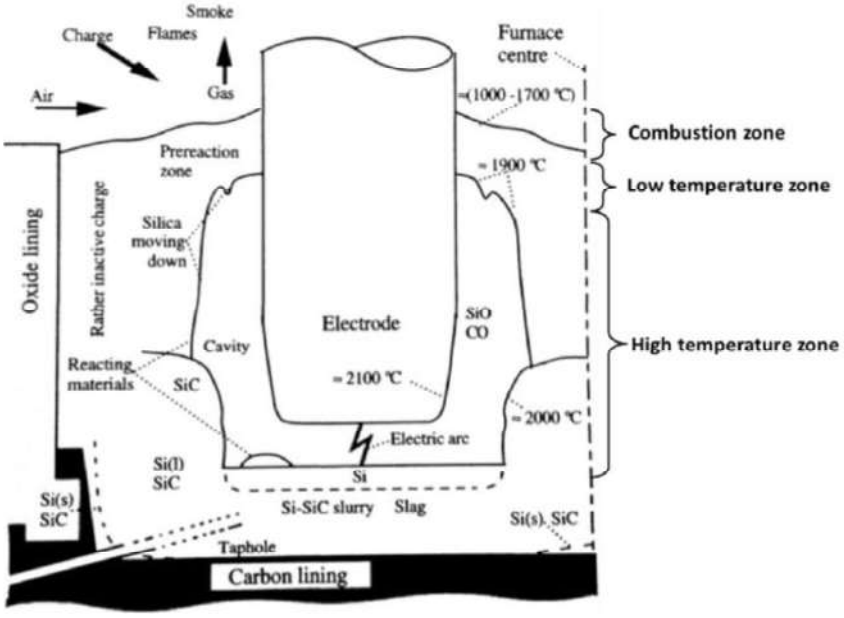

Figura 2.1 - Structure and reaction zones in silicon production furnace. Source: (LI, 2018).

It is observed in Figure 2.1 that there is a temperature variation inside the furnace, presenting a lower temperature near the tips of the electrodes that reach values of approximately 2200 °C, while at the top of the furnace, it is around 1400 °C (Tangstad,

2013). Li (2018), based on Schei *et al*. (1998), described the production of silicon by dividing the furnace into three distinct zones - combustion zone, external zone, and internal zone - as can be seen in Figure 2.1. The specific reactions of each zone will be described in the next topic.

It is also verified that near the electrodes, there are empty spaces called cavities or craters. These form because of the excess of gases generated in the internal reaction zone, the formation of sticky condensate ($Si + SiO_2$) in the external zone, and because of quartz melting in areas with temperature between 1.700-1.900 °C (Myrvågnes, 2008). The volume of raw material deposited above the craters is called the "furnace shaft", and this region is believed to be the most active part of the charge (Andresen, 1995).

In the furnace shaft, the formation of preferential channels and losses of the SiO gas directly to the gas outlet system may occur, and this compromise the Si yield. In the industrial process, to minimize the effect of these channels, the walls are broken at regular intervals and raw materials are added to increase the thickness of the furnace shaft (Myrvågnes, 2008).

1.3.1.1. Reactions in the combustion zone

The combustion zone is located at the top of the furnace, where the raw materials are loaded. In this area of the furnace, there is atmospheric air intake, and therefore, oxidation and heat release reactions occur. Both the exhaust gases from the furnace and part of the reducing material added to the charge undergo oxidation.

The exit gases (SiO, CO), when entering the combustion zone, will be oxidized and form silica powder (SiO_2) and CO_2, according to Equation 2 and Equation 3, respectively (Li, 2018). Both are exothermic reactions. The heat produced helps to heat the raw material and, consequently, the top of the furnace. From the combustion zone, the waste gases either leave the chimney or be sent to the energy recovery and gas cleaning system.

$$SiO_{(g)} + 0.5O_2 \longrightarrow SiO_2(s,l) \quad \Delta H°_{25°C} = -781 \text{ kJ/mol} \tag{2}$$

$$CO + 0.5O_2 \longrightarrow CO_2 \quad \Delta H°_{25°C} = -279 \text{ kJ/mol} \tag{3}$$

Additionally, volatile materials present in the charcoal and wood chips are released and burned as they pass through the combustion zone and also produce heat in this region. According to Tangstad (2013), the energy from the volatiles represents approximately 15 % of the energy input in the silicon furnace. In addition, part of the fixed carbon in the reducing material can be burned, especially when using material of smaller particle size, causing a lack of control of the amount of carbon in the process (Schei *et al.,* 1998).

The submerged electric arc furnace, depending on the technological feature, may have the combustion zone fully open, semi-open, or closed with an air inlet control. Closed furnaces are generally large (30 MW) and coupled to an energy recovery plant (Schei *et al.,* 1998).

1.3.1.2. Reactions in the outer zone

In the outer zone of the furnace, the carbon present in the reducing material reacts with the SiO gas in the furnace, generating SiC (s) - Equation 4, which shifts or moves with the downward flow of raw materials to the internal zone of the furnace, thus maintaining the Si element in the process. For this reason, Equation 4 is also called the silicon recovery reaction. The reducing material acts as a "SiO gas filter" in the furnace, preserving the silicon and energy in the process (Raaness and Gray, 1995). Equation 4 occurs only at temperatures above 1535 °C, while below that temperature, part of the SiO gas can be recovered by Equation 5, known as the condensation reaction. Li (2018) presented the main reactions of the outer zone:

$$SiO_{(g)} + 2\,C_{(s)} \longrightarrow SiC_{(s)} + CO_{(g)} \quad \Delta H^{\circ}_{1500^{\circ}C} = -75\ kJ/mol \tag{4}$$

$$2SiO_{(g)} \longrightarrow Si + SiO_{2(g)} \quad \Delta H^{\circ}_{1500^{\circ}C} = -617\ kJ/mol \tag{5}$$

The SiO gas produced inside the furnace is an energy-rich intermediate component. It should be noted that approximately 93 % of the energy required for quartz reduction is consumed by SiO gas formation reactions (Myrvågnes, 2008).

In order to obtain a better understanding of the dominant reactions in the silicon furnace, the phase stability diagram of the SiO_2-SiC-C-SiO-Si system is shown in Figure

3.1. It is assumed that the total gas pressure is equal to 1 bar and consists only of SiO and CO, predominant gases in the furnace.

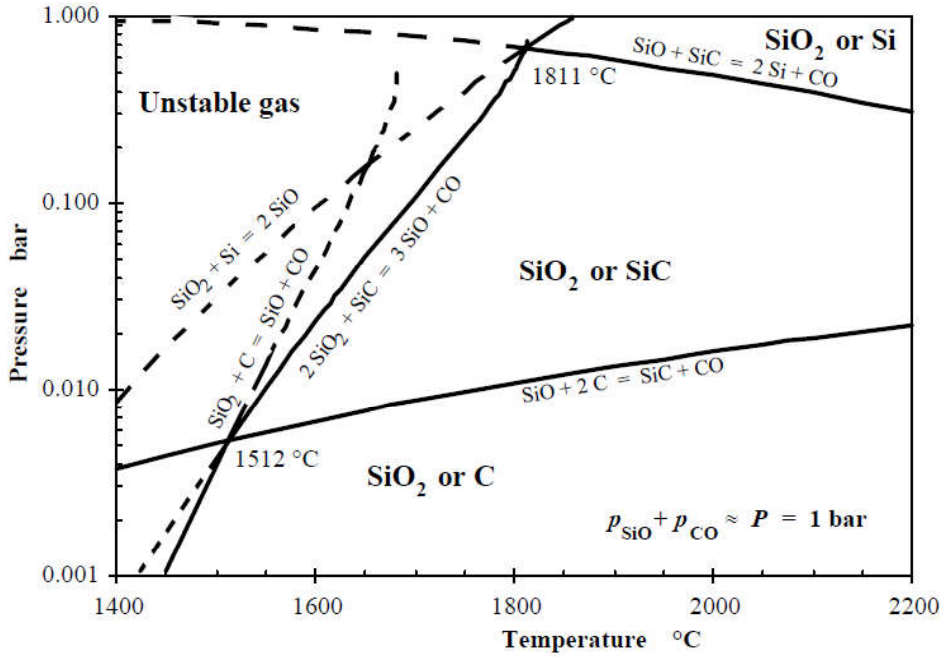

Figura 3.1 - Effect of temperature on SiO partial pressure. Source: (SCHEI *et al.*, 1998).

The condensation reaction, Equation 5, is exothermic, and thus, the amount of SiO gas that can be recovered as condensate is then limited by the heating capacity of the charge (Myrvågnes, 2008). As seen in Figure 3.1, the increase in temperature raises the equilibrium partial pressure of SiO gas, allowing more SiO gas to escape

According to Tangstad *et al.* (2010), losses of Si by the residual gas of the furnace are less than 1% when considering the temperature of 1400 °C on the surface of the charge and the equilibrium pressure of SiO below 0.01 atm. This, in turn, indicates a theoretical Si yield of greater than 99 %, significantly higher than the typical industrial yield of a silicon furnace (80-90 %). Therefore, non-equilibrium conditions are considered to dominate the top of the furnace.

1.3.2. Reactions in the inner zone

In the inner zone, SiC (s) and silica SiO_2 (s, l) react with each other to form SiO, CO, and Si. In this zone, the reactions require temperatures above 1800 °C in order to obtain sufficient partial pressure of SiO for silicon production. Li (2018) presented the main reactions in this zone:

$$2SiO_{2\,(s,l)} + SiC_{(s)} \longrightarrow 3SiO_{(g)} + CO_{(g)} \quad \Delta H^{\circ}{}_{1900^{\circ}C} = +1391 \text{ kJ/mol} \tag{6}$$

$$Si_{(l)} + SiO_{2(s,l)} \leftrightarrow 2SiO_{(g)} \quad \Delta H^{\circ}{}_{1900^{\circ}C} = +\,610 \text{ kJ/mol} \tag{7}$$

$$SiC_{(s)} + SiO_{(g)} \longrightarrow 2Si_{(l)} + CO_{(g)} \quad \Delta H^{\circ}{}_{1900^{\circ}C} = +171 \text{ kJ/mol} \tag{8}$$

For silicon formation – Equation 8 -, there must be a critical equilibrium condition in the Si-O-C system, being 0.67 bar at a minimum partial pressure of SiO at 1811 °C. At higher temperatures (~2000 °C), however, there is a drop to 0.5 bar because the SiO partial pressure is temperature dependent, as can be seen in Figure 2.1.

The formation of silicon occurs under high partial pressure of SiO, so reactions that consume SiO in the inner zone of the furnace will tend to reduce the recovery of silicon metal. According to Raaness and Gray (1995), the carbon fraction that does not react in the outer zone – Equation 4 - will react in the hotter zone of the furnace and will lead to an increase in the CO (g) production and, thus, there is an increase in the CO/SiO ratio in the inner zone. Therefore, the SiO pressure required in the internal zone will be further away from the chemical equilibrium, resulting in lower Si production and excess SiO circulation in the load. According to Schei *et al*. (1998), the theoretical silicon yield can decrease from 100 % to 50 % if reducing materials with a conversion degree of 67 % are used, i.e., 33 % of the carbon of the reductant did not react with the SiO gas in the outer zone of the furnace.

It is important to note that adding carbon above the stoichiometric optimum in order to reduce SiO losses, is not worthwhile, because this will result in the accumulation of SiC in the furnace, which will also cause losses in Si (Tangstad, 2013). It should be noted that the critical value of carbon to maximize silicon yield may vary slightly depending on the reactivity of the reducing material and the electric power of the furnace (Lund *et al.*, 2004).

1.3.3. Reaction between reductant material and SiO gas

A Most of the SiO gas produced in the inner zone of the furnace reacts with the carbon in the reducing material in the outer zone (Equation 9).

$$SiO_{(g)} + 2\ C_{(s)} \longrightarrow SiC_{(s)} + CO_{(g)} \quad (9)$$

This reaction is essential in two respects, according to Myrvågnes e Lindstad (2007):

(i) Minimize losses of Si (in the form of SiO) and, thus, increase the yield of silicon metal.

(ii) Maintain energy efficiency in the process because ~93% of the energy in Si production is used to form SiO gas.

The quality of the reducing material is of vital importance in order to maximize the conversion of C to SiC, because the free carbon on the surface of the reductant particle, when reacted with SiO, forms a layer of SiC that hinders the access of the SiO gas inside the particle. As this layer thickens, the reaction rate becomes slower. It is emphasized that, commonly, the reducing material has an unreacted carbon fraction when it reaches the inner zone of the furnace (Schei *et al*., 1998). These authors, using a stoichiometric model, simulated the influence of reactivity and partial pressure of SiO on the silicon yield. The influence of the reactivity is shown in Figure 4.1, where it can be observed that higher reactivities of the reducing material favor the performance in metallic silicon. The reactivity was calculated by the ratio of carbon moles reacted with SiO gas in the outer zone to total carbon moles.

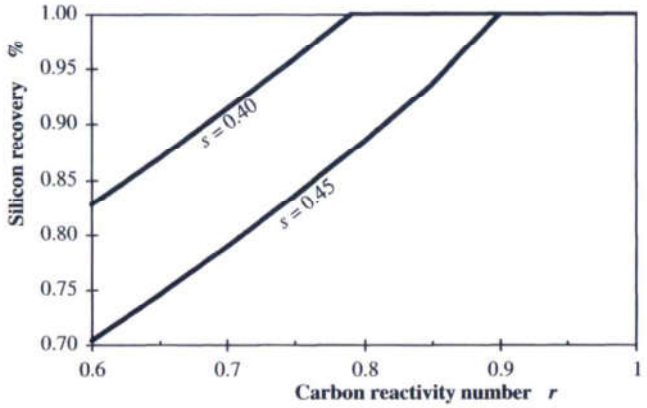

Figura 4.1 - Silicon yield model as a function of reactivity (r) evaluated under different partial pressure values of the SiO gas (s). Source: (SCHEI *et al.*, 1998).

In Figure 4.1, the negative influence of the SiO partial pressure on the silicon yield is also observed. According to the tested model presented by Schei *et al.* (1998), "*s 0.4*" provides a higher silicon yield than "*s 0.45*" regardless of the reactivity of the reducing material. A lower partial pressure in the internal zone of the furnace results in a lower concentration of SiO in the external zone and, consequently, lower losses of SiO in the SiO_2 form.

In the case of the SiO gas in the carbonaceous matrix of various reducing materials, Myrhaug *et al.* (2004) stated that the reaction of carbon with SiO gas, Equation 9, occurs from the outer surface to the inside of the particle, forming a layer of SiC around the unreacted central part , as can be seen in Figure 5.1. They concluded that the unreacted core model for spherical charcoal samples presented the best description of the kinetics of Equation 9. This model also proved to represent the best description of the behavior of the reducing material in a fixed bed of particles.

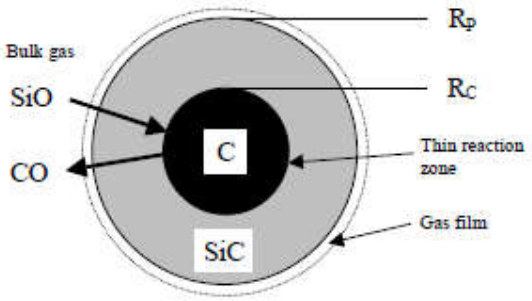

Figura 5.1 – Shrinking core model for reducing material sphere. Sphere of radius (Rp) and unreacted core ratius (Rc). Source: (MYRHAUG *et al*., 2003).

Myrhaug (2003) described the main steps of the reaction of a reductant particle with the SiO gas, based on Szekely *et al.* (1976).

1. Mass transfer of upward SiO gas into the furnace to the outer surface of the solid particle.

2. Penetration and diffusion of SiO gas through the pores of the solid matrix, which consist in SiC and C, to the surface of the unreacted nucleus.

3. Chemical reaction of SiO with available carbon on this surface.

4. Diffusion of the CO gas through the pores of the solid matrix, which consist in SiC and C, to the outer surface of the solid.

5. Transfer of masses of the CO gas from the outer surface of the solid particle to the upward gas in the furnace.

Vorob'ev (2017) stated that the formation of the silicon carbide (SiC) is topochemical. Hence, the SiO capture for SiC formation depends mainly on the accessible surface area of the SiO gas reducing material. For this reason, higher levels of porosity and surface area in the charcoal facilitate the diffusion of the SiO gas in the carbon matrix.

1.3.4. Factors that Affect Reactivity

Reactivity to SiO gas is a property commonly evaluated in coal and coke. Compared to the fossil reducers, there is practically no research involving this property when charcoal is the material researched, highlighting the study of Myrhaug (2003).

Analyzing the reactivity of reducing materials, Myrhaug (2003) found higher values of reactivity in samples of charcoal as compared to coal. The reactivity of charcoal ranged from 965 to 160 ml SiO, while coal varied from 1114 to 1275 ml SiO. The reactivity correlated positively with the porosity of the reducing material. Additionally, by evaluating the cross-section of charcoal with 50% converted, that is, half of the carbon converted to silicon carbide, an increase in the percentage of SiC along charcoal cell structures was observed, as can be seen in Figure 6.1-A. This seems to be due to two

distinct factors, namely: different anatomical characteristics of tracheids of latewood and initial wood of conifers or deposition of SiC in the wall of small diameter tracheids.

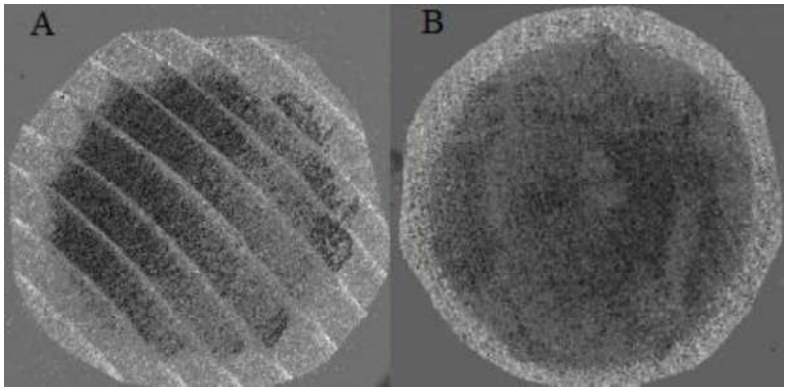

Figura 6.1 - Microprobe pictures of charcoal spheres partially reacted to the SiO gas. (A) softwood; (B) hardwood. The brighter areas represent SiC and the darker areas C. Source: Myrhaug (2003).

In this same study, the influence of charcoal particle size on reactivity was also evaluated. The results showed that the reactivity values of the charcoal increase with the reduction of the particle size. This phenomenon is observed in the ease of reaching of the active sites. Therefore, the larger particles have greater difficulty in the reactive gas accessing the active sites present in the center of the particle. In addition, it is emphasized that a particle of smaller particle size presents a larger specific area when compared to a particle of greater particle size (Nocentini *et al*., 2010)

Analyzing the reactivity of different reducing materials, Li (2018) referred to porosity as an important property that influences reactivity. In this study, charcoal presented higher reactivity and porosity. The reactivity values, expressed as conversion rates of SiO, of charcoal, coke, black carbon and coal were 87.7 %, 85.9 %, 56.5 %, and 46.5 %, respectively.

In the case of reducing materials of fossil origin, several reactivity studies are found. Tuset and Raaness (1976) verified a strong positive correlation of reactivity with the effective diffusivity of SiO gas in the pores of mineral coals. Raaness and Gray (1995), investigating the SiO reactivity of fossil reducers, correlated it with petrographic properties (Grade, Type, and Rank). Based on some assumptions, they showed that increasing rank in coal tends to decrease reactivity. Raaness and Gray (1995) and

Myrhaug (2003), examining the petrography of SiO gas-reacted coal and coke samples, identified reactive and non-reactive carbon forms. Raaness *et al*. (1998) established a multivariate regression model to predict reactivity as a function of the petrographic properties of the fossil reductant. Buø *et al*. (2000) concluded that coal and coke characteristics, such as low bulk density, large amount of binder phases, low amount of filling phases, high porosity, and less pore distance, were beneficial for increasing reactivity.

Considering the presence and quantity of minerals in the reducing material, Romero *et al*. (1999) reported that the presence of Group VIII metals in cokes, such as Fe and Ni, are effective catalytic agents in the production of SiC. Myrvågnes and Lindstad (2007) observed that the high amount of Si in the coke, in the form of inclusions of quartz, favored reactivity. This was related to the reaction of SiO_2 with carbon at temperatures above 1400 °C.

Although the use of charcoal has tradition and has had extensive use, the evaluation of charcoal properties for silicon production has been rarely reported in the literature. The behavior of the SiO gas in the carbon matrix of different charcoals, that is to say, coming from different species and processes of carbonization, still remains a little understood aspect and suggests the need for more investigation in this field.

1.4. SiO reactivity test

The reactivity of the reducing materials is one of the most important parameters when discussing the properties of carbonaceous agents for the production of silicon. The ease by which the carbon in the reducing material reacts with the SiO gas can be measured, and the value is recognized as SiO reactivity.

Gas analysis, thermogravimetry, and chemical determination of silicon carbide (SiC) are procedures used to evaluate the reaction between the SiO gas and the reducing material. A more in-depth discussion of these techniques will be provided in the following sections.

It is emphasized that, despite the development of different methods for testing the reactivity of reducing materials to SiO gas, such procedures are still very expensive to

perform. In this sense, the development of a simpler and more economical method to test reactivity is desirable.

1.4.1. Gas analysis technique

One of the most recognized tests for evaluating the reactivity of reducing materials to SiO gas is the SINTEF SiO reactivity test. This was first mentioned by Tuset and Raaness (1976) and further improved by Lindstad *et al*. (2007).

The principle of the SINTEF method is to simulate the reaction between a bed of particles of previously calcined reducing material and the flow of gas in the furnace. The gas used in the test consists of a gaseous mixture of SiO and CO, produced by the reaction between SiO_2 and SiC and is carried by the argon gas. The carbon in the reducing material will react with the SiO gas and produce CO, which is continuously monitored in the furnace effluent gas. When using a high reactivity reducing material, the CO content remains at a maximum value for a long period and, then, drops suddenly to a minimum value. In contrast, the CO drop occurs over a long period of time with a material of low reactivity, and some of the SiO gas is lost.

Figure 7.1 shows the reactions and the internal structure of an electric furnace used for the SINTEF SiO reactivity test. The furnace consists of three sections: SiO generator, reaction chamber, and condensation chamber. In the SiO generator, 4.5 % CO and 13.5 % SiO are produced by heating the pellets made of SiO_2 + SiC at 1650 °C. The gases are transported to the reaction chamber through the flow of argon gas at the constant flow of (320 ml min^{-1}). The reaction chamber has a volume of 20 cm^3, where the sample of the reducing material is placed. The upward SiO gas reaches the reaction chamber, and the reaction of the carbon with the SiO gas occurs. The SiO gas - which does not react with C - is condensed in the condensation chamber.

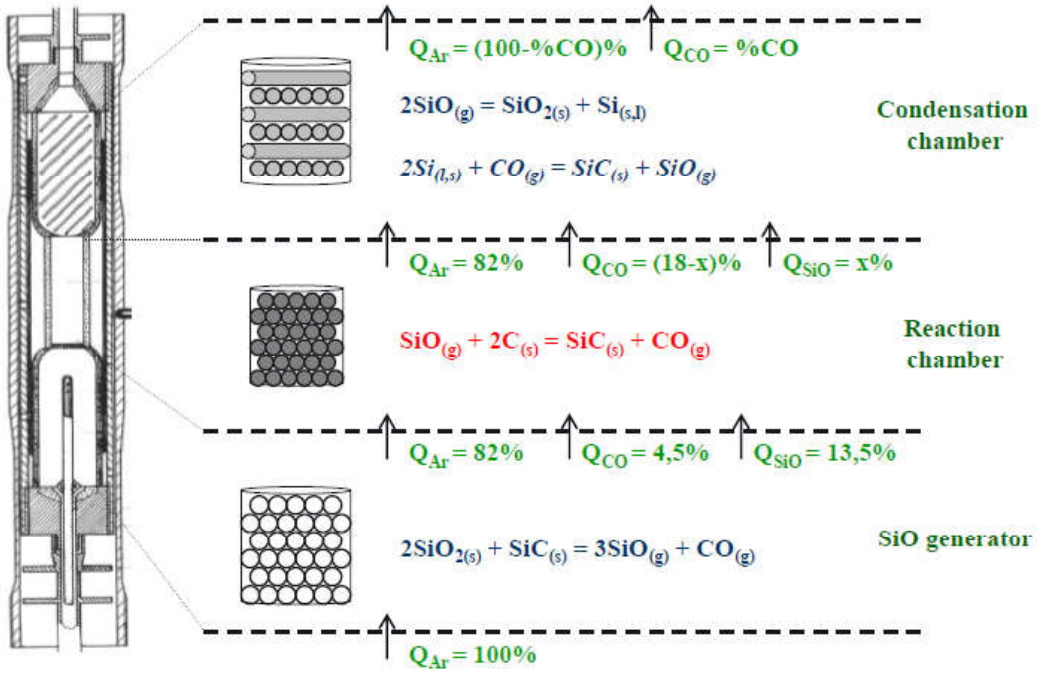

Figura 7.1 - Reactions and gas composition (vol%) in the three main units of the reactivity apparatus. Source: (Myrvågnes, 2017).

In the SINTEF standard test, 20 cm^3 particles of the reducing material are used in the particle size fraction of 4 - 6.3 mm. The SiO generator is filled with pellets produced from a mixture of grinds and fines α-SiC quartz at a molar ratio 2:1.05, respectively.

Figure 8.1 shows the CO profile versus time in the SINTEF SiO reactivity test (Monsen, 2015). The reactivity of the reducing material is evaluated on the basis of the R10 value, which expresses the amount of SiO gas (ml) passing through the reactor chamber without reacting with C. This is over the interval in which the concentration of CO in the effluent gas decreases from 18 to 10 %, calculated by Equation 10. High reactivity materials have a low R10 value.

$$R10 = \sum_{18 \rightarrow 10} \frac{Qar(18 - \%CO)}{82 - 0.82 * \%CO} * \Delta t \qquad (10)$$

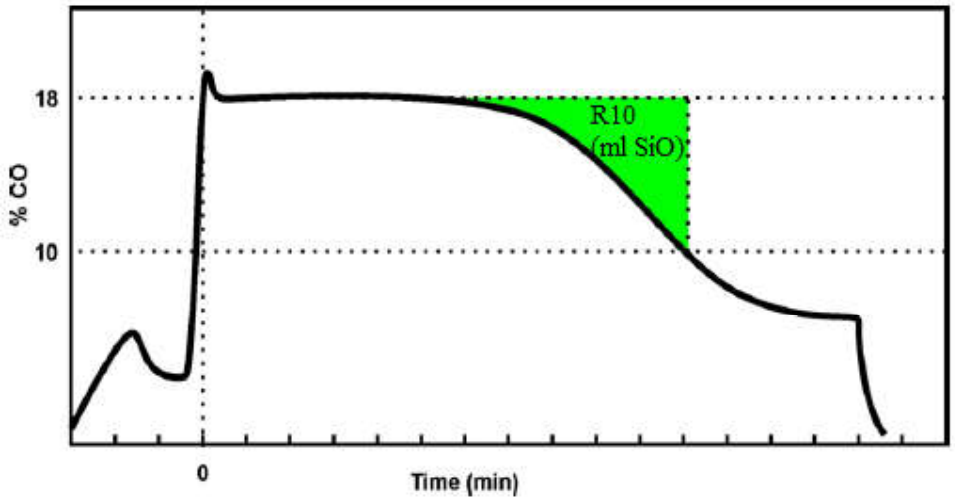

Figura 8.1 - Illustration of CO profile as a function of time - green area expresses SiO reactivity. Source: (Monsen, 2015).

Advances and improvements in the SINTEF SiO reactivity test were performed and are described in Lindstad *et al*. (2007), however the basis of the procedure is identical to the original test. In addition, Myrvågnes (2008) used the SINTEF test and proposed the calculation of the tangent slope at the point of inflection on the % CO curve as an alternative of reactivity measurement.

Figure 9.1 shows examples of reducing materials with different reactivities used for silicon production (Monsen, 2015). A low volume of SiO (mL) indicates high reactivity of the reducing material.

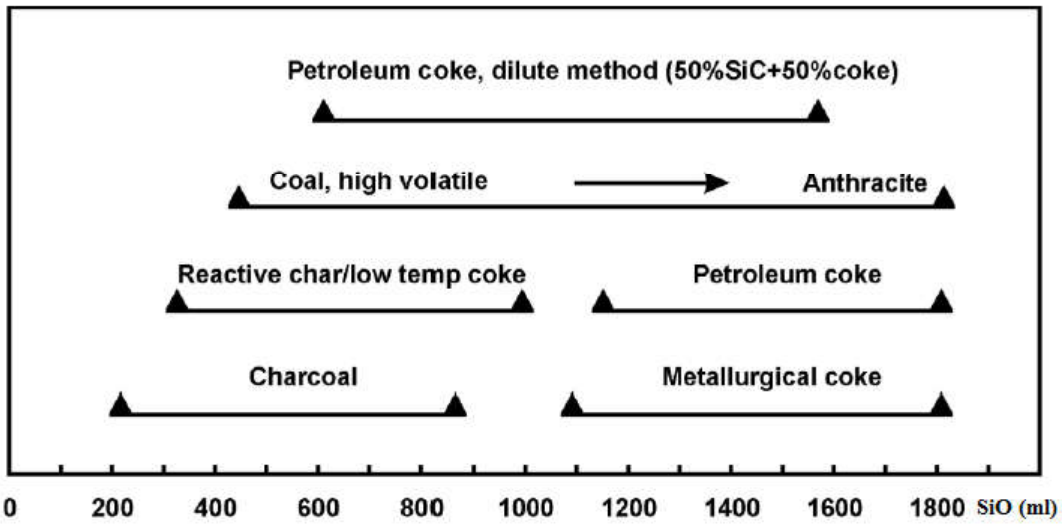

Figura 9.1 - Examples of reducing materials with different SiO reactivity. Source: (Monsen, 2015).

Paull and See (1978) presented a gas analysis technique similar to the SINTEF SiO reactivity test. The authors, however, concluded that the test was ineffective in assessing the ability of reducing materials to react with SiO gas. The main causes were the difficulty in controlling and maintaining the temperature at 1650 °C and, consequently, the instability of the SiO gas concentration during the tests. This difficulty occurred because the oven used did not have an automatic temperature control system. Adisty (2013) point out that SiO gas formation through the SiO_2 + SiC reaction is very temperature sensitive.

In the determination of the reactivity by the technique of gas analysis, in addition to the acquisition of a furnace for heating the sample, a gas analyzer of high precision is necessary, burdening this procedure. In addition, other points that must be considered are the need for calibration of the gas analyzer and the frequency of calibrations.

1.4.2. Thermogravimetric procedure

Thermogravimetry or the thermogravimetric procedure is a destructive technique in the field of thermal analysis, in which the mass variation of a sample is continuously monitored as a function of time in an environment of controlled temperature and

atmosphere. One of the first scientific studies that characterize the reactivity of reducing materials by thermogravimetric technique was published by Kozhevnikov *et al.* (1972). In this study, graphite discs, metallurgical coke, and charcoal were used as reducing materials, and they were subjected to temperatures of 1480 – 1680 ºC under SiO gas flow. This was generated by heating briquettes, made of SiO_2 and Si, at 1680 ºC. Based on the graphs of mass change of the sample as a function of the reaction time, the authors observed that there was no significant variation of the reactivity at the temperatures investigated. However, in the case of the different reducing materials, the charcoal was more reactive than the other reducing materials, especially in the initial reaction phase.

Another thermogravimetric method used to test the reactivity of reducing materials was reported by Videm (1995). In this procedure, the particles of the reducing material, of 4 - 6.3 mm particle size, were immersed in a crucible filled with pellets produced from a mixture of ground quartz and silicon carbide (SiC). Heating the pellets produced the SiO gas. The reaction temperature used was 1690 °C and is maintained for a certain time. During the experiment, both the sample and the reactor were continuously weighed. Reactivity is calculated using crucible mass change data. The reactivity value expresses the percentage of the carbon converted into silicon carbide (SiC). The illustration of the apparatus used in the reactivity experiment can be seen in Figure 10.1.

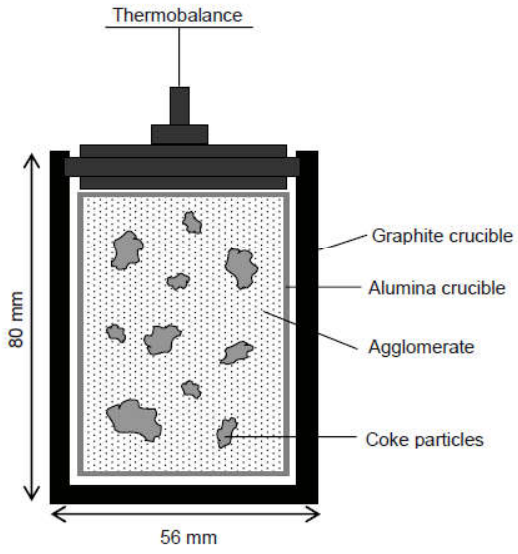

Figura 10.1 – Reactor for reactivity test. Source: Videm *et al.* (1995) adapted.

Buø *et al.* (2000), using the same procedure to test the reactivity combined with the petrographic characterization of the reducing materials, the authors developed models to estimate reactivity based on the petrographic characterization of the reducing material.

Myrhaug (2003) used a sample of reducing materials in the form of a sphere connected to a scale and monitored the mass increase of the sphere as it reacted with the SiO gas. The beads had diameters in the range of 8 to 25 mm and were connected to the balance by a tungsten wire. A simplified illustration of the equipment used in his work is shown in Figure 11.1. Similar to the SINTEF procedure, the SiO generator is placed below the reaction chamber, and the reaction temperature used was 1650 °C.

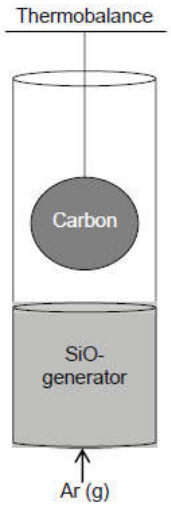

Figura 11.1 - Simplified illustration of the thermogravimetric apparatus used by Myrhaug (2003).

The reactivity, that is the degree of conversion of the C to SiC, was calculated on the basis of the sample mass change data during the experiment and the fixed carbon content of the reducing material, as presented in Equation 11.

$$X = (m2 - m1)/m1\,.\;C1\,(\frac{MSiC - 2MC}{2MC}) \qquad (11)$$

Where: "m" is the mass of the sample, 1 and 2 refer to the initial mass and current mass of the sphere, respectively. "*C1*" is the initial fixed carbon content. *MSiC* and *MC* are the molecular mass of SiC and C, respectively.

In this study, several kinetic models were tested in different reducing materials, based on the relationship obtained between the reaction time and the conversion of the sphere. In charcoal samples, the unreacted core model represented the best description of the kinetics of the reaction, while for the coke, both the shrinking core model and the grain model presented satisfactory results. Furthermore, it was possible to perform simulations in fixed bed models of particles, based on the kinetic models and parameters found.

According to Tuset and Raaness (1976), a simple way to evaluate the degree of conversion of the reducing material can be calculated by measuring the sample mass increase during the reaction, as shown in Equation 12.

$$X = \frac{(m2 - m1)}{m1} \tag{12}$$

Where:
X = Conversion rate (%)
m1 = initial mass of the calcined sample (g)
m2 = final sample mass after reactivity experiment (g)

Considering Equation 4 and the molecular mass of C and SiC, the theoretical maximum conversion rate will be 67%. This value is only obtained if the reducing material consists of pure carbon, and this material is totally converted to SiC. It is emphasized that this parameter does not take into account the carbon content in the reducing material, being ineffective in evaluating reducing materials with a wide range in carbon content (Myrvågnes, 2008).

1.4.3. Chemical analysis of SiC

Chemical analysis of silicon carbide (SiC) is performed for the purpose of determining the degree of conversion of the reducing material, i.e. the conversion efficiency of carbon to silicon carbide (SiC).

The procedures for quantification of silicon carbide (SiC) are based on the determination of total carbon and free carbon in the sample of the reducing material and are described in detail in ISO 21068 (2008). For determination of total carbon, the sample

is mixed with accelerators (iron, copper, tungsten carbide) and then melted in an induction furnace. Carbon is detected as CO_2 form by IR cells. The free carbon is determined by heating the sample under an oxygen atmosphere at a specific temperature (usually 900-1000 °C) in a tubular furnace. Carbon is detected as CO_2 form by IR cells.

After determination of total carbon and free carbon, the degree of conversion can be calculated, according to Lindstad *et al.* (2007) using Equation 13. In a simplified way, it can also be calculated by analyzing only the sample of reducing material after the reactivity experiment, according to Monsen *et al*. (2013) using Equation 14.

$$X = \frac{2\,.\,(C2,tot - C2,liv)}{C1,tot\,.\,m1}\,.100\% \tag{13}$$

$$X = (C2,tot - C2,liv).\frac{MSiC}{MC} \tag{14}$$

Where:
C,tot and *C,liv* are total and free carbon, respectively. The mass of the sample tested is referred to as "m", and indices 1 and 2 define the sample before and after the reactivity test, respectively. *MSiC* and *MC* are the molecular mass of SiC and C, respectively.

Li (2018) presented a procedure to test reactivity of reducing materials using a thermogravimetric furnace associated with chemical analysis of silicon carbide. Details of the equipment and reactor used in the experiment can be seen in Figure 12.1. A perforated cap alumina crucible was used inside the reactor to divide the reactor into two sections. In this test of reactivity, 5 g of pellets (mixture of SiC and SiO_2) were used inside the alumina crucible and 3 g of the reducing material on the cap. The experiment was carried out under a constant flow of Ar gas (0.5 l min^{-1}) at a temperature of 1650 °C. The SiO conversion rate was calculated by the ratio of generated SiO to captured SiO, based on the amount of SiC produced. This was analyzed according to ISO 21068 (2008) and determined according to Monsen *et al.* (2013).

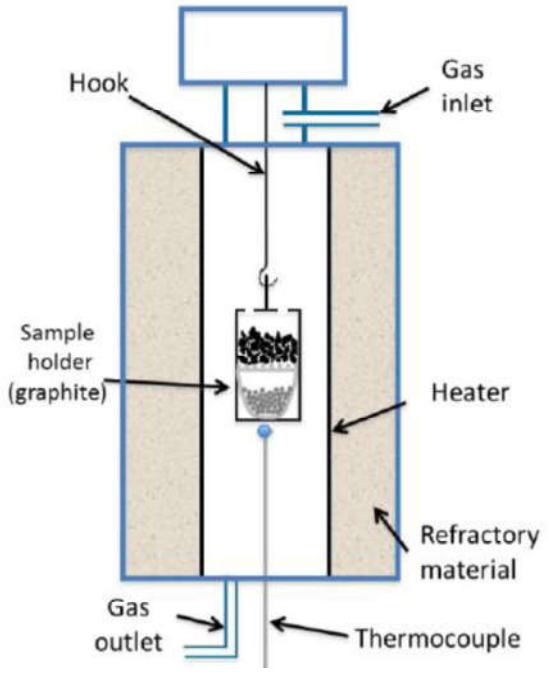

Figura 12 - Schematic diagram of the thermogravimetric furnace used by Li (2017). The gray materials at the base of the reaction crucible are SiO_2 + SiC pellets, while in the upper part, they are particles of the reducing material.

In determining the reactivity of the reducing material by means of the SiC chemical analysis, only a furnace is required for sample heating. Another point that can be considered is the use of simple equipment without scale, in order to reduce the cost of the analysis.

1.5. CONSIDERATIONS

The use of charcoal as a reducing material is a sole opportunity for Brazilian silicon production, since the concept of charcoal corresponds to a renewable coal mine. Therefore, the development of studies regarding charcoal characterization and selection for use in silicon production, technical-environmental improvements of the biomass to charcoal conversion process and the performance of industrial silicon furnaces using different kinds of charcoal are indispensable.

The reactivity towards SiO gas is an important parameter to measure the influence of a reduction material on the silicon recovery in the silicon production process. However, it is emphasized that, despite the development of different methods for testing this reactivity, such procedures are still very expensive to perform. In this sense, the development of a simpler and more economical method to test reactivity is desirable.

1.6. REFERENCES

ADISTY, D. **Kinetic study of SiO_2 + SiC reaction in silicon production**. 2013. 118 (Ph.D.). Department of Materials Science and Engineering, Norwegian University of Science and Technology

ANDRESEN, B. **Process model for carbothermic production of silicon metal**. 1995. 256 (Ph.D). Metallurgisk Institutt, Norwegian University of Science and Technology, Trondheim.

ANDRESEN, B. Operational Aspects of the Metallurgical Silicon Process. Silicon for the Chemical and Solar Industry XIII, 2016, Kristiansand, Norway. p.63-74.

ASADULLAH, M. et al. Effects of biomass char structure on its gasification reactivity. **Bioresource Technology,** v. 101, p. 7935–7943, 2010.

ASSIS, M. R. et al. Factors affecting the mechanics of carbonized wood: literature review. **Wood Sci Technol,** v. 50, p. 519-536, 2016.

BARROS, N. F. D.; NOVAIS, R. F. D. **Relationship Soil-*Eucalyptus***. Viçosa: 1990.

BRAND, M. A. Forest biomass energy. Joinvile, Brazil: 131 p. 2010.

BEN. **Brazilian Energy Balance**. ENERGY, M. O. M. A. Rio de Janeiro: 296 p. 2017.

BUØ, T. V.; GRAY, R. J.; PATALSKY, R. M. Reactivity and petrography of cokes for ferrosilicon and silicon production. **International Journal of Coal Geology,** v. 43, n. 1-4, 243-256, 2000.

CARDOSO, M. T. **Drying of logs using combustion gases of a kiln-furnace system**. 2015. 76 (Ph.D). Forest Engineering, Federal University of Viçosa, Viçosa.

CARNEIRO, A. D. C. O. et al. Potential energy of *Eucalyptus sp*. wood according to age and different genetic materials. **Revista Árvore,** v. 38, n. 2, p. 375-381, 2014.

COSTA, A. C. S. et al. Properties of heartwood and sapwood of *Eucalyptus camaldulensis*. **Brazilian Journal of Wood Science,** v. 8, n. 1, p. 10-20, 2017.

COUTO, A. M. et al. Quality of charcoal from Corymbia and *Eucalyptus* produced at different final carbonization temperatures. **Scientia Forestalis,** v. 43, n. 108, p. 817-831, 2015.

DAMÁSIO, R. A. P. et al. Thermal profile and control of carbonization on circular kiln through the internal temperature. **Brazilian Journal of Wood Science,** v. 6, n. 1, p. 11-22, 2015.

DONATO, D. B. **Development and evaluation of a furnace for the combustion of wood carbonization gases**. 2018. 100 (Ph.D). Forest Engineering, Federal University of Viçosa, Viçosa.

FAO. **The charcoal transition: greening the charcoal value chain to mitigate climate change and improve local livelihoods**. Rome, p.184. 2017

GALVÃO, A. P. M.; JANKOWSKY, I. **Proper wood drying** São Paulo: 1985. 112.

GŁADYSZ, J.; KARBOWNICZEK, M. Carbon reducers for the processes of ferroalloy production in the electric furnace. European Electric Steelmaking Conference, 2008, Krakow, Poland. p.30-59.

GRISCHENKO, S. G. et al. Production of special kinds of carbonaceous reducing agents for ferroalloy smelting. The thirteenth International Ferroalloys Congress, 2013, Almaty, Kazakhstan. june 9-13. p.505-510.

HAYKIRI-ACMA, H.; YAMAN, S.; KUCUKBAYRAK, S. Comparison of the thermal reactivities of isolated lignin and holocellulose during pyrolysis. **Fuel Processing Technology,** v. 91, n. 7, p. 759-764, 2010.

IBÁ. **Brazilian Tree Industry**. Pöyry Consultoria em Gestão e Negócios Ltda. Brasília, p.80. 2017

KAN, T.; STREZOV, V.; EVANS, T. J. Lignocellulosic biomass pyrolysis: A review of product properties and effects of pyrolysis parameters. **Renewable and Sustainable Energy Reviews,** v. 57, p. 1126-1140, 2016. ISSN 1364-0321.

KOZHEVNIKOV, G. N.; VODOPYANOV, A. G.; NEFEDOV, P. Y. Russian Metallurgy. In: (Ed.). **Influence of oxides in the ash on the reaction between carbon and silicon monoxide**. Moscow, Russian, 1972.

KRUGER, P. V. **Ferroalloy production chain in Brazil**. J Mendo Consultoria Belo Horizonte, p.112. 2009

KUMAR, M.; GUPTA, R. C.; SHARMA, T. Effects of carbonisation conditions on the yield and chemical composition of *Acacia* and *Eucalyptus* wood chars. **Biomass and Bioenergy,** v. 3, n. 6, p. 411-417, 1992. ISSN 0961-9534/9.

LI, F. **SiC production using SiO_2 and C agglomerates**. 2018. 217 Thesis (Ph.D). Materials Science and Engineering, Norwegian University of Science and Technology, Trondheim, Norway.

LINDSTAD, T. et al. Improved sintef sio-reactivity test. INFACON XI

2007, New Dehli, India. February 18-21

LUND, B. F. et al. Sensitivity analysis of a dynamic model for submerged arc silicon furnaces. INFACON X, 2004, Cape Town, South Africa. February 1-4. p.1-10.

MANABE, T. et al. Effect of Carbonization Temperature on the Physicochemical Structure of Wood Charcoal. **Transactions of the Materials Research Society of Japan,** v. 32, p. 1035-1038, 2007.

MITRAŠINOVIĆ, A. M.; UTIGARD, T. A. Refining silicon for solar cell application by copper alloying. **Silicon,** v. 1, p. 239-248, 2009.

MONSEN, B. et al. The use of biocarbon in norwegian ferroalloy production. INFACON IX, 2000, Quebec City, Canada. June 3-6

MONSEN, B. et al. Possible use of natural gas for silicon or ferrosilicon production. Thirteenth international ferroalloys congress, 2013, Almaty, Kazakhstan. p.467-478.

MONSEN, B. E. **Carbon materials: Fundamentals and measurement of SiO reactivity.** Silicon Seminar. Trondheim, Norway 2015.

MORELLO, T. F. **Charcoal based iron and steelmaking: from primitive technological model to solution for a post-Kyoto world**. 2009. 171 (M.Sc.). Economics, Administration and Accounting, USP, São Paulo.

MYRHAUG, E. H. **Non-fossil reduction materials in the silicon process - properties and behaviour**. 2003. 242 (Ph.D). Department of Materials Technology, Norwegian University of Science and Technology, Trondheim.

MYRHAUG, E. H.; TUSET, J. K.; TVEIT, H. Reaction mechanisms of charcoal and coke in the silicon process. INFACON X, 2004, Cape Town, South Africa. 1-4 February. p.108-121.

MYRVÅGNES, V. **Analyses and characterization of fossil carbonaceous materials for silicon production**. 2008. 248 (Ph.D.). Department of Materials Science and Engineering, Norwegian University of Science and Technology

MYRVÅGNES, V.; LINDSTAD, T. The importance of coal and coke properties in the production of high silicon alloys. INFACON XI, 2007, New Delhi, India. 18-21 February. p.402-413.

NOCENTINI, C. et al. Nature and reactivity of charcoal produced and added to soil during wildfire are particle-size dependent. **Organic Geochemistry,** v. 41, n. 7, p. 682-689, 2010.

NOUMIA, S. et al. Upgrading of carbon-based reductants from biomass pyrolysis underpressure. **Journal of Analytical and Applied Pyrolysis,** v. 118, p. 278-285, 2016.

OLIVEIRA, A. C. et al. Artificial cooling in rectangular kilns for charcoal production. **Revista Árvore,** v. 39, n. 4, p. 770-778, 2015.

OLIVEIRA, A. C. et al. Quality parameters of *Eucalyptus pellita* F. Muell. mood and charcoal. **Scientia Forestalis,** v. 38, n. 87, p. 431-439, 2010.

PANSHIN, A. J.; ZEEUW, C. D. **Textbook of wood technology**. New York: 1980. 722.

PAULL, J. M.; SEE, J. B. The interaction of silicon monoxide gas with carbonaceous reducing agents. **Journal of the South African Institute of Mining and Metallurgy,** v. 78, n. 7, p. 35-41, 1978.

PENG, X. et al. Temperature- and duration-dependent rice straw-derived biochar: characteristics and its effects on soil properties of an Ultisol in southern China. **Soil & Tillage Research,** v. 112, n. 2, p. 159-166, 2011.

PEREIRA, B. L. C. et al. Influence of chemical composition of *Eucalyptus* wood on gravimetric yield and charcoal properties. **bioresources,** v. 8, n. 3, p. 4574-4592, 2013.

PEREIRA, B. L. C. et al. Study of thermal degradation of *Eucalyptus* wood by thermogravimetry and calorimetry. **Revista Árvore,** v. 37, n. 3, p. 567-576, 2013c. ISSN 0100-6762.

PEREIRA, B. L. C. et al. Quality of wood and charcoal from *Eucalyptus* clones for ironmaster use. **International Journal of Forestry Research,** v. 2012, p. 1-8, 2012.

PEREIRA, B. L. C. et al. Correlations among the heart/sapwood ratio of *Eucalyptus* wood, yield and charcoal properties. **Scientia Forestalis,** v. 41, n. 98, p. 217-225, 2013b.

PEREIRA, E. G. et al. Pyrolysis gases burners: Sustainability for integrated production of charcoal, heat and electricity. **Renewable and Sustainable Energy Reviews,** v. 75, p. 592-600, 2017.

PROTÁSIO, T. D. P. et al. **Influence of heating rate of carbonization on the charcoal properties of Acacia mangium**. II CBCTEM. Belo Horizonte 2015.

PROTÁSIO, T. D. P. et al. Quality and energetic evaluation of the charcoal made of babassu nut residues used in the steel industry. **Ciência e Agrotecnologia,** v. 38, p. 435-444, 2014. ISSN 1413-7054.

PROTÁSIO, T. D. P. et al. Canonical correlation analysis between characteristics of *Eucalyptus* wood and charcoal. **Scientia Forestalis,** v. 40, n. 95, p. 317-326, 2012.

RAAD, T. J.; PINHEIRO, P. C. D. C.; YOSHIDA, M. I. General equations of carbonization of *Eucalyptus spp* kinetic mechanisms. **CERNE,** v. 12, n. 2, p. 93-106, 2006. ISSN 0104-7760.

RAANESS, O.; GRAY, R. Coal in the production of silicon rich alloys. INFACON XII, 1995, Trondheim, Norway. 11-14 June. p.201-220.

RAANESS, O.; KOLBEINSEN, L.; BYBERG, J. A. Statistical Analysis of Properties for coals used in the production of silicon rich alloys. INFACON VIII

1998, Beijing, China. June 7-10

RAMOS, D. C. et al. Quality of wood and charcoal from *Eucalyptus* clones for use in silicon production. INFACON XV, 2018, Cape Town. 25-28 February p.200-214.

RAMOS, D. C. et al. **Evaluation of charcoal resistance based on the diameter of charcoal lumps**. Simpósio de Integração Acadêmica SIA UFV. Viçosa 2015.

REIS, A. A. D. et al. Wood composition and charcoal of *Eucalyptus urophylla* in different planting locations. **Brazilian Journal of Foresty Research,** v. 32, n. 71, p. 277-290, 2012.

REZENDE, J. B.; SANTOS, A. C. D. **The charcoal production chain in Minas Gerais: critical points and potentialities**. EPAMIG. Viçosa**:** 80 p. 2010.

ROMERO, F. J. N.; REINOSOA, F. R.; DÍEZB, M. A. Influence of the carbon material on the synthesis of silicon carbide. **Carbon,** v. 37, p. 1771-1778, 1999.

ROUSSET, P. et al. Pressure effect on the quality of *Eucalyptus* wood charcoal for the steel industry: A

statistical analysis approach. **Fuel Processing Technology,** v. 92, n. 10, p. 1890–1897, 2011.

SANTOS, R. C. D. et al. Correlation of quality parameters of wood and charcoal of clones of *Eucalyptus*. **Scientia Forestalis,** v. 39, n. 90, p. 221-230, 2011.

SCHEI, A.; TUSET, J. K.; TVEIT, H. **Production of High Silicon Alloys**. Trondheim, Norway: 1998.

SIEBENEICHLER, E. A. et al. Influence of temperature and heating rates on mechanical resistance, density and yield of the wood charcoal of *Eucalyptus cloeziana*. **Brazilian Journal of Wood Science,** v. 8, n. 2, p. 82-94, 2017.

SILVEIRA, R. C. D.; CARMA, W. F. D.; NETO, M. V. B. Technical analysis of charcoal to use in the ferroalloy industry in Brazil. INFACON 86, 1986, Rio de Janeiro, Brazil. September 31. p.481-500.

SOARES, V. C. et al. Properties of eucalyptus wood hybrids and charcoal at three ages. **CERNE,** v. 21, n. 2, p. 191-197, 2015.

SZEKELY, J.; EVANS, J. W.; SOHN, H. Y. **Gas-Solid Reactions**. New York: 1976.

TANGSTAD, M. **Metal Production in Norway**. Trondheim: Akademika forlag, 2013. 240.

TANGSTAD, M. et al. Small scale laboratory experiments simulating an industrial silicon furnace. The Twelfth International Ferroalloys Congress, 2010, Helsinki, Finland. 6-9 June p.661-670.

TITILADUNAYO, I. F.; MCDONALD, A. G.; FAPETU, O. P. Effect of temperature on biochar product yield from selected lignocellulosic biomass in a pyrolysis process. **Waste Biomass Valor,** v. 3, p. 311-318, 2012.

TRUGILHO, P. F. et al. Evaluation of *Eucalyptus* clones for charcoal production. **CERNE,** v. 7, n. 2, p. 104-114, 2011.

TUSET, J. K.; RAANESS, O. Reactivity of reduction materials in the production of silicon, silicon-rich ferroalloys and silicon carbide. 34th Electric Furnace Conference, 1976, St.Louis. December 7-10

VANEGAS, J. D. B. et al. Thermal inertia effects of the structural elements in heat losses during the charcoal production in brick kilns. **Fuel,** v. 226, p. 508-515, 2018.

VIDEM, T. Reaction rate of reduction materials for the (ferro)silicon process. INFACON VII, 1995, Trondheim, Norway. June 11-14. p.221-230.

VILELA, A. D. O. et al. A new technology for the combined production of charcoal and electricity through cogeneration. **Biomass and Energy,** v. 69, p. 222-240, 2014.

VOROB'EV, V. P. Carborundum-bearing reducing agents in high-silicon alloy production. **Steel in Translation,** v. 47, n. 10, p. 688-690, 2017.

WANG, L. et al. Study of CO_2 gasification reactivity of biocarbon produced at different conditions **Energy Procedia,** v. 142, p. 991-996, 2017.

YIP, K. et al. Biochar as a fuel: 3. mechanistic understanding on biochar thermal annealing at mild temperatures and its effect on biochar reactivity. **Energy Fuels,** v. 25, p. 406-414, 2010.

CHAPTER II

2. REACTIVITY ASSESSMENT OF CHARCOAL FOR USE IN SILICON PRODUCTION

Abstract – Silicon metal as a commodity material is produced by carbothermic reduction of quartz in electric submerged arc furnaces, where CO_2 forms as a by-product. Replacing the use of fossil reductants with charcoal has a great potential with respect to the reduction of CO_2 emissions and to the contribution from this industry to the increasing greenhouse gas effect. Nevertheless, charcoals can be produced from different raw materials and under various process conditions, and have different properties influencing further applications. As charcoal is used in the silicon process, reactivity towards SiO is one of the most important properties that has strong effects on silicon recovery. The purpose of this study was defining a procedure to express the SiO reactivity in a simpler and more cost-efficient manner and indicate one or more clones of *Eucalyptus* with the greatest potential for production of charcoal to silicon use. In addition, the SiO-reactivity of metallurgical coke was also carried out for comparison purpose. The SiO-reactivity was conducted using agglomerates made of quartz and silicon carbide (SiC) mixtures and carbon material which have been heated in an electric tube vertical furnace at 1650 °C in an inert atmosphere for 120 minutes. Charcoal before and after SiO reactivity test were studied using the SEM photomicrograph to trace the gas diffusion paths of SiO gas and the formation of silicon carbide. It was found that there is wood variability between the clones evaluated and strong correlations among wood and charcoal properties. All charcoals had significantly higher SiO-reactivity than coke. In addition, an increasing trend of charcoal SiO-reactivity was found with a reducing of apparent density and fiber wall area of charcoal, these indices are connected to pore development in charcoal. The charcoal from the clone 3 stood out concerning charcoal production for silicon use, since it showed better results for SiO reactivity and readily available fixed carbon stock in charcoal. The developed procedure used for SiO reactivity measurements was a useful tool to classify charcoal for use in the silicon production process.

Keywords: SiO-reactivity; biocarbon; *Eucalyptus* clone

2.1. INTRODUCTION

Brazil is one of the countries with the highest potential for biomass production and use. It is the world's leading producer of charcoal for industrial purposes, with charcoal mainly stemming from *Eucalyptus* planted tree. In 2016, charcoal consumption reached 4.5 million tons, of which approximately 84% were derived from planted trees (Ibá, 2017). Around 11% of the consumption was directed towards ferroalloy and silicon production (Ben, 2017). In Brazil, charcoal is mainly used as a reductant in the silicon production. In other countries charcoal is also used, but to a lesser degree. Other silicon producers use mainly coal.

The use of charcoal in the metallurgical industry presents some advantages compared to fossil reductants. Charcoal has a high reactivity, a high porosity, a high resistivity and a low percentage of ash (e.g. sulphur and phosphorus). Additionally, compared to coal, the use of charcoal radically reduces SO_2 emissions, and allows to reduce the environmental impact of CO_2, a decisive movement in the Paris Agreement context (Unfccc, 2015). On the other hand, charcoal has much lower mechanical strength compared to coal, which might be challenging for some metal production processes. It is worth mentioning that the silicon production process involves low-shaft furnaces which imply moderate requirements on the charge in terms of mechanical strength (Silveira *et al.*, 1986; Grischenko *et al.*, 2013).

Elemental silicon is produced industrially by the reduction of quartzite with carbonaceous materials (coal, and charcoal) in an electric arc furnace following $SiO_2(s) + 2C(s) \longrightarrow Si(l) + 2CO(g)$. The use of charcoal as a reductant is well established in Brazil, but the assessment of its properties, especially for the silicon production process, has rarely been reported. Charcoals produced from different woods and under various conditions exhibit different properties, which can affect metallurgical processes.

Reactivity towards SiO is one of the most important process parameter to evaluate carbon materials for silicon production (Myrvågnes e Lindstad, 2007). In the silicon production process, the carbon reductant reacts with the SiO gas in the outer zone of the furnace to produce silicon carbide and carbon monoxide following $SiO\ (g) + 2\ C\ (s) \longrightarrow SiC\ (s) + CO\ (g)$. This reaction is essential to minimize the loss of silicon, in the form of

SiO, and thereby increase the silicon yield. A high SiO reactivity of the reduction materials leads to high silicon recovery, a good furnace operation and lower operating costs (Buø *et al.*, 2000; Myrvågnes, 2008). It is worth pointing out that the cost of reduction materials constitutes about 40% of the total material costs in the silicon production (Videm, 1995).

One of the most acknowledged tests to evaluate the reactivity of reductant materials towards SiO gas is the SINTEF SiO reactivity test, first mentioned by Tuset e Raaness (1976) and later improved by Lindstad *et al.* (2007). The principle of this method is to simulate the reaction between the carbon materials and the gas flow in the furnace. A gas mixture of SiO and CO, generated by the reaction between SiO_2 and SiC, is carried by argon through a carbonaceous packed bed. The carbon materials react with the SiO-gas and the composition of the effluent gas is continuously monitored. The SINTEF SiO reactivity test is an expensive technique. However, it is very robust and its reliability has been studied extensively. For the aim of this study, a simpler and more economical test was desirable. As a result, a simpler method was developed based on the SINTEF test procedure. Additionally, the properties of wood and charcoal and the effect of charcoal properties on SiO reactivity were evaluated.

2.2. EXPERIMENTAL SETUP AND METHODS

2.2.1. Raw material: sampling and characterization

Three short-rotation forestry, clones of *Eucalyptus urophylla* vs *grandis* hybrid, named as CL-1, CL-2 and CL-3, were used for the study. Samples of 7-year old wood were collected from a Brazilian forestry company located in State of Minas Gerais. These materials were selected due to the variation of their densities. Logs with diameters from 60 to 140 mm were selected and sawn in approximately 1.0 m height for carbonization. Six logs, representative of diameter variation, were sawn into 50-mm thick discs, then divided in four to be used in chemical, physical and anatomical analyses.

Measurements of anatomical characteristics were made in the Laboratório de Painéis e Energia da Madeira (LAPEM) and Laboratório de Propriedades Físicas e Mecânicas da Madeira (LPM) at the Universidade Federal de Viçosa (MG), Brazil, following the standard presented by Iawa (1989) and recommendations of Foelkel *et al.* (1975). The number of replications used to determine the dimensions of each anatomical characteristic is shown in Table 2.1. The percentage of vessels was also determined. The wood basic density was determined according to NBR 11941 (Brazilian Association of Technical Standards, 2003). Measurements of the heartwood and sapwood were done, according to the methodology described by Pereira *et al.* (2013b)

Table 2.1 - Parameters used in the anatomical properties' tests of *Eucalyptus* spp.

Anatomical characteristics	Measure site	Number of replications
Fiber length (L) (mm)	macerated	18
Fiber diameter or fiber width (D or W) (µm)	macerated	18
Fiber lumen diameter (d) (µm)	macerated	18
Fiber wall thickness (e) (µm)	macerated	18
Fiber slenderness ratio (L/D) (dimensionless)	macerated	18
Wall fraction (D - d/D) (dimensionless)	macerated	18
heartwood/sapwood (dimensionless)	wood disc	15
Vessels or pores frequence/mm²	Transverse sections	90
Vessel or pores transverse diameter (µm)	Transverse sections	90
Vessel percentage (%)	Transverse sections	90

2.2.2. Charcoal preparation and sampling

The charcoal produced from each clone and one type of mettalurgical coke were used in this study. The coke was investigated as a comparison purpose. The charcoal was produced using a laboratory kiln built of refractory bricks, with a diameter of 1.2 m and height 1.1 m, with 1.04 m^3 of usable volume. A volume of 0.6 m^3 of logs were loaded into the kiln for pyrolysis. Internal heating was used to initiate pyrolysis and maintain temperatures during the process. The temperature was monitored by five thermocouples, one inserted at the dome of the kiln and the others in the wall. The temperature control of the carbonization process was according to a pre-set theoretical tracks (Table 2.2). The peak temperature of carbonization process was about 380 °C. This temperature was used to maximizing charcoal yield.

Table 2.2 - Theoretical tracks temperature for carbonization control in laboratory kiln to be measured at dome of kiln.

Steps	Temperature Range	Heating time
1	25-200 °C	16-18 h
2	200-290 °C	12-13 h
3	290-380 °C	7-8 h
4	380 °C	7-8 h

After carbonization, the charcoal was unloaded from the kiln, homogenized and quartered, based on standard NBR 6923 (Brazilian Association of Technical Standards, 1981). Thereafter, a volume of 30 Liter charcoal from each clone was sampling to analyse charcoal properties.

2.2.3. Charcoal properties

Proximate analysis of produced charcoals was performed according to procedures described in ASTM standard D1762 (American Society for Testing and Materials, 1984). The quantification of the carbon (C), hydrogen (H) and nitrogen (N) relative to the charcoal dry mass was performed according to the standard SS-EN ISO 16948 (European Standard, 2015). Sulfur (S) was measured according to SS-EN ISO 16994 (European Standard, 2016). The oxygen content was determined by difference, i.e., by disregarding

the contents of carbon, hydrogen, nitrogen, sulfur and ash. The concentrations of inorganic elements in the produced charcoal were measured by means of an inductively coupled plasma optical emission spectrometry (ICP-OES) according to the standard CEN/TS 15290 (European Committee for Standardization, 2006). The silicon content was determined by the X-ray fluorescence technique (XRF).

The apparent density (AD) was determined by the hydrostatic method, in which the samples were immersed in mercury (Vital, 1984). Therefore, it was possible to obtain the fixed carbon stock (FCS), expressed in units of (kg m^{-3}), by the product of the apparent density and the fixed carbon content of charcoal.

The absolute density was determined by gas displacement technique using an AccuPyc 1330 Helium Pycnometer, according to the standard ISO 12154 (International Organization for Standardization, 2014). The porosity of material was obtained by the following equation:

$$Porosity = \left[1 - \left(\frac{apparent\ density}{absolute\ density}\right)\right] x\ 100\% \quad (1)$$

The pore structure of the samples was characterized by nitrogen adsorption/desorption at -196 °C. The Brunauere-Emmete-Teller (BET) method, described in DIN 66131 (Germany Committee for Stardardization, 1993), was used to determine the BET specific surface area (S_{BET}) using an automated gas adsorption analyzer (The TriSTAR 3000, Micromeritics). Prior to BET, 0.4 g of each sample, particle size of 500-200 μm, was vacuum degassed for 12 h at 250 °C in the built-in degas port of the instrument.

Surface morphology of the chars was investigated by field-emission scanning electron microscopy (LVFESEM, Zeiss Supra 55VP). The samples were investigated before and after the SiO reactivity tests. The samples after SiO reactivity test were embedded in epoxy resin, ground and polished, in order to study the carbonaceous structures compared to silicon carbide formation and structure. Twelve samples from each clone were randomly collected from the kiln. The transversal section of charcoal samples were previously sanded for better visualization of the charcoal microstructure and the images were obtained using a magnifying glass coupled to an image acquisition system

and were measured by software *Axio Vision* 4.3. To calculate the fiber wall area on charcoal (FWA%) the SEM photomicrograph from transversal section of charcoal samples was used. The (FWA%) was calculated by the difference between fiber lumen area and fiber area selected on the SEM image. The software *solution DT* was used to measure the images.

The friability (denoted F, expressed in %) also called "impact strength" indicates the extent of breakage that will occur during loading, transportation and screening of reductant material. In this study, the drum test was used to determine the index or degree of friability of the charcoal and coke. The samples were crushed and screened to the fraction +18-22 mm to use in the drum test. The procedure was performed according to Noumia *et al.* (2016).

2.2.4. SiO reactivity apparatus and procedures

Charcoal samples were calcined in an induction furnace to remove volatile matter, prior to SiO reactivity tests at 1200 °C for 20 min. Thereafter the samples were crushed and screened to the fraction of +2-4.5 mm to be used in the SiO reactivity test. The SiO reactivity test was performed in an electric tube vertical furnace, using a graphite crucible as shown in Figure 2.1.

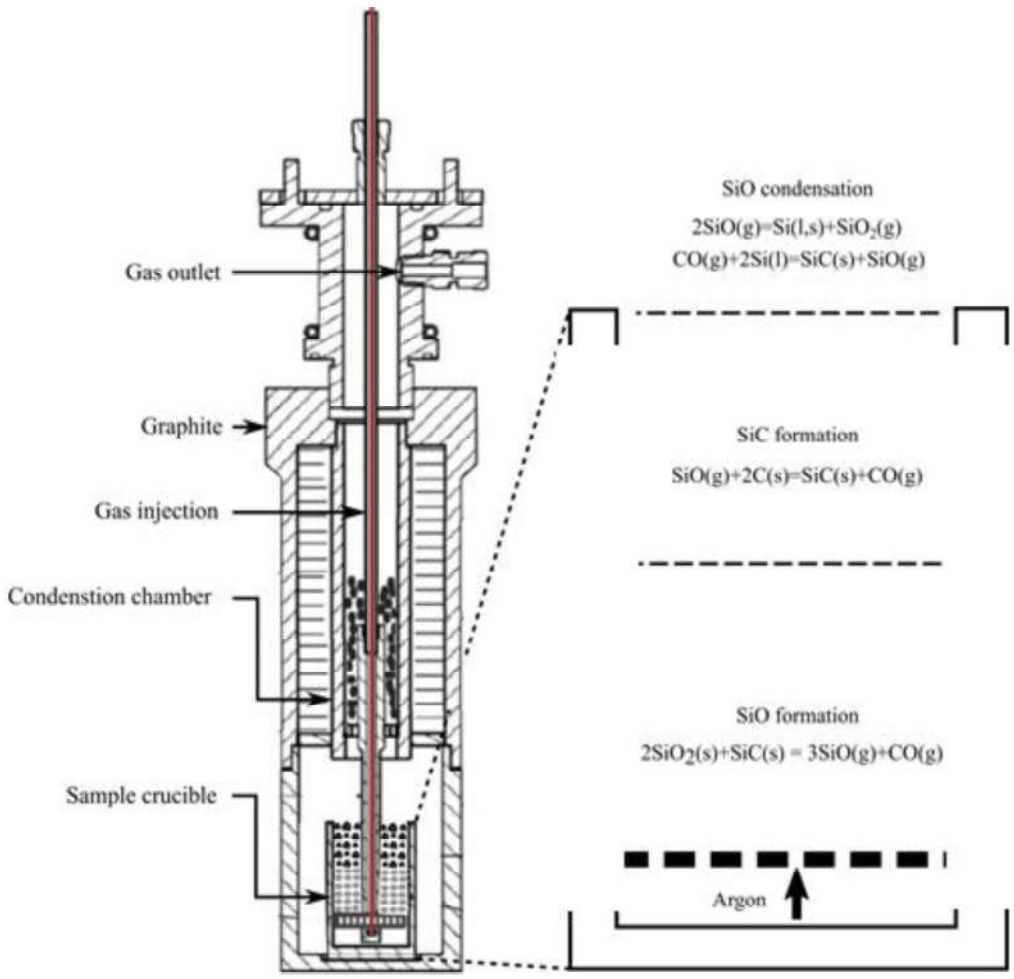

Figure 2.1 - Schematic diagram of graphite crucible used in experimental setup for SiO reactivity test (Drawings by P.Tetlie at SINTEF). In the sample crucible, the grey part is SiO_2+SiC and the black is charcoal.

The SiO reactivity test was carried out with use of pellets made by mixing SiC+SiO_2 powders (the mole ratio of 1:2 respectively) to generate SiO-gas, which will react with the charcoal above it. Both materials were loaded in the sample crucible, with dimension of 32 mm in diameter and 60 mm in height. The internal surfaces of the sample crucible were lined with SiC coating to protect the graphite from reacting with SiO gas. The sample crucible was placed inside the reaction chamber (Figure 1). In the experiment 15 g of pellets and 15 mL of lump charcoals were loaded, corresponding to a carbonaceous packed bed 20 mm high. This set-up was defined by the stoichiometric analysis of the pellets reaction and mass of carbon used to reach SiO-gas levels which do

not restrict conversion rate of the carbon materials. For coke, the reductant used for comparison purpose, the test was fixed by mass (3g) to avoid restrictions in conversion. In addition, SiC particles were placed in the condensation chamber above the crucible to capture unreacted SiO-gas.

The loaded crucible was heated up to 1650 °C at a constant heating rate of 30°C min^{-1}, under a constant flow of argon (0.4 l min^{-1}). Argon was used as a carrier gas, transporting SiO generated from the pellets through the packed bed of carbonaceous material. The temperature of 1650 °C and the argon gas flow through the furnace were maintained for 2 hours. The experiment was then cooled down to room temperature. The gas analyzer ABB2020 was connected to the off-gas lance to detect the concentration of CO gas. The %CO change and temperature were recorded in the logging program where values were registered automatically every 5 seconds. The weight of charcoal, pellets and the set-up crucible were measured before and after the tests.

The number of reactivity, based on the SiO reactivity test, were calculated in five different protocols: based on the profile of CO% versus time, referred to as Diego-Ramos (*DR)* and calculated according to Eq. (*1*); degree of conversion (*X1*), (*X2*) and (*X3*) according to Tuset e Raaness (1976), Myrhaug (2003) and Monsen *et al.* (2013) expressed in the form of Eq. (*2*), Eq. (*3*) and Eq. (*4*) respectively; and, lastly, the degree of conversion (*X4*) was determined based on Si content investigated by X-ray fluorescence technique (XRF) according to Eq. (5). The formulas are given below:

$$DR = \frac{\left(\sum_{7,6}^{10,8} f(\%co)\ .\ \Delta t\right)}{m1\ .\ C1,free} \tag{1}$$

$$X1(\%) = (m2 - m1)/m1 \tag{2}$$

$$X2(\%) = (m2 - m1)/m1\ .\ C1,free\ (\frac{MSiC - 2MC}{2MC}) \tag{3}$$

$$X3(\%) = (C2,total - C2,free)\ .(\ MSiC/MC) \tag{4}$$

$$X4(\%) = \%Si\,.\,(MSiC/MSi) \quad (5)$$

Where: "m" is mass of sample, 1 and 2 refer to before and after the test, respectively. "C" is carbon content in %, 1 and 2 refer to before and after. The %Si was found by X-ray fluorescence (*XRF*) analysis; M_{SiC}, M_C and M_{Si} are molar mass of SiC, C and Si respectively.

The chemical analysis of total carbon and free carbon were conducted according to ISO 21068:2008 using the Eltra CS-2000 and the Leco R RC-612 instruments respectively. Measurement uncertainly specified with 95pct confidence intervals are for C: 0.3%, free C: 0.1%, and Si: 0.4%. Due to temperatures used in the experiment, the Si content found by *XRF* was assumed to correspond to SiC.

The *DR* was evaluated by performing a numerical integration of %CO from (10.8%) defined as the starting point, to (7.6%) designated as the end point. The starting point was the common carbon monoxide peak reached in all experiments soon after reaching the temperature of 1650 °C. The end point was defined according to the reaction rate of the pellets. The latter was found in preliminary experiments using only pellets in the same experimental setup. The equation designed to express DR parameter is divided by the mass fraction of free carbon loaded in the sample, since the test was performed at constant volume of reducing material. A high value of *DR* is related to high CO generation from the carbon reaction which indicates high SiO-reactivity of reductant material. It is worth mentioning that the SiO_2+SiC-pellets conversion, hence SiO gas generated, exhibited narrow variation in all experiments with a standard deviation of 3.5%.

In order to classify the charcoal with the greatest potential for silicon use, the parameter (ECS), a readily available fixed carbon stock in charcoal per weight, was created. The FCS is expressed in ($kg_{FC}\ kg^{-1}_{char}$); it was calculated using the important charcoal properties, such as apparent density, fixed carbon, friability and the degree of conversion (X) according to Eq. 6:

$$ECS = [FCS * (1 - F) * X]/AD \quad (6)$$

Where: *FCS* (kg m^{-3}) is the fixed carbon stock in charcoal; *F* (%) is the friability; *X* (%) is the degree of conversion of C to SiC according to the experiment's conditions used and

AD (kg m^3) is the apparent density of charcoal. The friability value was defined as losses in carbon stock.

2.2.5. Statistical analysis

Reductant materials properties were evaluated according to a randomized design with 4 treatments (three charcoal and one coke). Data were subjected to analysis of variance, and, when significant differences were established, treatments were compared through the Tukey test at 5% probability.

The experimental reactivity test was conducted according to a factorial design of 4x4 - four reactivity protocols and four reductant material - with two replicates (two-sample) totaling 32 sampling units. Additionaly, the *DR* reactivity protocol, which is expressed based on gas analysis, was evaluated singly.

2.3. RESULTS AND DISCUSSIONS

2.3.1. Wood characterization

As can be seen in Figure 2.2, the basic density of wood ranged from 459.8 to 559.2 kg m^{-3} between the evaluated clones. The clone CL-1 presented the highest average basic density of 559.2 kg m^{-3}, being 21.6% and 14.9% higher than the CL-3 and CL-2, respectively. The basic density should be considered one of the main criteria for selection of species and clones of *Eucalyptus* for charcoal production. The wood with high basic density usually is preferred, because the use of denser woods results in higher production of charcoal for a certain volume of wood loaded in the kiln (Pereira *et al.*, 2012; Carneiro *et al.*, 2014; Assis *et al.*, 2016). Moreover, denser woods produce a denser charcoal, thus it is expected to have higher mechanical strength (Assis *et al.*, 2016).

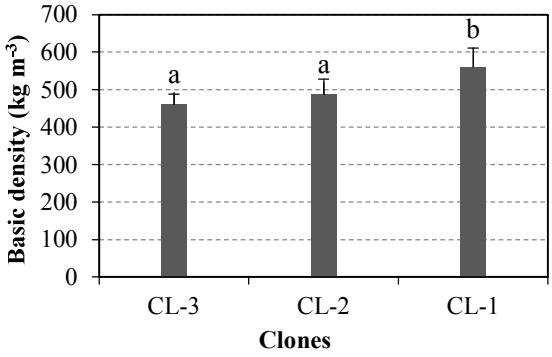

Figure 2.2 - Mean values of basic density of *Eucalyptus* spp. clones kg m^{-3}. The bars on top of column graph are the standard deviations. Number of samples (N = 36). Means followed by same letter do not differ at 95% probability by Tukey test.

The parameters that characterize the anatomical properties of *Eucalyptus* spp. wood are shown in Table 2.3. The diameter and frequency of vessels in wood ranged from 115 to 130 µm and 9.8 to 12.9 vessels mm^{-2}, respectively. The vessels were larger and had less frequency in CL-1 clone, while they were smaller and more frequent in CL-3. Despite the differences of the vessel's diameter and frequency between clones, the percentage of vessels in the wood showed a narrow variation, with an average of 16.1%. This result is similar to those cited by Palermo *et al.* (2015), who found the vessel's percentage of wood from *Eucalyptus grandis* from 15.8 to 17.2%.

Table 2.3 - Anatomic analysis of wood samples.

Anatomical characteristics	Clone		
	CL-3	CL-2	CL-1
Fiber length (L) (mm)	0.9 ±0.1	1.0 ±0.2	1.0 ±0.2
Fiber diameter or fiber width (D or W) (µm)	20.1 ±1.3	20.6 ±0.5	20.4 ±0.9
Fiber lumen diameter (d) (µm)	8.5 ±1.9	8.6 ±2.2	8.0 ±2.2
Fiber wall thickness (e) (µm)	5.7 ±1.1	6.0 ±1.1	6.2 ±1.3
Fiber slenderness ratio (L/D) (dimensionless)	49.1 ±2.0	49.9 ±4.5	49.9 ±3.8
Fiber wall fraction [(2.e)/D] .100 (%)	57.2 ±1.9	58.3 ±4.7	60.5 ±3.7
Heartwood/sapwood ratio (dimensionless)	0.4 ±0.2	0.4 ±0.2	0.6 ±0.3
Vessels/mm²	12.9 ±3.5	11.6 ±3.1	9.8 ±2.5
Vessel diameter (µm)	115.2 ±18	119.9 ±17.1	130.0 ±15
Vessel percentage	16.4 ±2.1	15.9 ±2.4	15.7 ±2.1

(±) Standard deviation.

The properties of fiber showed narrow variation between clones. Regarding heartwood/sapwood ratio (H/SW), it is observed that the clone CL-1 presented the highest H/SW ratio, with an average of 0.65, followed by CL-2 and CL-3, the latter two presenting values close to each other. In heartwood, the vessels are usually obstructed by tyloses, which reflects it low permeability (Silva *et al.*, 2010). In the initial stage of the carbonization process, the low permeability of heartwood makes it difficult to transport water from the inner part of the wood to the outer part. Under these conditions, the vapor pressure of the gases increases inside the anatomical elements, possibly rupturing the cells, which than leads to the formation of fissures in carbonized pieces with representative heartwood areas and a tendency to form fines when handling charcoal (Assis *et al.*, 2016; Costa *et al.*, 2017). According to Costa *et al.* (2017) low values of H/SW are suggested for charcoal production. It is worth mentioning that the H/SW ratio in the wood increases with the age of the tree. Thus, the only way to control the formation of heartwood is using younger trees, that is, reducing the cutting age (Assis *et al.*, 2016).

Table 2.4 shows the properties of vessels as a function of the clones and the regions of wood. The vessels, in the sapwood region, exhibited a larger diameter and lower frequency in comparison to heartwood. These results are similar to those cited by (Evangelista *et al.*, 2010; Ferreira, 2013; Costa *et al.*, 2017) who characterized the anatomical properties of hybrid genetic materials of *Eucalyptus*. This is attributed to

intrinsic characteristics of anatomical elements of juvenile wood, in central region of logs, and mature wood, close to the bark. It is known that the juvenile wood has a lower density, shorter fibers, thinner cell wall and more parenchyma in comparison to mature wood (Trugilho *et al.*, 1996).

Table 2.4 - Mean values of wood morphological analysis of vessels as a function of the clones and the regions of wood

Clone	Wood region	Vessel diameter (μm)	Vessels mm^{-2}
CL-3	Sapwood	123.7 ±14	11.8 ±2.8
CL-3	Heartwood	106.7 ±13	14.0 ±3.6
CL-2	Sapwood	131.1 ±14	9.3 ±2.4
CL-2	Heartwood	108.7 ±11	13.9 ±2.1
CL-1	Sapwood	135.6 ±6	8.9 ±1.4
CL-1	Heartwood	124.7 ±16	10.9 ±2.3

(±) Standard deviation.

2.3.2. Reductant material characterization

The parameters that characterize the chemical properties of charcoal and coke are showed in Table 2.5. The inorganic elements are listed in Table 2.6.

Table 2.5 - Proximate and elemental analysis of reductant material samples (dry basis, wt%) (N=12)

Sample	Elemental analysis (wt %)					Mass ratio	Proximate analysis (wt%)		
	C	H	S	N	O	O/C	VM*	FC*	Ash
CL-1	75.2	3.5 a	0.01 b	0.6 a	20.7 a	0.27 a	28.7 a	70.9 b	0.4± c
CL-2	75.5	3.2 a	0.01 b	0.7 a	20.2 a	0.27 a	28.1 a	71.3 b	0.7 bc
CL-3	76.4	3.4 a	0.01 b	0.6 a	19.6 a	0.26 a	28.9 a	70.6 b	0.6 b
COKE	95.0	1.7 b	0.30 a	0.6 a	2.4 b	0.02 b	4.2 b	89.0 a	6.9 a

VM*: volatile matter. FC*: fixed carbon. Means followed by same letter do not differ at 95% probability by Tukey test. N: Number of samples.

Table 2.6 - Ash composition of the reductant material samples (N=8)

Sample	Chemical composition of ash (wt%)										
	AlO_3	Fe_2O_3	CaO	MgO	P_2O_5	MnO	K_2O	Na_2O	TiO_2	S	SiO_2
CL-1	2.0	2.5	28.1	10.1	8.4	1.2	32.0	9.5	0.1	1.5	4.6
CL-2	0.4	0.7	22.7	11.3	7.9	1.2	47.8	4.9	0.0	1.1	2.0
CL-3	1.3	1.1	31.3	8.6	8.9	3.8	31.3	9.5	0.1	0.8	3.4
COKE	17.4	15.9	14.5	8.7	0.1	0.6	0.9	2.3	0.7	4.3	34.5

N: Number of samples.

The fixed carbon showed a narrow variation between charcoals, which is explained by homogeneous pyrolysis conditions. The coke had the highest FC, as was expected. The levels of volatile matter are inversely proportional to the FC. The ash content of charcoal was less than 1% in all materials, whereas it was 6.9% in coke. In silicon production, the ash content in the reductant material is a source of contamination, as it will be transferred to the silicon metal and will affect the silicon quality. Thus, high amount of ash will negatively reflect on the silicon refining processes' cost (Schei *et al.*, 1998). According to Monsen *et al.* (2000) in a pilot furnace experiment, the trace elements in the silicon products were 1% when using charcoal, while they were 4% using coke. The most important case is the production of high purity silicon, with the intention to enter the market for solar grade silicon, where the control of trace elements is strongly required. It is pointed out that the impurity level for some elements in silicon for solar cell applications, should not exceed the level of 1 ppmw (Mitrašinović e Utigard, 2009). The main disadvantage of using charcoal is the relatively high phosfor content.

As can be seen in Table 2.6, the dominant species are Ca and K in all of the charcoal samples, which are essential nutrients for plant growth (Fromm, 2010). In general, the CL-2 wood char presented the highest amount of K and the lowest amount of Ca compared to the others. Even though some inorganics elements could be of high importance with respect to catalytic effects, the contribution of these elements to changing SiO reactivity seems to be negligible for the charcoals studied.

Romero *et al.* (1999) evaluating the influence of type of coke on the synthesis of silicon carbide, stated that certain types and amounts of impurities in reductant materials can act as catalysts during SiC formation. They observed that metals of Group VIII (Fe and Ni) within cokes are especially effective agents for catalysis during SiC formation. Myrvågnes e Lindstad (2007) investigated the SiO reactivity in fossil reductants materials; they stated that the high amount of Si in the form of clastic quartz inclusions on carbonaceous material lead to an increase in SiO-reactivity. This was related to the significant reaction rate between quartz and the surrounding carbon above 1400 °C.

There is significant variability of apparent density and fixed carbon stock between charcoal Figure 2.3. The CL-3 charcoal exhibited the lowest apparent density (319.2 kg m^{-3}) and fixed carbon stock (232.6 kg m^{-3}), followed by CL-2 and CL-1, respectively.

These results can be attributed to the variability found for the basic density of wood. The clones that stood out with the highest basic density, also presented the highest values of apparent density and fixed carbon stock in charcoal. It is worth noting that basic density of wood and pyrolysis conditions are two factors that significantly affect the charcoal apparent density (Assis *et al.*, 2016; Kan *et al.*, 2016). The apparent density and fixed carbon of coke were 1024.5 and 911.8 kg m^{-3}, respectively, about 3 times higher than the average of charcoal, which is mainly related to intrinsic characteristics of parental coal (Sakurovs e Burke, 2011).

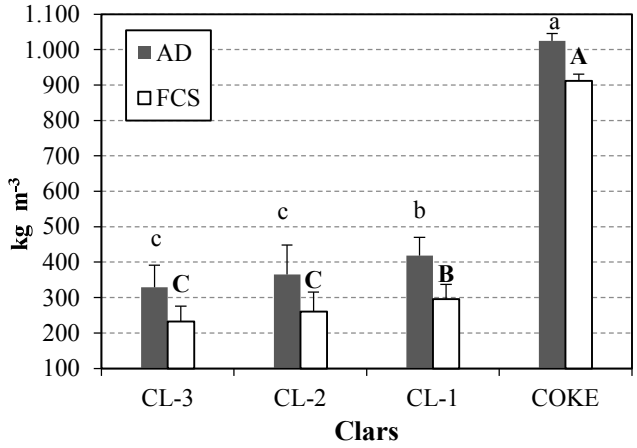

Figure 2.3 – Mean values of apparent density (AD) and fixed carbon stock (FCS) of reductant materials. The bars on top of column graph are the standard deviations. Number of samples (N = 12). Means followed by same letter do not differ at 95% probability by the Tukey test.

In regards to the microstructure of charcoal, independent of the *Eucalyptus* clones and the pyrolysis condition used, the wood structure kept its integrity as seen in Figure 2.4. In general, anatomical characteristics of wood, such as shape, arrangement and organization showed little or no alteration due to slow pyrolysis and the charcoal surface was well-defined. In addition, as seen in Figure 2.4, there is a fiber cell-wall thinning and the cell walls transform into a glazed and amorphous appearance with the carbonization. This was also observed by (Kwon *et al.*, 2009; Pereira *et al.*, 2016; Siebeneichler *et al.*, 2017).

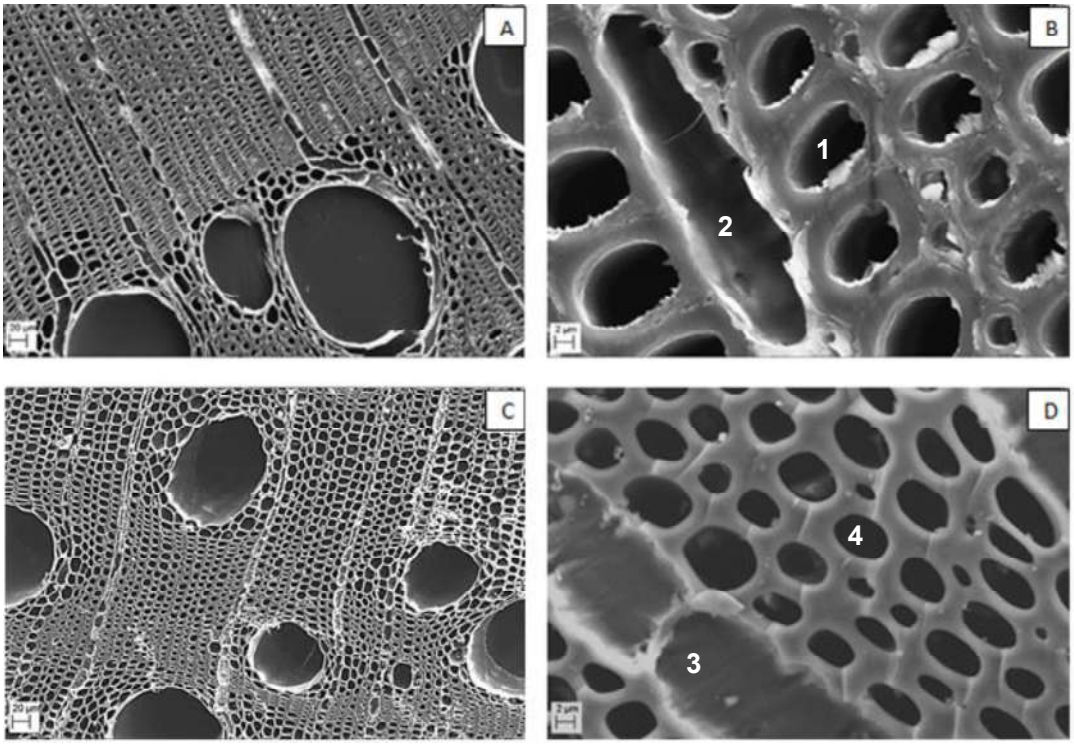

Figure 2.4 – Microphotography of the transversal section of CL-1 wood (A, B) and charcoal (C, D). Fibers (1), parenchyma cell (2), charred parenchyma cell (3), charred fibers (4).

Table 2.7 shows that the CL-1 and CL-3 wood char exhibited a vessel diameter average of 111.1 μm, it was 10.3% smaller compared to its parental wood. Although, the mean vessel diameter from clone CL-2 did not show reduction, this was not expected. This appears to be due to the position of the wood (sapwood or heartwood) from where the charcoal lumps were produced. Ferreira (2013), evaluating the morphology of vessels from kind of *Eucalyptus* at different regions of wood and its respective charcoals, observed that the charcoal retains the form and structure of the biomass from which it is produced. In this study the large vessels in the wood were related to larger vessels in charcoal.

Table 2.7 - Mean values of morphology of vessels and fibers of charcoal, transversal section. (N = 48)

Charcoal	Fiber wall area (%)	Vessel diameter (μm)	Vessels/mm²
CL-3	49.0 ±8.1 b	106.3 ±10.7 b	18.5 ±1.3 a
CL-2	50.2 ±5.8 b	123.8 ±8.6 a	14.9 ±2.4 b
CL-1	59.3 ±10 a	115.7 ±23 ab	18.2 ±4.5 a

Means followed by same letter do not differ at 95% probability by Tukey test. N: Number of samples.

The frequency of vessels on charcoal increased 50.3% in comparison to parental wood. Despite the vessels in charcoal being smaller in size than in wood, the high frequency of vessels will contribute to the higher porosity of charcoal. This is related to the retraction of wood when it is charred.

As observed in Table 2.7, the CL-1 wood char exhibited the highest fiber wall area (*FWA*), whereas the CL-2 and CL-3 showed a narrow variation. A strong positive correlation between fiber wall area and apparent density of charcoal was found. The values of fiber wall area are inversely proportional to the fiber lumen area (void area on charcoal), thus the reduction in fiber wall area will influence other properties that are connected to the porous matrix of charcoal.

The porosity of charcoals and coke is shown in Figure 2.5, the porosity ranging from 42.2% to 77.2%. The coke had the lowest porosity, at 43% lower than the average of the other charcoals. In addition, the high porosity and, hence, the low apparent density were related to higher friability of charcoal. This result was similar to that found by several authors, among them Noumia *et al.* (2016) and Siebeneichler *et al.* (2017).

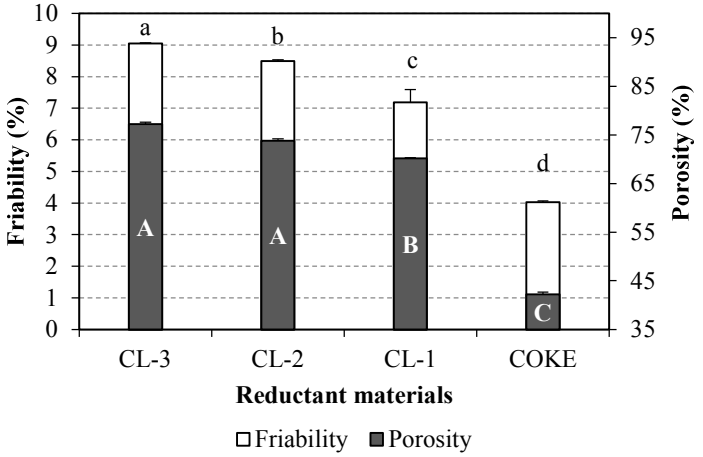

Figure 2.5 - Friability and porosity of Eucalyptus wood chars and coke. The bars on top of column graph are the standard deviations. Number of samples (N = 12). Means followed by same letter do not differ at 95% probability byTukey test.

The charcoal is classified as a friable material due to its low mechanical strength. The parameter friability gives an idea of the extend breakagede of charcoal when it is subjected to abrasion, friction or fall. As can be seen in Figure 2.5 the charcoal friability ranged from 7.1 to 9.1%. The CL-1 wood char exhibited the lowest friability between the charcoals, but still higher than coke. The high coke apparent density, and low porosity, explains, in part, its lower friability. According to the classification of the "Technical Center for Tropical Forest" cited by Silva *et al.* (2007), whatever the *Eucalyptus* clone used, all the charcoal obtained was hardly friable (i.e. mass loss in the form of fines was less than 10%).

The specific surface area (S_{BET}) of charcoal and coke is presented in Table 2.8, the charcoal S_{BET} ranging from 7.4 to 10.9 $m^2 g^{-1}$. The charcoal CL-3 exhibited the highest S_{BET}, at 34% higher than the others charcoal. Keeping in mind that all of the charcoal was obtained in same carbonization conditions, it is clear that the differences are related to the wood origins. Additionally, low values of S_{BET} on all of the charcoals tested have been found, which may be explained by low peak temperature of carbonization (380 °C), also by the presence of tyloses in charcoal microstructure which then blocks the diffusion of nitrogen. As reported by Mackay e Roberts (1982), the microporosity in lignocellulosic chars is established only near 500 °C. Additionally, Khalil (1999) stated that the very

narrow microporosity or the presence of constrictions in the micropore entrances on lignocellulosic materials restricted the activated diffusion of nitrogen.

Table 2.8 - Mean values of BET specific surface area of reductants materials (S_{BET})

Reductant material	Number of replications	BET specific surface area ($m^2\ g^{-1}$)
CL-3	3	10.9 ±0.4 b
CL-2	3	7.4 ±0.02 c
CL-1	3	7.5 ±0.02 c
COKE	3	14.6 ±0.3 a

Means followed by same letter do not differ at 95% probability by Tukey test.

Table 2.8 also shows that the S_{BET} of coke was much higher than those of charcoal tested. This may be attributed mainly to the chemical, physical and petrographic properties from its parental coal. It is worth mentioning that despite the largest S_{BET}, the coke had the lowest porosity.

2.3.3. Char SiO-reactivity

The SiO-reactivity tests were carried out on charcoals and a coke reductant as a reference. Figure 2.6 shows the mean curves (% CO vs. time) for all of the reductant materials. With a CL-3 charcoal, the CO content stays at a maximum value for a long time until it reaches the designated end point, followed by CL-2 and CL-1. On the other hand, with coke, the CO drop occurs in a short time. High CO levels translates into a higher conversion of carbon to SiC, according to SiO (g) + 2C (s) = SiC (s) + CO (g).

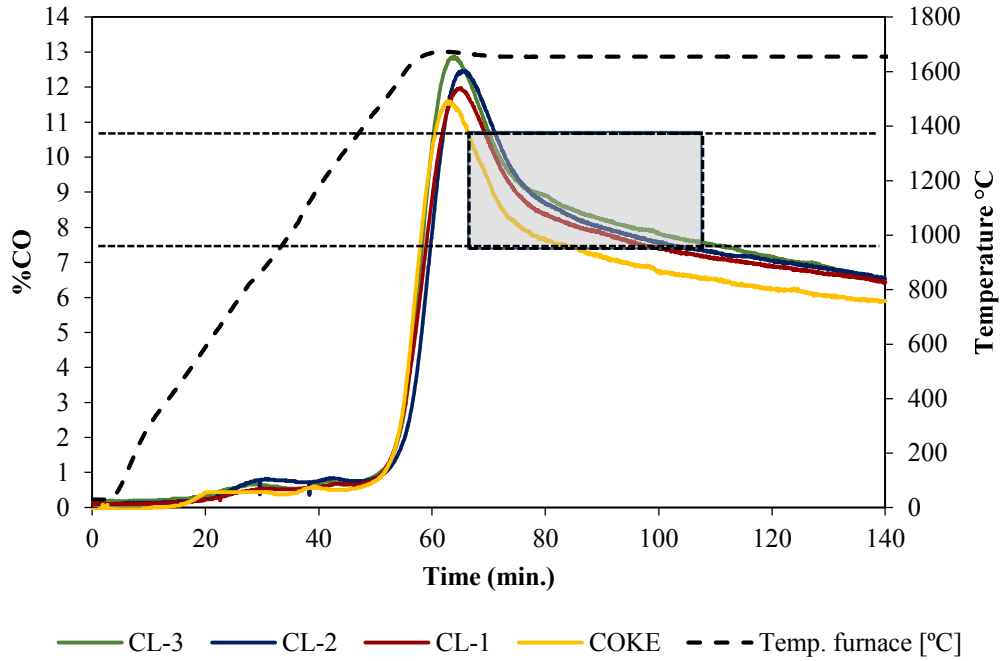

Figure 2.6 – Mean curve of the %CO versus time for the reductant materials tested.

Reactivity results given as "DR parameter" can be seen in Table 2.9. This value expresses the numerical integration of %CO from 10.8 to 7.6%. A high value of DR indicates high SiO-reactivity of reductant material.

Table 2.9 - Reactivity values based on the profile of CO% of the reductant materials (N=12)

Parameter	CHARCOAL			COKE
	CL-3	CL-2	CL-1	
DR (%CO g^{-1})	204.1±15 a	182.5±11 ab	156.4±14 b	100.7±10 c

DR: Reactivity number based on the profile of CO% versus time. N: Number of samples. Means followed by same letter do not differ at 95% probability by Tukey test.

The CL-3 had the highest SiO reactivity. The characteristics of CL-3 wood char, such as the high porosity, the low apparent density and the low fiber wall area, which are indices connected to the development of pores in charcoal, may facilitate the diffusion of silicon monoxide into the carbon matrix. In accordance with Myrhaug (2003) and Li (2018), high values of charcoal SiO reactivity were related to a lower fiber wall area and higher porosity. It is worth pointing out that the reaction between C and SiO-gas is

topochemical, thus, the SiO capture and SiC formation mainly depend on the surface area of the carbon accessible to the SiO gas (Vorob'ev, 2017).

There was a significant effect of the reductant material and reactivity parameters on degree of conversion, but no interaction between them ($p > 0,05$). All of the parallel protocols tested based on the SiO reactivity test exhibited a very similar trend between charcoal as seen in Figure 2.7, where the CL-3 wood char had the highest values, followed by CL-2 and CL-1. The coke had the lowest conversion in all cases, except for SiC (*X4*) parameter. The latter had been done using X-ray fluorescence technique, which did not represent a suitable tool to analyse coke conversion, a high ash content material. This may be explained due to interferences of the amount of minerals present in ash, especially the Si. The small values of (*X1*) parameter is explained due to the theoretical limit of a 67% weight increase.

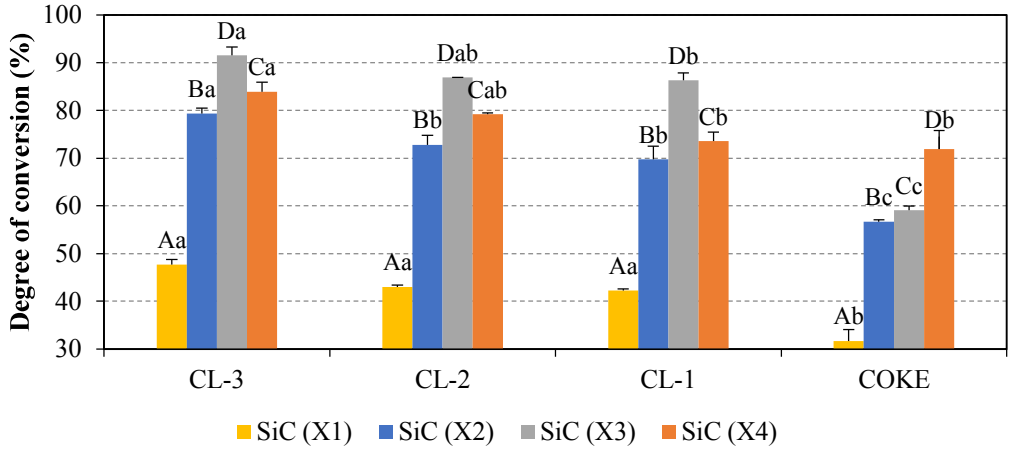

Figure 2.7 - Effect of reactivity protocols and reductant material on degree of conversion. The bars on top of column graph are the standard deviations. Number of samples (N = 12). Means followed by same uppercase letter among the reactivity parameters and lowercase among the clones do not differ at 95% of probability by Tukey test.

To summarize, all the parameters tested in this study can be used to evaluate the ability of charcoal to react with SiO(g). The degree of conversion (*X2*) was found to be the best parameter tested to evaluate charcoal reactivity due to its smaller deviation and simplicity; it also takes in account the carbon content of samples before reaction.

The CL-3 charcoal was 13.7% higher than the others charcoal, across all reactivity parameters. Regarding microstructure of CL-3 wood chars, it presented the highest

frequency of vessels, the smallest vessel diameter and fibers with the lowest wall area. Additionally, the CL-3 charcoal had the highest porosity and lowest apparent density.

The readily available fixed carbon stock (*ECS*) can be seen in Figure 2.8. This parameter was created by a combination of important charcoal properties, such as carbon stock (fixed carbon stock discounting losses by fines generation) and the quality of the carbon (degree of conversion to SiC), in order to indicate one or more charcoals with the greatest potential for use in silicon production. Based on *ECS*, there was no statistical difference ($p>0.05$) between the reductant materials. There is only a trend of increasing *ECS* from the CL-1, followed by the CL-2 and CL-3 charcoal. Besides the CL-3 wood char presenting the highest values of *ECS*, the use of biocarbon in metallurgical industries has a great potential with respect to reducing CO_2 emissions and the contribution from this industry to the increasing greenhouse gas effect also may improve the silicon quality.

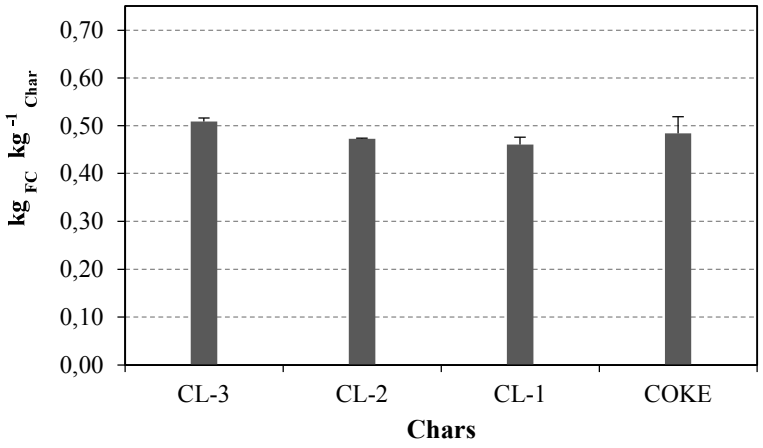

Figure 2.8 - Mean values of readily available fixed carbon stock (ECS). The bars on top of column graph are the standard deviations. Number of samples (N = 12).

2.4. CONCLUSIONS

The evaluated genetic materials showed differences in their wood properties which affect the charcoal quality. The anatomical characteristics of wood, such as shape, arrangement and organization showed little or no modification due to carbonization. The observed changes from wood to charcoal were mainly related to fiber wall thinning.

The developed SiO reactivity procedure test was a useful tool to classify charcoal for use in silicon production process. All the parallel indices used to express SiO reactivity can be used to evaluate the ability of charcoal to react with SiO(g).

The charcoal SiO reactivity increased with a decreasing apparent density, fiber wall area, and increasing porosity. The coke exhibited lower reactivity compared to the charcoals.

Based on the parameters investigated and under the experimental conditions, the charcoal from the clone 3 stood out concerning charcoal production for silicon use, since it showed better results for SiO reactivity and readily available fixed carbon stock in charcoal.

2.5. REFERENCES

ASSIS, M. R. et al. Factors affecting the mechanics of carbonized wood: literature review. **Wood Sci Technol,** v. 50, p. 519-536, 2016.

BUØ, T. V.; GRAY, R. J.; PATALSKY, R. M. Reactivity and petrography of cokes for ferrosilicon and silicon production. **International Journal of Coal Geology,** v. 43, n. 1-4, 243-256 2000.

BEN. **Brazilian Energy Balance**. ENERGY, M. O. M. A. Rio de Janeiro:**:** 296 p. 2017.

CARNEIRO, A. D. C. O. et al. Potential energy of *Eucalyptus sp*. wood according to age and different genetic materials. **Revista Árvore,** v. 38, n. 2, p. 375-381, 2014.

COSTA, A. C. S. et al. Properties of heartwood and sapwood of *Eucalyptus camaldulensis*. **Brazilian Journal of Wood Science,** v. 8, n. 1, p. 10-20, 2017.

EVANGELISTA, W. V. et al. Quantitative anatomical features of the wood of *Eucalyptus camaldulensis* Dehnh. and *Eucalyptus urophylla* S. T. Blake clones. **Scientia Forestalis,** v. 38, n. 86, p. 273-284, 2010.

FERREIRA, A. T. B. **Evaluation of anatomical structure and apparent density of wood and charcoal from *Eucalyptus sp*. and *Corymbia* sp. trees**. 2013. 131 (Ph.D). Forest Engineering, ESAUQ/USP, Piracicaba, São Paulo.

FOELKEL, C. E. B.; BARRICHELO, L. E. G.; MILANEZ, A. F. **Comparative study of *Eucalyptus saligna*, *E. paniculata*, *E. citriodora*, *E. maculata* and *E. tereticornis* wood for cellulose sulfate production**. IPEF. São Paulo, Brazil, p.17-37. 1975

FROMM, J. Wood formation of trees in relation to potassium and calcium nutrition. **Tree Physiology** v. 30, p. 1140-1147, 2010.

GRISCHENKO, S. G. et al. Production of special kinds of carbonaceous reducing agents for ferroalloy smelting. The thirteenth International Ferroalloys Congress, 2013, Almaty, Kazakhstan. june 9-13. p.505-510.

IAWA, C. **List of microscopic features for hardwood identification**. BULLETIN, I. Leuven, Belgium. 10**:** 219-332 p. 1989.

IBÁ. **Brazilian Tree Industry**. Pöyry Consultoria em Gestão e Negócios Ltda. Brasília, p.80. 2017

KAN, T.; STREZOV, V.; EVANS, T. J. Lignocellulosic biomass pyrolysis: A review of product properties and effects of pyrolysis parameters. **Renewable and Sustainable Energy Reviews,** v. 57, p. 1126-1140, 2016. ISSN 1364-0321.

KHALIL, L. B. Porosity characteristics of chars derived from different lignocellulosic materials. **Adsorption Science & Technology** v. 17, n. 9, p. 729-739, 1999.

KWON, S. M.; KIM, N. H.; CHA, D. S. An investigation on the transition characteristics of the wood cell walls during carbonization. **Wood Science and Technology,** v. 46, n. 5-6, p. 487-498, 2009.

LI, F. **SiC production using SiO_2 and C agglomerates**. 2018. 217 Thesis (Ph.D). Materials Science and Engineering, Norwegian University of Science and Technology, Trondheim, Norway.

LINDSTAD, T. et al. Improved sintef sio-reactivity test. INFACON XI

2007, New Dehli, India. February 18-21

MACKAY, D. M.; ROBERTS, P. V. The influence of pyrolysis conditions on yield and microporosity of lignocellulosic chars **Carbon,** v. 20, n. 2, p. 95-104, 1982.

MITRAŠINOVIĆ, A. M.; UTIGARD, T. A. Refining silicon for solar cell application by copper alloying. **Silicon,** v. 1, p. 239-248, 2009.

MONSEN, B. et al. The use of biocarbon in norwegian ferroalloy production. INFACON IX, 2000, Quebec City, Canada. June 3-6

MONSEN, B. et al. Possible use of natural gas for silicon or ferrosilicon production. Thirteenth international ferroalloys congress, 2013, Almaty, Kazakhstan. p.467-478.

MYRHAUG, E. H. **Non-fossil reduction materials in the silicon process - properties and behaviour**. 2003. 242 (Ph.D). Department of Materials Technology, Norwegian University of Science and Technology, Trondheim.

MYRVÅGNES, V. **Analyses and characterization of fossil carbonaceous materials for silicon production**. 2008. 248 (Ph.D.). Department of Materials Science and Engineering, Norwegian University of Science and Technology

MYRVÅGNES, V.; LINDSTAD, T. The importance of coal and coke properties in the production of high silicon alloys. INFACON XI, 2007, New Delhi, India. 18-21 February. p.402-413.

NOUMIA, S. et al. Upgrading of carbon-based reductants from biomass pyrolysis underpressure. **Journal of Analytical and Applied Pyrolysis,** v. 118, p. 278-285, 2016.

PALERMO, G. P. D. M. et al. Anatomical properties of *Eucalyptus grandis* wood and transition age between the juvenile and mature woods. **European Journal of Wood and Wood Products,** v. 73, n. 6, p. 775–780, 2015.

PEREIRA, B. L. C. et al. Effect of wood carbonization in the anatomical structure and density of charcoal from *Eucalyptus*. **Ciência Florestal,** v. 26, n. 2, p. 545-557, 2016.

PEREIRA, B. L. C. et al. Quality of wood and charcoal from *Eucalyptus* clones for ironmaster use. **International Journal of Forestry Research,** v. 2012, p. 1-8, 2012.

PEREIRA, B. L. C. et al. Correlations among the heart/sapwood ratio of *Eucalyptus* wood, yield and charcoal properties. **Scientia Forestalis,** v. 41, n. 98, p. 217-225, 2013b.

ROMERO, F. J. N.; REINOSOA, F. R.; DÍEZB, M. A. Influence of the carbon material on the synthesis of silicon carbide. **Carbon,** v. 37, p. 1771-1778, 1999.

SAKUROVS, R.; BURKE, L. Influence of gas composition on the reactivity of cokes. **Fuel Processing Technology** v. 92, n. 6, p. 1220-1224, 2011.

SCHEI, A.; TUSET, J. K.; TVEIT, H. **Production of High Silicon Alloys**. Trondheim, Norway: 1998.

SIEBENEICHLER, E. A. et al. Influence of temperature and heating rates on mechanical resistance, density and yield of the wood charcoal of *Eucalyptus cloeziana*. **Brazilian Journal of Wood Science,** v. 8, n. 2, p. 82-94, 2017.

SILVA, M. G. D. et al. Charcoal from timber industry residues of three tree species logged in the municipality of Paragominas, PA. **Acta Amazonica,** v. 37, n. 1, p. 61-70, 2007.

SILVA, M. R. D. et al. Permeability measuremens of brazilian *Eucalyptus*. **Materials Research,** v. 13, n. 3, p. 281-286, 2010.

SILVEIRA, R. C. D.; CARMA, W. F. D.; NETO, M. V. B. Technical analysis of charcoal to use in the ferroalloy industry in Brazil. INFACON 86, 1986, Rio de Janeiro, Brazil. September 31. p.481-500.

TRUGILHO, P. F.; LIMA, J. T.; MENDES, L. M. Influence of age on the physical-chemical and anatomical characteristics of the wood of *Eucalyptus saligna* **Cerne** v. 2, n. 1, p. 96-111, 1996.

TUSET, J. K.; RAANESS, O. Reactivity of reduction materials in the production of silicon, silicon-rich ferroalloys and silicon carbide. 34th Electric Furnace Conference, 1976, St.Louis. December 7-10

UNFCCC. **Paris Agreement** NATIONS, U. Paris**:** 27 p. 2015.

VIDEM, T. Reaction rate of reduction materials for the (ferro)silicon process. INFACON VII, 1995, Trondheim, Norway. June 11-14. p.221-230.

VITAL, B. R. **Methods for wood density determination**. SIF, Universidade Federal de Viçosa. Viçosa, Brazil, p.21. 1984

VOROB'EV, V. P. Carborundum-bearing reducing agents in high-silicon alloy production. **Steel in Translation,** v. 47, n. 10, p. 688-690, 2017.

CHAPTER III

3. EFFECT OF PYROLYSIS CONDITIONS ON CHARCOAL QUALITY FOR SILICON PRODUCTION

Abstract: A primary factor for determining the silica reduction process efficiency is the reactivity of the carbon reductants. The ability of the carbon reduction materials to react with SiO gas is commonly assumed to be of large importance to the performance of the process. Nevertheless, charcoals can be produced from different raw materials and under various process conditions, having different properties that influence further applications. The purpose of this study was to examine the effects of pyrolysis conditions on SiO reactivity. In this work, charcoal was produced from *Eucalyptus spp*., under peak temperature (380 °C) and holding times (2 and 8 hours). In addition, an industrial metallurgical charcoal produced at 460 °C was used for comparison. Proximate and elemental analysis, surface area BET, friability, porosity and apparent density of the charcoal produced were determined. The SiO reactivity was conducted using agglomerates made of quartz and silicon carbide (SiC) mixtures and charcoal, which have been heated in a resistance heating furnace at 1650 °C in an inert atmosphere for 120 minutes. Charcoal samples, before and after SiO reactivity test, were studied using the SEM photomicrograph to trace the gas diffusion paths of SiO gas and the formation of SiC. The results reveal an increasing trend of degree of conversion of carbon to SiC with increasing holding time. In addition, the degree of conversion for charcoal produced at 460 °C was lower than those prepared at 380 °C. The decreasing degree of conversion with increasing temperature from 380 °C up to 460 °C was attributed to the increase of aromatic C in charcoal.

Keywords: SiO reactivity, *Eucalyptus*, carbonization

3.1. INTRODUCTION

Elemental silicon, traditionally called metallurgical grade silicon, is produced industrially by reduction of silica (SiO_2) with carbon materials in an submerged arc furnace (SAF) according to $SiO_{2(s)} + 2C_{(s)} \longrightarrow Si_{(l)} + 2CO_{(g)}$. However, the chemistry of the process is more complicated than what is expressed by the overall reaction, since a series of reactions take place in different zones of the furnace. Schei *et al.* (1998) described the Si process by dividing the furnace into an inner and outer zone. The inner zone is described as areas where silicon carbide (SiC) produced in the upper parts of the furnace will react with the molten quartz, and silicon will be produced according to $3SiO_{2(s)} + 2SiC_{(s)} \longrightarrow Si_{(l)} + 4SiO_{(g)}\ 2CO_{(g)}$. The outer zone is where one of the most important gas-solid reaction takes place: $SiO_{(g)} + 2C_{(s)} \longrightarrow SiC_{(s)} + CO_{(g)}$, where the content of SiO-gas coming from the inner zone must be recovered, or it will be lost. The carbon materials capture SiO gas from the inner zone, producing SiC, which transfers the silicon back to the inner zone with the descending charge material, improving the silicon recovery. SiC is an intermediate product in the process that is essential for the silicon producing reactions in the inner zone.

The ability of carbon material to react with SiO-gas is referred to as the SiO reactivity. This is one of the most important properties of carbon materials used as reductants during silicon production processes. This parameter defines how efficient a given reduction material can recover the SiO-gas in a packed bed, for example in a silicon furnace (Myrvågnes, 2008). A high SiO reactivity of the reduction materials leads to high silicon recovery, good furnace operation, and low costs (Buø *et al.*, 2000; Myrvågnes e Lindstad, 2007). It is worth pointing out that the cost of reduction materials constitutes about 40% of the total material costs in silicon production (Videm, 1995).

The charcoal is the best reduction material to use in silicon production. The low content of impurities favors the higher purity silicon production, and the developed pores structure leads to a high SiO reactivity (Myrhaug *et al.*, 2004; Kim *et al.*, 2013). There is, however, the question of charcoal having a lower mechanical strength. Nevertheless, charcoals can be produced from different raw materials and under various carbonization process conditions, having different properties that influence further applications.

Carbonization is a process of thermal decomposition of biomass in inert atmosphere, and the main goal is to eliminate most of the oxygen and hydrogen using heat and, therefore, increase the carbon concentration in the residual structure. Changes in carbonization conditions affects physical, chemical, and morphological properties of the charcoal (Protásio *et al.*, 2014; Assis *et al.*, 2016; Kan *et al.*, 2016), which may influence their respective SiO reactivity. Some studies (Myrhaug, 2003; Li, 2018) on the SiO reactivity of charcoal have been carried out; however, the effects of carbonization conditions remain a poorly understood aspect, suggesting the need for further investigation in this field.

Given the differences in pyrolysis conditions used for metallurgic charcoal production and the lack of research related to the wood char SiO reactivity, the aim of the present work was to investigate the effects of pyrolysis process conditions on charcoal quality for silicon use.

3.2. EXPERIMENTAL SETUPS AND METHODS

3.2.1. Raw material: sampling and characterization

A short rotation forestry species, clones of *Eucalyptus urophylla* vs *grandis* hybrid, named CL-1 clone, was used for the study. Samples of 7-year old wood were collected from a Brazilian forestry company. Logs with diameters from 6 to 14 cm were selected and sawn in approximately 1.0 m length for carbonization. Six logs, representative of diameter variation, were sawn into 50-mm thick (discs) and then divided in four to be used in chemical and physical analyses. Firstly, measurements were taken of the heart wood and sapwood of each disc, according to methodology described by Pereira *et al.* (2013b).

Measurements of anatomical characteristics were made in the Laboratory of Anatomy and Quality of Wood (LAPEM) and Laboratório de Propriedades Físicas e Mecânicas da Madeira (LPM) at the Federal University of Viçosa (MG), Brazil, following the standard presented by Iawa (1989) and recommendations of Foelkel *et al.* (1975). Wood basic density was determined according to NBR 11941 (Brazilian Association of Technical Standards, 2003).

To determine chemical composition (lignin, extractives and holocellulose content) and ash content, the samples were crushed and sieved between 40 - 60 mesh. Wood extractive content was determined according to TAPPI 204 om-88, using the total extractive method but substituting ethanol/benzene for ethanol/toluene. Lignin content was obtained by summing soluble and insoluble lignin. Insoluble lignin was determined using Klason method and soluble lignin by spectrophotometry. Holocelluloses content was determined by difference, based on extractive-free wood and disregarding ash.

The characteristics of the *Eucalyptus* clone used in this work are listed in Table 3.1. The parameters that characterize the anatomical properties is shown in Table 3.2.

Table 3.1 - Chemical composition, basic density and H/S ratio of *Eucalyptus* clone.

Parameter	Value	Standard deviation
Lignin total (%)	29.6	0.03
Holocelulloses (%)	65.8	0.03
Extratives total (%)	4.5	0.01

Ash (%)	0.3	0.01
Basic density (kg m^{-3})	559.1	51.5
Heartwood/Sapwood (H/S)	0.64	0.3

Table 3.2 - Anatomical characteristics of *Eucalyptus* clone.

Parameter	Value	Standard deviation
Fiber length (L) (mm)	1.0	0.2
Fiber diameter (D) (μm)	20.4	0.9
Fiber lumen diameter (d) (μm)	8.1	2.2
Fiber wall thickness (e) (μm)	6.2	1.3
Fiber slenderness ratio (L/D)	49.9	3.8
Wall fraction (D - d/D)	60.5	3.7
Frequency (vessels /mm²)	9.8	2.5
Vessels diameter (μm)	130.0	15
Vessels area (%)	15.7	2.1

3.2.2. Charcoal preparation

The charcoals were produced in a laboratory kiln built of masonry bricks, with a diameter 1.2 m and height 1.1 m, with 1,04 m^3 of usable volume. A volume of 0,6 m^3 of logs were loaded into the kiln for slow pyrolysis. Internal heating was used to initiate pyrolysis and maintain temperatures during the process. The temperature was monitored by five thermocouples, one inserted at the dome of the kiln and the others in the walls. The temperature control of the carbonization process was agreed with a pre-set theoretical model. The peak temperature of the carbonization was 380 °C and used to two different hold times (2h and 8h). In addition, an industrial charcoal (control), supplied by the Laboratório de Painéis e Energia da Madeira LAPEM - Universidade Federal de Viçosa, was investigated for comparison purpose. This charcoal was produced in an industrial kiln-furnace system with combustion of pyrolysis gases during the carbonization, the peak temperature of carbonization was around 460 °C for 17h. Further details about this kiln-furnace system can be found elsewhere (Oliveira *et al.*, 2013; Damásio *et al.*, 2015).

After carbonization, six bags with charcoal, 20 liter each, were randomly collected, homogenized and quartered, based on standard NBR 6923 (Brazilian Association of Technical Standards, 1981). Thereafter, 20 liters of charcoal for each experiment was taken to determine charcoal properties.

3.2.3. Charcoal separation and experimental design

Given the heterogeneity of the wood samples and, consequently, the charcoal produced, the charcoal lumps in this study were separated into density fractions in order to obtain greater homogeneity between samples, as well as a better understanding of the parameter selected for evaluation. The charcoal was first crushed and sieved to a size fractions between 18-22 mm, and then, the apparent density of each lump of charcoal. Thereafter, the lumps of charcoal were screened into 2 different fractions, denoted as high and low density, which was defined from the mean value of apparent density. The experiment design can be seen in Table 3.3.

Table 3.3 - Experimental design

Pyrolysis treatment (PT)	Temperature (T) °C	Hold time (HT) hours	Density fraction (DF)	Experiment identification
1	380	2	Low	380 °C_L_2h
2	380	8	Low	380 °C_L_8h
Control	460	17	Low	460 °C_L_IC
1	380	2	High	380 °C_H_2h
2	380	8	High	380 °C_H_8h
Control	460	17	High	460 °C_H_IC

IC: Industrial charcoal.

3.2.4. Charcoal properties

Proximate analysis of produced charcoals was performed according to procedures described in ASTM standard D1762 (American Society for Testing and Materials, 1984). The quantification of the carbon (C), hydrogen (H), and nitrogen (N) relative to the charcoal dry mass was performed according to the standard SS-EN ISO 16948 (European Standard, 2015). Sulfur (S) was according to SS-EN ISO 16994 (European Standard, 2016). The oxygen content was determined by the difference, i.e., by disregarding the contents of carbon, hydrogen, nitrogen, sulfur, and ash. The concentrations of inorganic elements were measured by means of an inductively coupled plasma optical emission spectrometry (ICP-OES) according to the standard CEN/TS 15290 (European Committee

for Standardization, 2006). The Si content was determined by the X-ray fluorescence technique (XRF).

Fourier Transform Infrared Spectroscopy (FTIR) were performed in a IFS 25-Bruker (Germany), equipped with an attenuated total reflection crystal (ATR) made of diamond for identifying types of molecular components and structures of charcoal. The FTIR was recorded with PC based software controlled instrument operation and data processing. An aperture setting of 6 mm with a wave-number range of 4000-500 cm^{-1} and scan speed of 10 kHz was applied for spectra collection. For each sample, 16 scans were utilized to improve the signal-to-noise ratio. According to Peng *et al*. (2011) the band around 3400 cm^{-1} was assigned to O–H stretching, 2900 cm^{-1} to aliphatic C–H stretching, and 800–1600 cm^{-1} to C–C, C=C, C=O stretching (aromatic).

The crystallographic structure of the samples was studied using X-ray Diffraction (XRD) analysis on a Bruker AXS D8 Advance X-ray Diffractometer with Cu Kα 1 radiation, 40 kV and 30 mA. The charcoal powder was prepared in a sample holder for X-ray diffraction with the dimensions of 1 mm (thickness) 20 mm (diameter). The X-ray unit used in this study was in the angular ranges of 10-75° (2θ) at a scanning speed of 2° min^{-1}, and a variable divergence slits opens automatically such that the illuminated length on the sample always remains 6 mm.

The apparent density (AD) was determined by the hydrostatic method, in which the samples were immersed in mercury. The absolute density was determined using an AccuPyc 1330 Helium Pycnometer, according to the standard ISO 12154 (International Organization for Standardization, 2014). The porosity (%) of material was obtained by the following equation:

$$Porosity = \left[1 - \left(\frac{apparent\ density}{absolute\ density}\right)\right] x\ 100\% \quad (1)$$

The fixed carbon stock on charcoal per unit volume (FCS), expressed in units of - $kg.m^{-3}$-, was obtained by multiplying the charcoal's fixed carbon content (FC) by the apparent density (AD), as presented in the Equation 2:

$$FCS = (AD * FC) \quad (2)$$

In this equation, *AD* is the apparent density of charcoal (kg m^{-3}) and *FC* (%) is the fixed carbon content of charcoal.

The pores structure of the charcoal samples was characterized by nitrogen adsorption/desorption at 196 °C. The Brunauere-Emmete-Teller (BET), Standard DIN 66131 (Germany Committee for Stardardization, 1993) was used to measure the total surface area using an automated gas adsorption analyzer (The TriSTAR 3000-Micromeritics). Prior to BET all materials, 0.4g of each sample, particle size of 500-200μm, was degassed for 12 h under a vacuum at 250 °C in the built-in degas port of the instrument.

The charcoal morphology was investigated by field-emission scanning electron microscopy (LVFESEM, Zeiss Supra 55VP). The samples were investigated before and after the SiO reactivity test. The samples after SiO reactivity test were embedded in epoxy resin, ground, and polished in order to study carbonaceous structures in relationship to silicon carbide formation. To investigate the microstructure of charcoal measurements of vessel in the transversal section, the vessels diameter (μm), frequency (vessels mm^{-2}), and vessels area (%) of 5 samples from each material were randomly collected. The transversal section of charcoal samples was previously sanded for better visualization of the charcoal microstructure, and the images were obtained using a magnifying glass coupled to an image acquisition system, as well as being measured by software "Axio Vision 4.3".

The measurements of fibers on charcoal surface are rarely reported due to their small size and, hence, are difficult to measure. In this work, a new measurement procedure was applied using SEM microphotography, followed by handling of the images using the software "solution DT". At the traversal section, four charcoal samples were randomly evaluated for each treatment. The fiber wall area on charcoal (FWA%) was calculated by difference between fiber lumen area and selected fiber area on the SEM image (Figure 3.1). A high contrast was used to get better differentiation between fiber lumen area and fiber wall area.

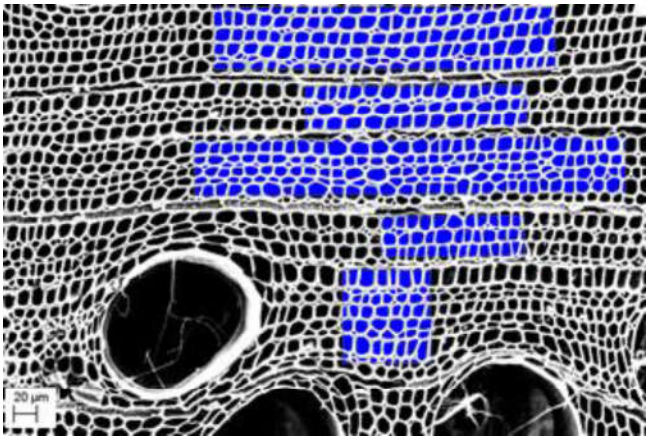

Figure 3.1 - Measurements of fiber wall fraction on charcoal surface, transverse section, by use of SEM photomicrograph with software solution DT. The squares on the image are the fiber selected areas to measure, while the blue and white color in the selected area represent the fiber lumen and fiber wall, respectively.

The friability (denoted F, expressed in %), also called "impact strength", gives an idea of the extent of breakage that will occur during loading, transportation, and screening of charcoal. In this study, the drum test was used to determine the index or degree of friability of the charcoal. The procedure was performed according to Noume *et al*. (2016).

3.2.5. SiO reactivity apparatus and procedures

Charcoal samples were calcined in an induction furnace to remove volatile matter, prior to SiO reactivity tests. Thereafter, the samples were crushed and screened to the fraction size of +2-4.5 mm to use in the SiO reactivity test. The SiO reactivity test was performed in an electric tube vertical furnace, using a graphite crucible as shown in Figure 3.2.

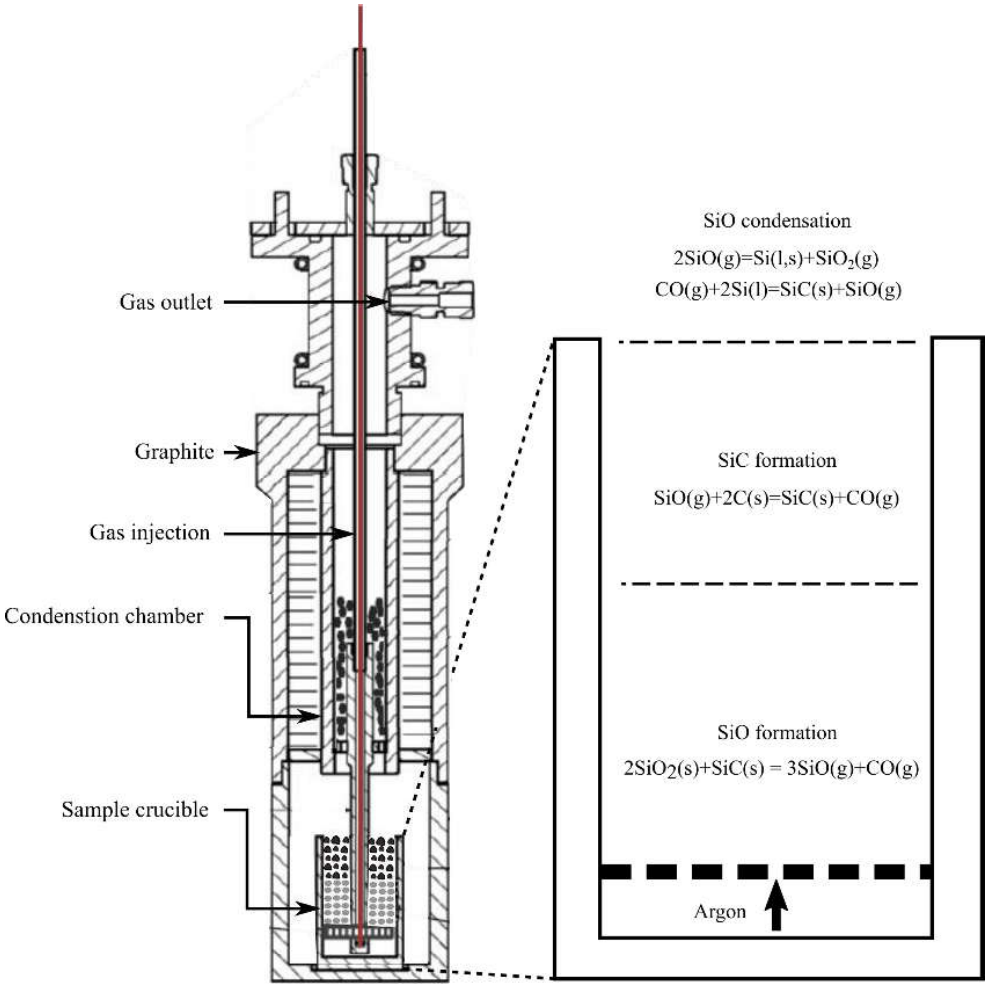

Figure 3.2 - Schematic diagram of graphite crucible used in experimental setup for SiO reactivity test (Drawings by P.Tetlie at SINTEF). In the sample crucible, the grey part is SiO_2+SiC and the black is charcoal.

The SiO reactivity test was carried out with use of pellets made by mixing SiC+SiO_2 powders (the mole ratio of 1:2 respectively) to generate SiO-gas, which will react with the charcoal above it. Both materials were loaded in the sample crucible, with dimensions of 32 mm in diameter and 60 mm in height. The internal surfaces of the sample crucible were lined with SiC coating to protect the graphite from reacting with SiO gas. The sample crucible was placed inside the reaction chamber (Figure 3.2). In the experiment, 15g of pellets and 15ml of lump charcoals were loaded, corresponding to a carbonaceous packed bed 20 mm high. This setup was defined by the stoichiometric analysis of the pellets reaction and mass of carbon used to reach SiO-gas levels that do

not restrict conversion rate of the carbon materials. In addition, SiC particles were placed in the condensation chamber above the crucible to capture unreacted SiO-gas.

The loaded crucible was heated up to 1650 °C at a constant heating rate of 30 °C min^{-1} under a constant flow of argon (0.4 l min^{-1}). Argon was used as a carrier gas, transporting SiO generated from the pellets through the packed bed of carbonaceous material. The temperature of 1650 °C and the argon gas flow through the furnace were maintained for 2 hours. The experiment was then cooled down to room temperature. The gas analyzer ABB2020 was connected to the off-gas lance to detect the concentration of CO gas. The %CO change and temperature were recorded in the logging program where values were registered automatically every 5 seconds.

The weight of charcoal, pellets, and the setup crucible were measured before and after the tests. The reactivity tests in this study were carried out a minimum of two parallel runs for each reductant materials. It is worth mentioning that the SiO_2+SiC-pellets conversion, hence SiO gas generated, exhibited narrow variation in all experiments with a standard deviation of 3.5%.

The degree of conversion (*X*) for the particle during conversion can be expressed based on the Reaction 3:

$$SiO + 2C \rightarrow xSiC + xCO + (2-2x)C + (1-x)SiO \quad (3)$$

The total conversion of carbon to SiC is then expressed by the carbon reaction $SiO_{(g)} + 2C_{(s)} \rightarrow SiC_{(s)} + CO_{(g)}$ when x=1. The degree of conversion (*X*) on the SiO reactivity test was calculated trough Equation 4, marked as:

$$X(\%) = (m2 - m1)/(m1\,.\,C1free\left(\frac{MSiC - 2MC}{2MC}\right)) \quad (4)$$

Where "*m*" is mass of sample, 1 and 2 refer to before and after the test, respectively. "$C1_{free}$" is free carbon content before test. The M_{SiC} and M_C are molar mass of SiC and C respectively.

The chemical analysis of free carbon was conducted by free carbon Leco Rc-412, based on EN ISO 21068:2008 with IR detection. Measurement uncertainly specified with 95 pct. confidence intervals is 0.1% for free C.

In order to classify the charcoal with the greatest potential for silicon use, the parameter (ECS), readily available fixed carbon stock in charcoal per volume, was created. The *ECS* is expressed in ($kg_{CF}\ kg_{char}^{-1}$), and it was calculated using the important charcoal properties, such as apparent density, fixed carbon, friability, and the degree of conversion (X), according to the Eq. 5.

$$ECS = [FCS * (1 - F) * X]/\mathrm{AD} \quad (5)$$

Where FCS ($kg\ m^{-3}$) is the fixed carbon stock on charcoal; *F*(%) is the friability; AD($kg\ m^{-3}$) is the apparent density; *X* (%) is the degree of conversion of C to SiC, according to the experimental conditions used.

The friability value in Equation 5 was assumed as the percentage of charcoal fines removed by the practice of sifting charcoal before its introduction in the furnace, and thus, it was defined as losses in carbon stock.

3.2.6. Statistical analysis

The reactivity experiment of charcoal from each density fracion was conducted according to a randomized design with two treatments (heating time) with two replicates (two-sample). Thereafter, data were subjected to Dunnett's method to test if treatment means were different from the control. The accuracy of the measurements was assessed with the sample standard deviation. The 95% level of significance was always considered.

Additionally, a nonlinear model was adjusted to predict (degree of conversion) from the (FC and AD), two important properties easily determined and strictly controlled in the metallurgical industry.

3.3. RESULTS AND DISCUSSIONS

3.3.1. Charcoal characterization

3.3.1.1. Chemical composition of charcoal

The parameters that characterize the chemical properties of charcoal are shown in Table 3.4. The chemical composition of ash is listed in Table 3.5.

Table 3.4 - Properties of *Eucalyptus* charcoal produced at different pyrolysis conditions. (N = 12).

Experiment	Elemental analysis (wt %)					Mass ratio		Proximate analysis (wt%)		
identification	C	H	N	O	S	O/C	H/C	VM^+	FC^+	Ash
380°C_L_2h	74.5	3.6	0.8	21.0	<0.05	0.28	0.05	32.4±0.3b*	67.2±0.5a*	0.28±0.04a*
380°C_L_8h	77.0	3.4	0.5	19.1	<0.05	0.25	0.04	23.9±0.1a*	75.5±0.2b*	0.38±0.04a
460°C_L_IC	87.2	3.9	0.6	8.3	<0.05	0.10	0.04	12.9±0.2	86.2±0.1	0.58±0.07
380°C_H_2h	71.9	3.6	0.7	23.8	<0.05	0.33	0.05	33.8±0.3b*	65.7±0.4a*	0.33±0.02a*
380°C_H_8h	77.0	3.4	0.5	19.1	<0.05	0.25	0.04	25.2±0.1a*	74.2±0.1b*	0.41±0.01a*
460°C_H_IC	88.0	3.4	0.4	8.2	<0.05	0.09	0.04	15.8±0.1	83.6±0.2	0.62±0.02

VM^+ volatile matter; FC^+ fixed carbon. Means followed by same letter do not differ at 95% probability by test F. Means labeled with the (*) are significantly different from the control at 95% probability by test Dunnett. N = Number of samples.

Table 3.5 -Mean values of ash composition of *Eucalyptus* charcoal. (N=6)

Chemical composition of ash (wt%)									
K_2O	MgO	CaO	P_2O_5	Na_2O	SiO_2	MnO	Fe_2O_3	AlO_3	TiO_2
32.1±1.3	10.7±1.2	27.7±1.6	8.1±1.6	9.9±1.2	3.8±1.2	1.8±1.2	2.3±0.5	1.8±0.5	0.1±0.01

N = Number of samples.

As can be seen in Table 3.4, fixed carbon (*FC*) content is highly dependent on pyrolysis conditions, and the values obtained range from 61.2 to 86.2%. The *FC* substantially increased with rising peak temperature and hold time, which is related to drive off of volatile matter of the charcoal. It is known that the peak temperature and hold time controls the quality (i.e., the volatile matter content) and other properties of the charcoal product (Protásio *et al.*, 2014; Protásio *et al.*, 2015; Kan *et al.*, 2016).

In metallurgical industrial practice, carbon reductants with a wide range of fixed carbon are used. There is no consent in the industry about the best fixed carbon content

in charcoal for metallurgical purposes, and there is a lack of scientific research on this subject. The choose of fixed carbon content and, hence, volatiles in charcoal should be based on set of reasons, such as yield of charcoal, mechanical strength, porosity and chemical properties. Gładysz e Karbowniczek (2008) stated that excessive conditions of volatile materials in the charcoal can form a kind of pyrolytic carbon film that leads to scorching on the surface of the charge and a decrease in gas permeability, as well as decreasing the reactivity of the reducing material and the electrical resistance of the charge.

The ash content of charcoal was less than 1% in all materials. There was a slight increase of ash when increasing the temperature in charcoal produced at 460 °C. This factor is associated with reduction of charcoal mass fraction due to the loss of volatiles materials during degradation and volatilization. In silicon production, the ash content in the reductant material is a source of contamination; it will be transferred to the silicon metal and will affect the silicon quality. The lower ash content in charcoal has a potential to significantly reduce the trace elements in the silicon produced. According to Monsen *et al.* (2000), in a pilot furnace experiment, the trace elements in the silicon products were 1% when using charcoal, while it was 4% with the reference coke. The most important case is the production of high purity silicon, intended for use in the solar grade silicon market, where the control of trace elements is strongly required. Thus, high amount of ash will negatively reflect on the silicon refining processes cost (Schei *et al.*, 1998). It is worth mentioning that the impurity level for some elements in silicon for solar cell applications should not exceed the 1 ppm level (Mitrašinović e Utigard, 2009). The main disadvantage of using charcoal is the relatively high P content.

The O/C ratio in charcoal range from 0.09 to 0.28. The charcoal produced at 460 °C presented the lowest O/C, differing significantly from the others charcoal. While the H/C showed a narrow range between charcoals, high values were found for charcoal at 460 °C. This result corroborates the findings of Protásio *et al.* (2014) and Titiladunayo *et al.* (2012). The sharp decrease of O/C from 380 °C to 460 °C is mainly attributed to cellulose volatilization, which have the structure of branching chain of polysaccharides rich in oxygen and no aromatic compounds that are easily volatilized (Lv *et al.*, 2010).

The FTIR spectra of charcoal samples is shown in Figure 3.3. Significant differences between spectrums on charcoal produced at 460 °C and 380 °C were found. The charcoal produced at 460 °C showed loss of adsorption intensities at the band 2900 $cm^{-1}$and 1740 cm^{-1}, indicating that the high peak temperature used on the pyrolysis leads to reduction of O, H and aliphatic C–H bonds. On the other hand, the adsorption at the 1400 cm^{-1} band was intensified, indicating an increase in aromatic C. These results are attributed to cellulose and hemicelluloses decomposition (Peng *et al.*, 2011; Nanda *et al.*, 2013) and increase in structural ordering of the carbon matrix with an increasing carbonization temperature (Kumar *et al.*, 1993; Asadullah *et al.*, 2010).

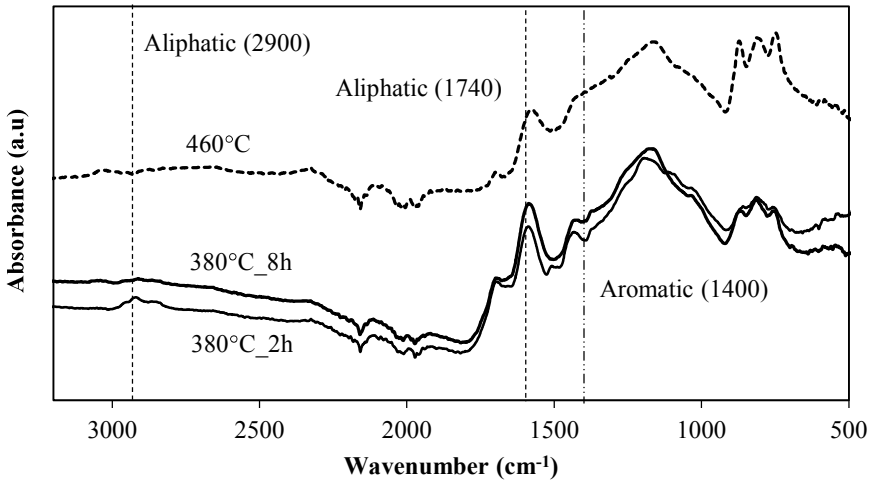

Figure 3.3 - FTIR spectra of charcoal produced at different pyrolysis conditions. Number of samples (N = 18).

Hajaligol *et al.* (2001) evaluated the formation of aromatic hydrocarbon from slow pyrolysis of cellulosic materials at low temperatures. They found that simple hydrocarbon products begin to evolve above 350 °C, where the primary decomposition of cellulose is completed and the remaining char has begun the carbonization/aromatization process. Most aromatic products such as benzene, naphthene, toluene, and anthracene are detected between 400 and 600 °C.

The X-ray diffraction patterns of the charcoal are presented in Figure 3.4. The diffraction profiles attributed to the 2θ = 22.7° appear to be very informative. The charcoal produced at 460 °C showed less intensity at the 25° peak when compared to the 380 °C charcoal, which can be attributed to the transition from amorphous C into ordered

turbostratic crystallites. This phenomenon is further supported by the increase in true absolute density of charcoal with carbonization temperature. The absolute density of *Eucalyptus* wood char was 1387 kg m^{-3} for 380 °C_2h and 1535 kg m^{-3} for 460 °C_IC, respectively. Keiluweit *et al.* (2010) studied the dynamic molecular structure in pine wood and grass using the in-situ X-ray diffraction in the carbonization temperature range of 100-700 °C. They reported that the narrowing of this peak, 2θ about 23°, with increasing temperature above 400 °C, and this indicates developing atomic order in the increasingly carbonized plant material. This was attributed to the formation and evolution of turbostratic crystallites. Similar results of X-ray diffraction patterns were also found by Kwon *et al.* (2009) and Nishimiya *et al.* (1998).

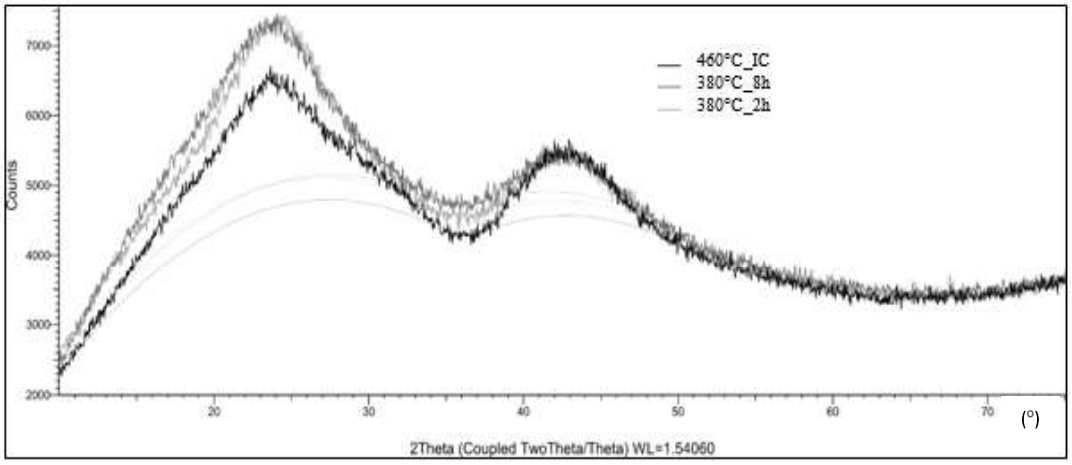

Figure 3.4 - The equatorial X-ray diffractograms of *Eucalyptus* charcoal charred at different pyrolysis conditions. Number of samples (N = 12).

3.3.1.2. *Physical properties of charcoal*

As can be seen in Figure 3.5, the effect of the peak temperature and holding time were significant with respect to the apparent density of charcoal. The charcoal produced at 460 °C exhibited the lowest apparent density, average of 356.1 kg m^{-3}, followed by the 380 °C_8h (397.2 kg m^{-3}) and 380 °C_2h (441.2 kg m^{-3}). The increase in peak temperature and hold time of carbonization led to a significant reduction in charcoal apparent density. On average, there was a density loss of 9.9% and 10.3% with increasing holding time and peak temperature, respectively. The mass loss caused by the extraction of volatiles

between the temperatures of 380 °C and 460 °C is much larger than the size reduction of charcoal, which explains the decrease in apparent relative density. These results indicate that the choice of pyrolysis conditions can be used to control the apparent density of charcoal in order to get the desired quality for different metallurgical processes. Values of charcoal apparent density from clones and *Eucalyptus* species found in the literature ranged from 266 kg m^{-3} to 490 kg m^{-3} (Santos *et al.*, 2011; Trugilho *et al.*, 2011; Castro *et al.*, 2016; Pereira *et al.*, 2016).

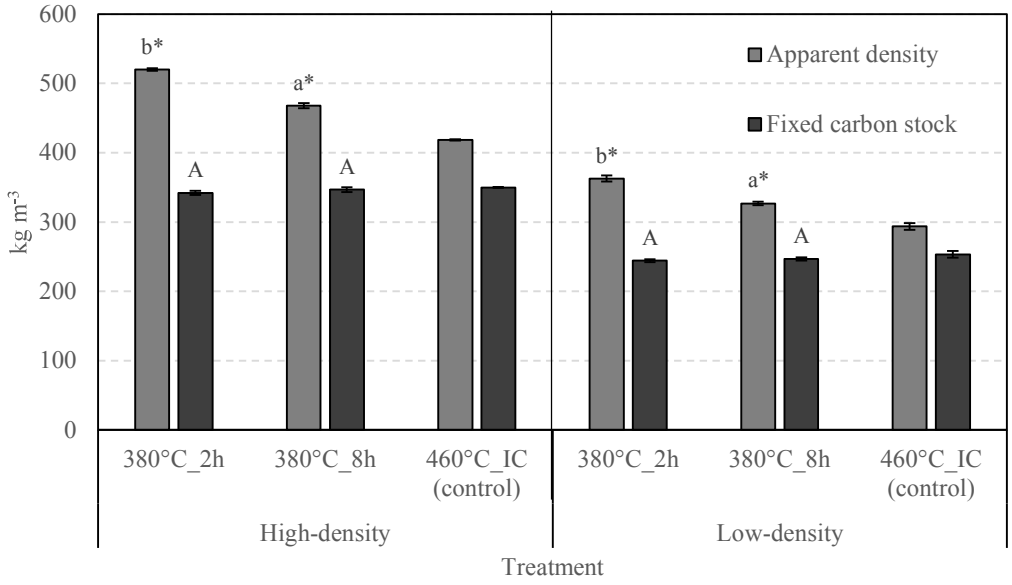

Figure 3.5 - Mean values of apparent density and fixed carbon stock of *Eucalyptus urograndis* wood char produced at different pyrolysis conditions. The bars on top of column graph are the standard deviations. Number of samples (N = 12). Means followed by same letter do not differ at 5% probability by test F. Me Means labeled with the (*) are significantly different from the control at 95% probability by test Dunnett.

In regard to the fixed carbon stock (FCS) per unit volume, different results were observed when compared to apparent density of charcoal, presented in Figure 3.5. Despite the lower values of charcoal apparent density with increasing temperature and holding time, the carbon stock of charcoal showed a narrow variation. This is attributed to the magnitude of FC rise (27.6%) as compared to the reduction of apparent density (19.3%) between charcoal. The charcoal produced at 460 °C showed an average FCS of 301.6 kg

m^{-3}, followed by the 380 °C_8h (296.6 kg m^{-3}) and 380 °C_2h (293.2 kg m^{-3}). This result demonstrates the importance of this variable, since it simultaneously considers two important characteristics for the selection of metallurgical charcoal: fixed carbon and density. In silicon processes, more carbon is better, however, you also have to take in account how reactive it is.

The porosity of charcoal is shown in Figure 3.6. The charcoal porosity ranged from 62.3% to 81.1%. The 380 °C_2h wood char showed the lowest porosity, being an average porosity of 68.2% and followed by the 380 °C_8h at 72.3% and 460 °C_IC at 76.7%. The charcoal porosity increased with peak temperature and holding time of carbonization. In addition, the charcoal porosity was strongly related to the apparent density, and either indices are connected to pore development in charcoal. It is generally known that the devolatilization and the volumetric shrinkage, which occur during the carbonization of biomass, play a role in the generation of porosity in charcoal.

A similar trend of increasing porosity with carbonization temperature were found by (Krzesińska e Zachariasz, 2007; Oliveira *et al.*, 2010; Chrzazvez *et al.*, 2014; Siebeneichler *et al.*, 2017). The higher porosity of the charcoal makes it easier for the gaseous reagent to diffuse throughout the solid particle of charcoal and, subsequently, reach the reaction sites for charcoal gasification (Wang *et al.*, 2017). It is worth noting that not only the volume of pores, but also their distribution in the solid matrix, can contribute to diffusion of gas inside the particle.

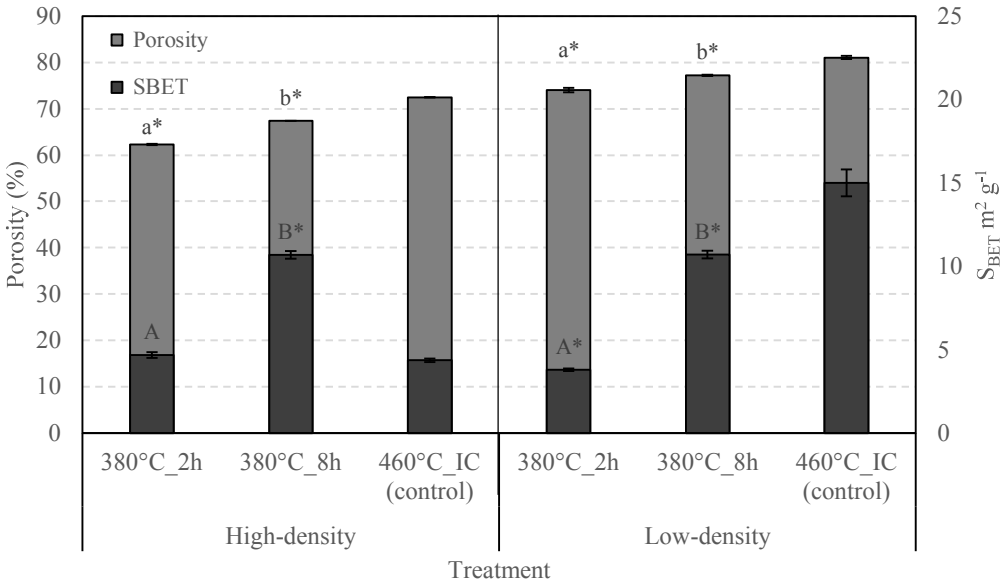

Figure 3.6 - Mean values of porosity and SBET specific surface area of *Eucalyptus* charcoal produced at different pyrolysis conditions. The bars on top of column graph are the standard deviations. Number of samples (N = 12). Means followed by same letter do not differ at 5% probability by test F. Me Means labeled with the (*) are significantly different from the control at 95% probability by test Dunnett.

The S_{BET} ranged from 3.8 to 14.9 m^2 g^{-1} Figure 3.6. The 460 °C_IC wood char, with the lowest density fraction, showed the highest value, average S_{BET} of 14.9 m^2 g^{-1}. At 380 °C carbonization temperature, the S_{BET} was very low. It is known that carbonization conditions, such as residence time, peak of temperature, heating rate and pressure greatly influence the surface area of charcoal (Duman *et al.*, 2014). Amutio *et al.* (2012) studied the pyrolysis of pinewood sawdust wood at final temperatures 400-600 °C range and found S_{BET} values ranging from 1.9 to 2.2 m^2 g^{-1} for the 400 °C to 450 °C. They also noted there was a sharply increase to 16.3 and 73.2 m^2 g^{-1} for the 450 °C to 600 °C, respectively. The latter was attributed to formation of smaller pores (meso and micropores) and, consequently, an increase of S_{BET}. The same behavior is also found by (Keiluweit *et al.*, 2010).

The S_{BET} of charcoal did not exhibit a clear relationship with porosity and apparent density. This appears to be due to two reasons. First, the poor microporosity of the charcoal was a result of the low pyrolysis temperature. It is worth mentioning that the

mean value of the micropore volume of charcoal was 0.0037 $cm^3\ g^{-1}$ in this study. Second, the presence of tyloses or tar in charcoal microstructure blocked the diffusion of nitrogen. Similarly, Khalil (1999) found that the very narrow microporosity or the presence of constrictions in the micropore entrances on lignocellulosic materials carbonized at low temperatures restricted the activated diffusion of nitrogen. He found S_{BET} values ranging from 6.1 to 16.2 $m^2\ g^{-1}$ for lignocellulosic chars produced under 550 °C in nitrogen atmosphere.

The charcoal is classified as a friable material due to its low mechanical strength. The friability parameter is defined as the property of charcoal that produces fines when subjected to abrasion, friction, or falling. As can be seen in Figure 3.7, the charcoal friability ranged from 5.5 to 11.4%. The 380 °C_2h charcoal showed an average friability of 6.5%, followed by the 380 °C_8h at 7.8% and 460 °C at 10.5%. The latter, in percentage terms, was 59% and 34% worse than that observed on 380 °C_2h and 380 °C_8h charcoal, respectively. The charcoal friability increased sharply with increasing peak carbonization temperature and holding time, probably due to shattering of the wood cells during pyrolysis. In addition, the charcoal from the lower-density fraction showed high values when compared to the high-density fraction under all pyrolysis conditions. According to Assis *et al*. (2016), a denser charcoal is usually related to lower friability.

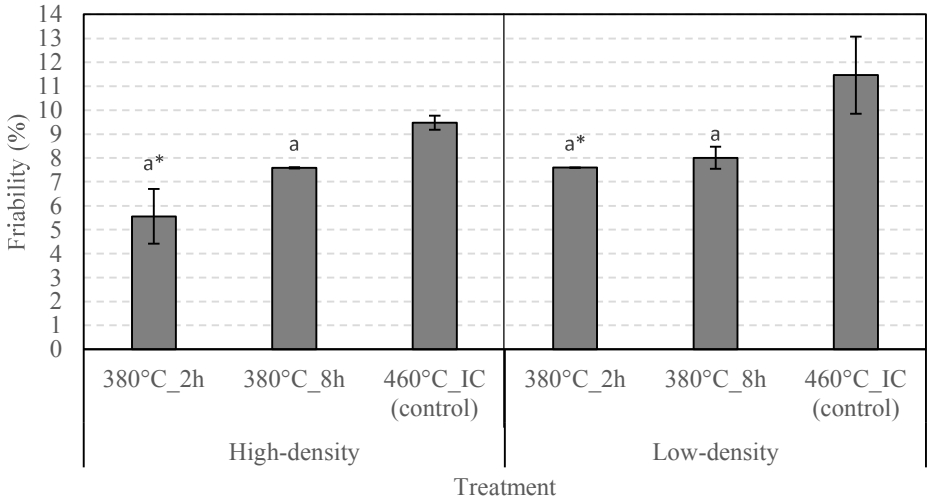

Figure 3.7 – Mean values of friability of charcoal from *Eucalyptus urograndis* clone produced at different pyrolysis conditions. The bars on top of column graph are the standard deviations. Number of samples (N = 18). Means

followed by same letter do not differ at 95% probability by test F. Me Means labeled with the (*) are significantly different from the control at 95% probability by test Dunnett.

According to the classification of the "Technical Center for Tropical Forest" cited by Silva *et al*. (2007), the charcoal produced at 460 °C is the only one that can be classified as easily friable (i.e. mass loss in the form of fines was higher than 10%). In silicon production, the charcoal smaller particles burn on the top of the furnace or may be carried into the gas outlet due to the high gas velocity in the furnace. This may lead to losing control with the amount of carbon in the process, hence, decreasing Si yield (Schei *et al.*, 1998). Additionally, charcoal fines may cause environmental problems due to very fine dust spreading in the atmosphere. In the charge, subgrain charcoal can affect negatively the gas permeability of the charge. Furthermore, the fine fraction is always increasingly contaminated (Gładysz e Karbowniczek, 2008). It is known that charcoal presents difficulties in maintaining uniform granulometry because of its high friability; however, even with such difficulties, this is relatively controlled by the practice of sifting charcoal before being fed to the silicon furnace.

3.3.1.3. *Charcoal microstructure*

In general, anatomical characteristics of wood, such as shape, arrangement, and organization, showed little or no alteration from slow pyrolysis at atmosphere pressure, and the charcoal surface presented well-defined structures, as shown in Figure 3.8.

However, in samples carbonized at 460 °C, the charcoal became brittle, and the cross section shows a considerable amount of charcoal fragments, which can be attributed to cracks in the charcoal. This explains, in part, the high friability of this charcoal compared to the others. The same observation was made by Kim and Hanna (2006) who examined the charcoal morphology of *Quercus variabilis*. The authors stated that for the charcoal prepared at 400 °C, most of the morphological characteristics remained relatively unchanged. However, from 400 °C to 1000 °C the cross-section became rougher and increasingly disrupted. This was attributed to an increase in cell wall thinning and excessive volumetric shrinkage.

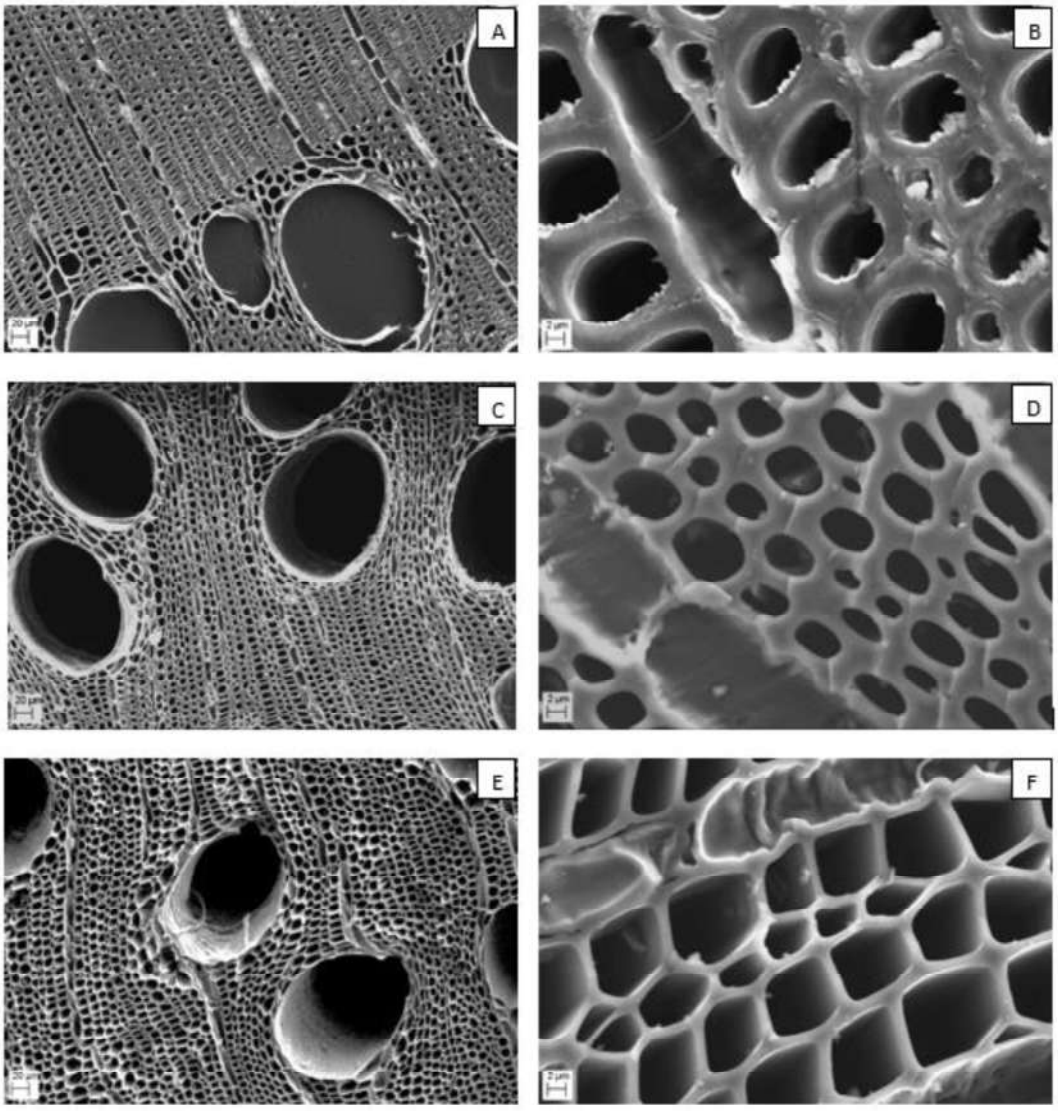

Figure 3.8 - Scanning electron microscopy of the transversal section of wood and charcoal from *Eucalyptus*: (A) Wood; (B) details of wood fibers and parenchyma in transversal section; (C) charcoal produced at 380 °C; (D) details of charred fibers and parenchyma on charcoal produced at 380 °C, (E) charcoal produced at 460 °C; (F) details of charred fibers and parenchyma on charcoal produced at 460 °C.

Measurements of charred vessels are showed in Table 3.6. The average vessels diameter ranged from 89.7 to 137.6 µm. The vessel diameter shrinkage observed in the transformation of wood to charcoal was in general 11%. Ferreira (2013) and Pereira *et al.* (2016) evaluated the charcoal from *Eucalyptus sp*. clones produced with the peak

temperature of 450 °C and found average pore diameter shrinkage of 15 and 18.6%, respectively. These values are higher than those found for *Eucalyptus* charcoal in this study. This result can be explained by the difference of wood characteristics between clones.

Table 3.6 - Mean values of diameter, frequency and area of vessels charred of *Eucalyptus*. (N=24)

Treatment	Separation	Charred vessels properties		
		Vessel diameter (μm)	Frequency (vessels/mm²)	Vessels area (%)
380°C_2h	Low	117.4 ±8 a	17.5 ±3.3 a	19.1 ±1.8 a
380°C_8h	Low	137.6 ±2 a	16.4 ±3.1 a	21.0 ±1.6 a
460°C_IC	Low	129.2 ±9	18.1 ±4.1	23.4 ±3.3
380°C_2h	High	124.5 ±2 a	14.9 ±4.7 a*	24.4 ±3.1 a
380°C_8h	High	110.9 ±6 a	21.5 ±5.7 a	25.6 ±2.2 a
460°C_IC	High	102.5 ± 2	24.9 ±2.2	25.8 ±1.7

Means followed by same letter do not differ at 95% probability by Test F. Means labeled with the (*) are significantly different from the control at 95% probability by Test Dunnett. N = number of samples.

In general, the frequency of vessels showed an increasing trend with increasing temperature and holding time. The 380 °C_2h charcoal showed the lowest frequency of pores, an average of 17.5 vessels mm^{-2}, followed by the 380 °C_8h at 19.0 vessels mm^{-2} and 460 °C_IC at 21.6 vessels mm^{-2}. The vessels frequency of the charcoal rose, on average, 2 times compared to its parental wood. Despite the vessels in charcoal presenting smaller sizes than in wood, the high frequency per mm² will contribute to the high porosity of charcoal.

In general, charcoal with high pore diameter showed lower pores frequency. The vessels area showed a tendency to increase with temperature and holding time. The average of pores area was 23.3%, denoting that the remaining carbonized tissue (76.7%) are mainly composed of fibers.

As observed in Figure 3.9 the fiber wall area (*FWA*) decreases with peak carbonization temperature and holding time. The charcoal produced at 460 °C presented average *FWA* of 45.71%, being 21.3% lower than the carbonization at 380 °C. Whereas, an increase in holding time from 2 to 8h showed only a *FWA* drop of 4.9%. Hence, peak carbonization temperature exhibits a larger influence on reduction of *FWA*. These results agree very well with those of Cutter *et al.* (1980), who examined the morphology of tracheids in a pine wood charred at 250-600 °C and heating rate of 1, 10, 50 °C min^{-1}.

They stated that the increasing charring temperature cause sharply decrease on cell wall thickness of tracheids from the earlywood and the latewood in all cases studied. Similarly, Siebeneichler *et al.* (2017) evaluated the effect of different pyrolysis conditions on samples of *Eucalyptus* ssp. They observed fiber cell-wall thinning with the increase of temperature and heating hate.

The fiber wall area had a strong correlation with apparent density and porosity of charcoal. The values of fiber wall fraction are inversely proportional to the fiber lumen area (void area in charcoal), and thus, a reduction in the fiber wall fraction will influence the charcoal properties that are connected to pore development in charcoal.

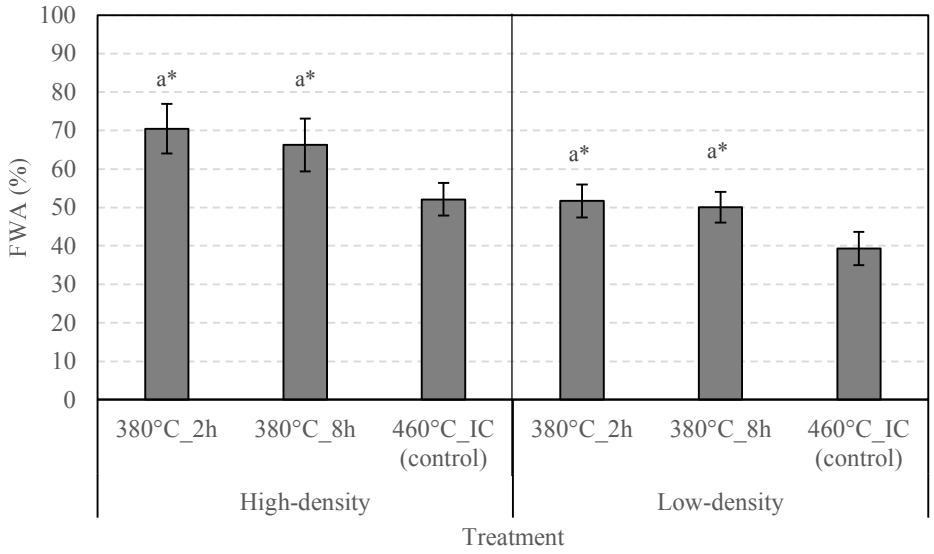

Figure 3.9 - Mean values of fiber wall area of *Eucalyptus* charcoal produced at different pyrolysis conditions. The bars on top of column graph are the standard deviations. Number of samples (N = 24). Means followed by same letter do not differ at 5% probability by test F. Means labeled with the (*) are significantly different from the control at 5% probability by test Dunnett.

3.3.2. Charcoal SiO-reactivity

The degree of conversion is shown in Figure 3.10. The results reveal a sharp increasing trend for the degree of conversion (*X*) with increasing holding time from 2 up to 8h at 380 °C. Otherwise, it decreases for charcoal produced at 460 °C, presenting an average reduction of 12%. Additionally, the drop in degree of conversion (*X*) at 460 °C

peak temperature was less pronounced for charcoals with higher density. The latter can be attributed to the transformation of wood to charcoal, and since the energy input in the process is the same (pyrolysis conditions), a higher specific mass of wood undergoes a low thermal degradation. Raad *et al*. (2006), in his study of kinetic mechanism of wood carbonization, showed that with higher specific mass of wood, the required carbonization time is longer, due to the mass and heat transfer effects.

The degree of conversion of *Eucalyptus* wood chars increased as the holding time at carbonization temperature of 380 °C was increased. This can be related to an increase of porosity and surface area of the charcoal. Though, the contribution of this parameter in increasing the degree of conversion of resulting wood chars was relatively small in comparison to the effect of peak carbonization temperature. The reduction in SiO reactivity with increasing temperature from 380 up to 460 °C can be attributed to its lower O/C ratio, as well as the increase of aromatic C. This can be determined by the increase of aromatic C, as seen in (Table 3.4) and (Figure 3.3), respectively. It is known that the aromatic carbon is less reactive, hence requiring a higher activation energy to start the reaction. In addition, the development of aromatic C by increasing pyrolysis temperature is related to a more ordered structure and loss of active sites of carbon (Kumar *et al.*, 1993; Keiluweit *et al.*, 2010). The latter is associated with reduction of CO_2 gasification reactivity (Wang *et al.*, 2017).

Since gas transport phenomena have similarities between SiO and CO_2, carbonization temperature increases can, at least in part, lead to reduction of SiO-reactivity. Buø *et al.* (2000) evaluated properties of fossil carbonaceous materials versus SiO-reactivity through petrographic analysis. They stated that an increase in the reactive carbon forms, such as binder phase and low amount of filler phase are favorable for SiO reactivity.

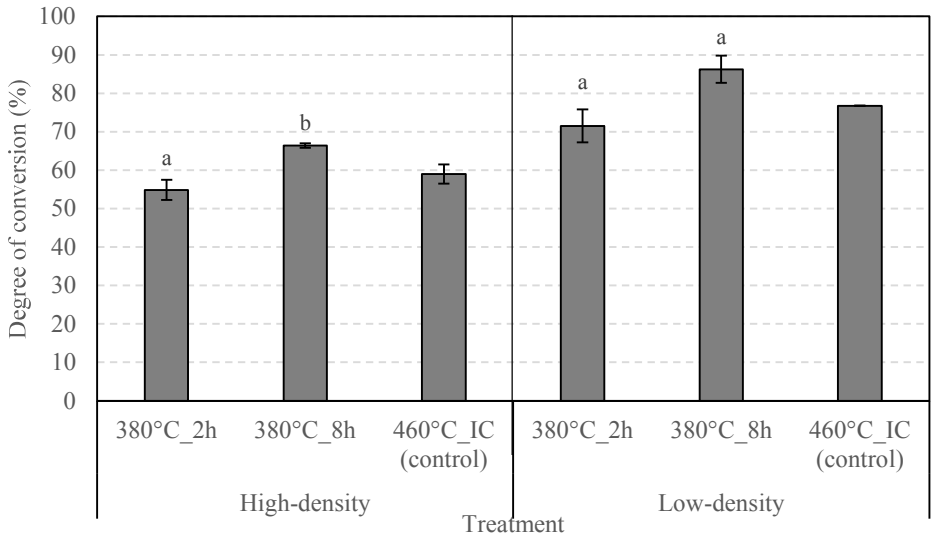

Figure 3.10 - Degree of conversion of *Eucalyptus* charcoal produced at different pyrolysis conditions. The bars on top of column graph are the standard deviations. Number of samples (N = 12). Means followed by same letter do not differ at 95% probability by test F. Means labeled with the (*) are significantly different from the control at 95% probability by test Dunnett.

Multivariate regression analysis was applied and a polynomial function was adjusted to predict the degree of conversion from the FC and AD, two important properties strictly controlled in metallurgical industry. Polynomial model best described the effect of the charcoal apparent density and fixed carbon on degree of conversion (X) and was significant by the F test. All model' coefficients were also significant by the T test. Base on the model, a response surface plot was created Figure 3.11. The results reveal that the fixed carbon at 75% and apparent density at 330 kg m^{-3} are the best values to maximizing degree of conversion.

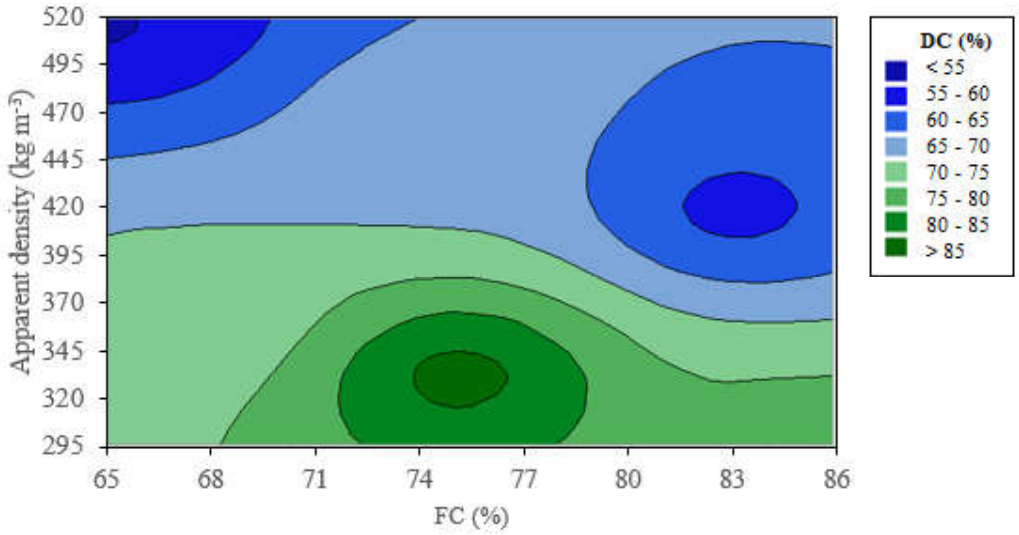

Figure 3.11 - Response surface plot for degree of conversion adjusted (DC) at different levels of fixed carbon (FC) and apparent density (AD). R^2: 97.22%, Model: $DC = -a + b\,AD + c\,FC - d\,FC^2 - e\,AD{*}FC$; *Coefficients:* $a = 9.16$; $b = 0.00351$; $c = 25.52$; $d = 15.39$; $e = 0.00656$

A general trend of data can be clearly seen where lower apparent density gives a higher degree of conversion (*X*). As mentioned earlier, the reason for the increase in charcoal SiO-reactivity by decreasing apparent density is related to the development of pores in the charcoal. In addition, an increasing trend of charcoal SiO-reactivity was found with increasing fixed carbon content from 65 up to 75%. However, after that, it decreased in charcoal with an average fixed carbon of 85%. This reduction was attributed to the increase of aromatic C on charcoal with higher fixed carbon content.

For the microstructure of charcoal, the increases in peak temperature and holding time led to an increase in cell-wall thinning of fiber, hence the increase of porosity and degree of conversion. It is believed that fibers with lower wall fraction and more frequent pores promote better accessibility of the SiO-gas to the internal surface of the particle. In addition, the fibers microstructure in charcoal tissue might have the largest impact on SiO reactivity, since they are the most abundant structural units. Similar results were observed by Myrhaug (2003), where high charcoal SiO-reactivity values was related to the lower fiber wall fraction. In that case, the fiber wall fraction was presented as the fiber wall thickness parameter. It also stated that the cell wall should be as thin as possible to make the diffusion patterns of SiO short.

The silicon carbide formation is of topochemical nature and is controlled by pore diffusion. The lump of carbon material reacts with the SiO in the gas, and the free carbon becomes covered with a layer of SiC; as the layer becomes thicker, the reaction gets slower (Schei *et al.*, 1998). Thus, higher levels of porosity should facilitate the diffusion of silicon monoxide into the carbon matrix. Li (2018), in his study of SiC production with different kind of carbon materials, observed an SiO gas conversion rate of 87.7 for charcoal samples with an average porosity of 85%, verifying the importance of charcoal porosity on SiO reactivity.

A typical structure of the parent wood was practically maintained in the reacted charcoal. The cross section of partially converted charcoal lump is shown in Figure 3.12. The distinct boundaries that represent the growth rings on wood, demarcated by thick-walled, can be seen in the cross section of reacted charcoal produced at 380 °C. The high conversion of C to SiC is observed in the charcoal region with a thicker wall of fibers. This can be explained by the presence of SiC depositions, bright areas in lumen of fibers, as can be seen in (Figure 6). The proposal mechanism to explain these depositions is the reaction between SiO(g) and CO(g) to produce SiC(s) and SiO_2(s), which are a very fine mix particles of SiO_2(s) and SiC(s). Therefore, the $SiO_{2(s)}$ may react with C(s) and produced SiO(g) and CO(g) again, so that only SiC(s) is left. As the gas has problems of leaving a more thick-walled structure (diffusion resistance), this may happen more easily.

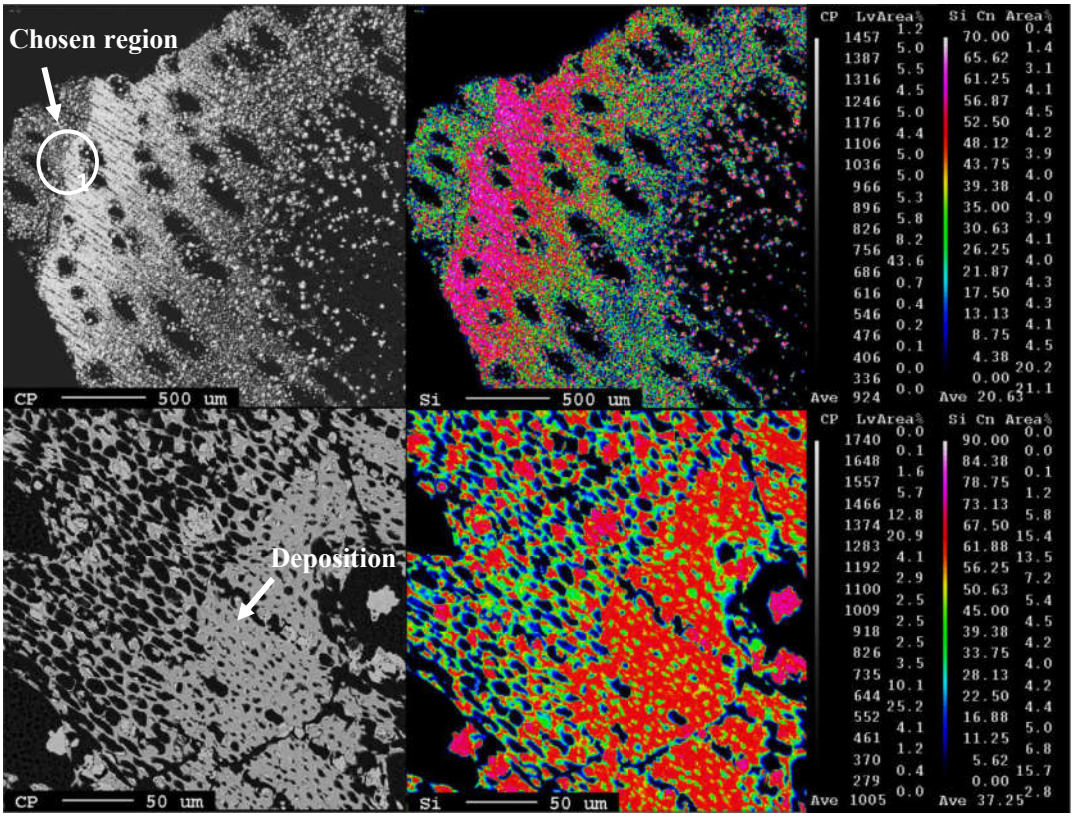

Figure 3.12 – Morphology of *Eucalyptus* charcoal transversal section produced at 380 °C_2h after SiO reactivity. Charcoal lump about 50% converted. Backscattering electron image (left), X-ray maps of Si (right). Details of the chosen region (1) on the the chosen region (1) on the bottom.

In Figure 3.12, it can also be seen that the reaction progresses from the outer surface of the solid (particle edge) towards the center. Similar results were observed by Myrhaug *et al.* (2004), where it was found that the charcoals exhibit a sharp boundary between an unreacted core and a product layer that provided a best description of the kinetic shrinking core model. They also stated an increase in degree of conversion along some parallel cell structures in the charcoal, indicating that these structures transport the SiO-gas better.

Figure 3.13 shows the effective fixed carbon stock (ECS). This variable was created in order to simultaneously evaluate the carbon stock (carbon stock discounting losses by fines generation) and the quality of the carbon (degree of conversion to SiC) in a simple global variable. This parameter has the purpose of classifying the charcoal for use in silicon production.

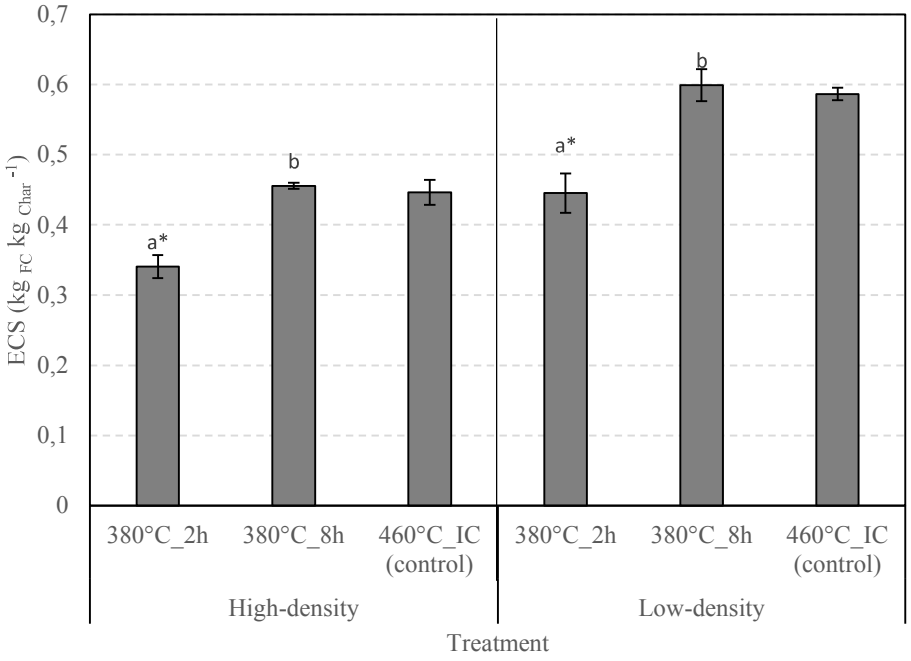

Figure 3.13 - Mean values of effective fixed carbon stock in charcoal (ECS) from *Eucalyptus* clone produced at different pyrolysis conditions. The bars on top of column graph are the standard deviations. Number of samples (N = 12). Means followed by same letter do not differ at 95% probability by test F. Means labeled with the (*) are significantly different from the control at 95% probability by test Dunnett.

The charcoal produced at 380 °C for 8h presented the greatest *ECS*, average of 0.527 kg $_{FC}$ kg $_{Char}^{-1}$, and 33% and 3% higher than the carbonization at 380 °C_2h and 460 °C_IC, respectively. Is worth pointing out that, despite the ECS from the charcoal produced at 380 °C_8h does not differ from the control, however, the carbonization at lower temperatures favors of obtaining a better yield of charcoal, which is an important parameter to be analyzed to defining the best carbonization process. In addition, the charcoal from the low-density fraction in all of cases showed lower *ECS* values when compared to the higher fraction; in other words, the charcoal apparent density has a relevant impact to changing of *ECS*.

3.4. CONCLUSIONS

The anatomical characteristics of wood, such as shape, arrangement, and organization showed little or no modification of the carbonization at 380 °C for 2 and 8h. Otherwise, the charcoal produced at 470 °C became brittle, and the cross section shows a large amount of charcoal fragments, which can be attributed to cracks of charcoal.

The apparent density decreases with peak temperature and holding time, whereas the porosity and friability increase.

There was an increasing trend of degree of conversion (X) with increasing holding time from 2 up to 8h at 380 °C. However, it decreased for charcoal produced at 460 °C. The charcoal SiO-reactivity depends on two main characteristics: carbon structure and apparent density.

Based on the parameters investigated and under the given experimental conditions, the charcoal produced by slow pyrolysis, under atmospheric pressure, at 380 °C peak temperature, 8h holding time and with a fixed carbon around 75% appears to be the most promising candidate for industrial use in Si production.

3.5. REFERENCES

AMUTIO, M. et al. Influence of temperature on biomass pyrolysis in a conical spouted bed reactor. **Resources, Conservation and Recycling,** v. 59, p. 23-31, 2012.

ASADULLAH, M. et al. Effects of biomass char structure on its gasification reactivity. **Bioresource Technology,** v. 101, p. 7935–7943, 2010.

ASSIS, M. R. et al. Factors affecting the mechanics of carbonized wood: literature review. **Wood Sci Technol,** v. 50, p. 519-536, 2016.

BUØ, T. V.; GRAY, R. J.; PATALSKY, R. M. Reactivity and petrography of cokes for ferrosilicon and silicon production. **International Journal of Coal Geology,** v. 43, n. 1-4, 243-256 2000.

CASTRO, A. F. N. M. et al. CORRELATIONS BETWEEN AGE, WOOD QUALITY AND CHARCOAL QUALITY OF *EUCALYPTUS* CLONES. **Revista Árvore,** v. 40, p. 551-560, 2016. ISSN 0100-6762.

CHRZAZVEZ, J. et al. Impact of post-depositional processes on charcoal fragmentation and archaeobotanical implications: experimental approach combining charcoal analysis and biomechanics. **Journal of Archaeological Science,** v. 44, p. 30-42, 2014.

CUTTER, B. E.; CUMBIE, B. G.; E. A. MCGINNES, J. Sem and shrinkage analyses of southern pine wood following pyrolysis. **Wood Science and Technology** v. 14, p. 115-130, 1980.

DAMÁSIO, R. A. P. et al. Thermal profile and control of carbonization on circular kiln through the internal temperature. **Brazilian Journal of Wood Science,** v. 6, n. 1, p. 11-22, 2015.

DUMAN, G.; UDDIN, M. A.; YANIK, J. Gozde Duman a, Md. Azhar Uddinb, Jale Yanikc. **Fuel ProcessingTechnology,** v. 118, p. 75-81, 2014.

FERREIRA, A. T. B. **Evaluation of anatomical structure and apparent density of wood and charcoal from *Eucalyptus sp*. and *Corymbia* sp. trees**. 2013. 131 (Ph.D). Forest Engineering, ESAUQ/USP, Piracicaba, São Paulo.

FOELKEL, C. E. B.; BARRICHELO, L. E. G.; MILANEZ, A. F. **Comparative study of *Eucalyptus saligna*, *E. paniculata*, *E. citriodora*, *E. maculata* and *E. tereticornis* wood for cellulose sulfate production**. IPEF. São Paulo, Brazil, p.17-37. 1975

GŁADYSZ, J.; KARBOWNICZEK, M. Carbon reducers for the processes of ferroalloy production in the electric furnace. European Electric Steelmaking Conference, 2008, Krakow, Poland. p.30-59.

HAJALIGOL, M.; WAYMACK, B.; KELLOGG, D. Low temperature formation of aromatic hydrocarbon from pyrolysis of cellulosic materials. **Fuel,** v. 80, n. 12, p. 1799-1807, 2001.

IAWA, C. **List of microscopic features for hardwood identification**. BULLETIN, I. Leuven, Belgium. 10**:** 219-332 p. 1989.

KAN, T.; STREZOV, V.; EVANS, T. J. Lignocellulosic biomass pyrolysis: A review of product properties and effects of pyrolysis parameters. **Renewable and Sustainable Energy Reviews,** v. 57, p. 1126-1140, 2016. ISSN 1364-0321.

KEILUWEIT, M. et al. Dynamic molecular structure of plant biomass-derived black carbon (biochar). **Environmental Science & Technology,** v. 44, n. 4, p. 1247–1253, 2010.

KHALIL, L. B. Porosity characteristics of chars derived from different lignocellulosic materials. **Adsorption Science & Technology** v. 17, n. 9, p. 729-739, 1999.

KIM, N.-H.; HANNA, R. B. Morphological characteristics of *Quercus variabilis* charcoal prepared at different temperatures. **Wood Science and Technology,** v. 40, n. 5, p. 392-401, 2006.

KIM, V. et al. Carbon reductant for silicon metal production. The thirteenth International Ferroalloys Congress, 2013, Almaty, Kazakhstan. June 9-13. p.519-526.

KRZESIŃSKA, M.; ZACHARIASZ, J. Correlation between the carbonization temperature and the physical parameters of porous carbons derived from *Yucca flaccida*. **Journal of Physics,** v. 79, p. 1-5, 2007.

KUMAR, M.; GUPTA, R. C.; SHARMA, T. X-ray diffraction studies of Acacia and *Eucalyptus* wood chars **Journal ff Materials Science** v. 28, p. 805-810, 1993.

KWON, S. M.; KIM, N. H.; CHA, D. S. An investigation on the transition characteristics of the wood cell walls during carbonization. **Wood Science and Technology,** v. 46, n. 5-6, p. 487-498, 2009.

LI, F. **SiC production using SiO_2 and C agglomerates**. 2018. 217 Thesis (Ph.D). Materials Science and Engineering, Norwegian University of Science and Technology, Trondheim, Norway.

LV, D. et al. Effect of cellulose, lignin, alkali and alkaline earth metallic species on biomass pyrolysis and gasification **Fuel Processing Technology** v. 91, n. 8, p. 903-909, 2010.

MITRAŠINOVIĆ, A. M.; UTIGARD, T. A. Refining silicon for solar cell application by copper alloying. **Silicon,** v. 1, p. 239-248, 2009.

MONSEN, B. et al. The use of biocarbon in norwegian ferroalloy production. INFACON IX, 2000, Quebec City, Canada. June 3-6

MYRHAUG, E. H. **Non-fossil reduction materials in the silicon process - properties and behaviour**. 2003. 242 (Ph.D). Department of Materials Technology, Norwegian University of Science and Technology, Trondheim.

MYRHAUG, E. H.; TUSET, J. K.; TVEIT, H. Reaction mechanisms of charcoal and coke in the silicon process. INFACON X, 2004, Cape Town, South Africa. 1-4 February. p.108-121.

MYRVÅGNES, V. **Analyses and characterization of fossil carbonaceous materials for silicon production**. 2008. 248 (Ph.D.). Department of Materials Science and Engineering, Norwegian University of Science and Technology

MYRVÅGNES, V.; LINDSTAD, T. The importance of coal and coke properties in the production of high silicon alloys. INFACON XI, 2007, New Delhi, India. 18-21 February. p.402-413.

NANDA, S. et al. Characterization of north american lignocellulosic biomass and biochars in terms of their candidacy for alternate renewable fuels. **BioEnergy Research,** v. 6, n. 2, p. 663–677, 2013.

NISHIMIYA, K. et al. Analysis of chemical structure of wood charcoal by X-ray photoelectron spectroscopy. **The Japan Wood Research Society,** v. 44, n. 1, p. 56–61, 1998.

OLIVEIRA, A. C. et al. Otimização da produção do carvão vegetal por meio do controle de temperaturas de carbonização. **Revista Árvore,** v. 37, p. 557-566, 2013. ISSN 0100-6762.

OLIVEIRA, A. C. et al. Quality parameters of *Eucalyptus pellita* F. Muell. mood and charcoal. **Scientia Forestalis,** v. 38, n. 87, p. 431-439, 2010.

PENG, X. et al. Temperature- and duration-dependent rice straw-derived biochar: characteristics and its effects on soil properties of an Ultisol in southern China. **Soil & Tillage Research,** v. 112, n. 2, p. 159-166, 2011.

PEREIRA, B. L. C. et al. Effect of wood carbonization in the anatomical structure and density of charcoal from *Eucalyptus*. **Ciência Florestal,** v. 26, n. 2, p. 545-557, 2016.

PEREIRA, B. L. C. et al. Correlations among the heart/sapwood ratio of *Eucalyptus* wood, yield and charcoal properties. **Scientia Forestalis,** v. 41, n. 98, p. 217-225, 2013b.

PROTÁSIO, T. D. P. et al. **Influence of heating rate of carbonization on the charcoal properties of Acacia mangium**. II CBCTEM. Belo Horizonte 2015.

PROTÁSIO, T. D. P. et al. Mass and energy balance of the carbonization of babassu nutshell as affected by temperature. **Pesquisa Agropecuária Brasileira,** v. 49, n. 3, p. 189-196, 2014.

RAAD, T. J.; PINHEIRO, P. C. D. C.; YOSHIDA, M. I. General equations of carbonization of *Eucalyptus spp* kinetic mechanisms. **CERNE,** v. 12, n. 2, p. 93-106, 2006. ISSN 0104-7760.

SANTOS, R. C. D. et al. Correlation of quality parameters of wood and charcoal of clones of *Eucalyptus*. **Scientia Forestalis,** v. 39, n. 90, p. 221-230, 2011.

SCHEI, A.; TUSET, J. K.; TVEIT, H. **Production of High Silicon Alloys**. Trondheim, Norway: 1998.

SIEBENEICHLER, E. A. et al. Influence of temperature and heating rates on mechanical resistance, density and yield of the wood charcoal of *Eucalyptus cloeziana*. **Brazilian Journal of Wood Science,** v. 8, n. 2, p. 82-94, 2017.

SILVA, M. G. D. et al. Charcoal from timber industry residues of three tree species logged in the municipality of Paragominas, PA. **Acta Amazonica,** v. 37, n. 1, p. 61-70, 2007.

TITILADUNAYO, I. F.; MCDONALD, A. G.; FAPETU, O. P. Effect of temperature on biochar product yield from selected lignocellulosic biomass in a pyrolysis process. **Waste Biomass Valor,** v. 3, p. 311-318, 2012.

TRUGILHO, P. F. et al. Evaluation of *Eucalyptus* clones for charcoal production. **CERNE,** v. 7, n. 2, p. 104-114, 2011.

VIDEM, T. Reaction rate of reduction materials for the (ferro)silicon process. INFACON VII, 1995, Trondheim, Norway. June 11-14. p.221-230.

VITAL, B. R. **Methods for wood density determination**. SIF, Universidade Federal de Viçosa. Viçosa, Brazil, p.21. 1984

WANG, L. et al. Study of CO_2 gasification reactivity of biocarbon produced at different conditions **Energy Procedia,** v. 142, p. 991-996, 2017.

CHAPTER IV

4. SIO REACTIVITY OF CHARCOAL FROM EUCALYPT CLONES

Abstract: A primary factor for determining the efficiency of the silica reduction process is the reactivity of the carbon reductants. The ability of the carbon reduction materials to react with SiO gas is of large importance to the performance of the process. The purpose of this study was to examine the impact of charcoal properties from *Eucalyptus* clones on SiO reactivity. The charcoal was produced in a laboratory kiln and the charcoal sampling was done into density fractions and positions in the kiln to get a better understanding of variables in this study. The SiO reactivity was conducted using agglomerates made of quartz and SiC mixtures and charcoal which have been heated in a resistance heating furnace at 1650 °C in an inert atmosphere for 120 minutes. Charcoal samples before and after SiO reactivity test were studied using the SEM photomicrograph to trace the gas diffusion paths of SiO gas and the formation of silicon carbide (SiC). The results reveal that there is charcoal variability between the clones. The indices that are connected to pore development in charcoal, such as apparent density, porosity and fiber lumen areas played an important role in SiO reactivity, and as a result in the degree of conversion of carbon to SiC. The increases in degree of conversion (X) was strongly related to lower apparent density, higher porosity and higher fibers lumen area.

Keywords: silicon production process, biocarbon, carbonization

4.1. INTRODUCTION

The high silicon alloy traditionally called “silicon metal” is produced industrially by reduction of silica (SiO_2) with carbon material (such as coke, coal and charcoal) in an electric arc furnace (EAF) according to $SiO_{2(s)} + 2C_{(s)} \rightarrow Si_{(l)} + 2CO_{(g)}$. However, the chemistry of the process is more complicated than what is expressed by the overall reaction, since a series of various reactions take place in different zones of the furnace. Schei *et al.* (1998) describe the Si process by dividing the furnace into an inner and outer zone. The inner zone is described by areas where silicon carbide (SiC) produced in the upper parts of the furnace will react with the molten quartz, and silicon will be produced according to $3SiO_2 + 2SiC \rightarrow Si + 4SiO + 2CO$. The outer zone is where one of the most important gas-solid reaction takes place: $SiO_{(g)} + 2C_{(s)} \rightarrow SiC_{(s)} + CO_{(g)}$, where the content of SiO-gas coming from the inner zone must be recovered or it will be lost. The carbon materials act as a barrier to capture SiO gas from the inner zone, producing silicon carbide (SiC) which transfers the silicon back to the inner zone with the descending charge material, improving the silicon recovery. Silicon carbide is an intermediate product in the process which is essential for the silicon producing reactions in the inner zone.

The ability of carbon materials to react with SiO-gas is referred to as the SiO reactivity. This is one of the most important properties of the carbon materials that is used as reductants during silicon production processes. This parameter defines how efficient a given reduction material can be in recovering the SiO-gas in a packed bed like in a silicon furnace (Myrhaug, 2003).

A high SiO reactivity of the reduction materials leads to high silicon recovery, good furnace operation and lower operating costs (Buø *et al.*, 2000; Myrvågnes e Lindstad, 2007). According to Raaness e Gray (1995) the fraction of carbon that does not react in the outer zone will react in the hottest zone of the furnace and will lead to an increased production of $CO_{(g)}$ and thereby an increase in CO/SiO ratio in the cavity zone. Thereafter the SiO pressure needed for the process will be farther from the chemical equilibrium, leading to lower Si production and excess circulation of SiO in the burden. The silicon monoxide which is not recovered will be lost as silica dust upon leaving the charge. Raaness e Gray (1995) also stated that about 80-90% of the electrical energy consumed in the process is used for the formation of $SiO_{(g)}$ from silica in the inner zone

of the furnace. It is therefore of vital importance that as much SiO-gas as possible is preserved within the process to achieve acceptable yields on raw materials and energy.

The quality of the reductant material is important to increase SiO-capture, because during the silicon process the lump of carbon material reacts with the SiO in the gas, and the free carbon becomes covered with a layer of silicon carbide. As this layer becomes thicker, the reaction gets slower (Schei *et al.*, 1998). Silicon carbide is formed first at the surface of the charcoal and at internal pores exposed to the surface, the shrinking core model represents the best description of this reaction kinetics (Myrhaug, 2003).

The formation of SiC is influenced by the variability of the characteristics of the reductant material, which is defined by a set of chemical, physical, mechanical, and anatomical properties, usually interdependent. When using charcoal as a reductant material, the apparent density of charcoal is one of the most important indices to be considered among the physical properties. The high density of charcoal normally is characterized by low porosity; hence it may bring negative consequences on the gas transport properties, which will reflect on the gas-solid reaction in the different metallurgical processes. Szekely *et al.* (1976) stated that in gas-solid reactions under conditions where the chemical reaction is fast, i.e. high temperature processes, the pore diffusion is expected to be the major resistance to the overall progress of reaction. The behavior of SiO gas towards different types of charcoal with different microstructures remains a poorly understood aspect, suggesting a need of further investigation in this field.

Assessment of charcoal properties is often the primary step to ensure proper and efficient utilization for a specific metallurgical process. The aim of the present study was thus to investigate how physical, chemical and morphological properties of charcoal influence the reactivity towards SiO gas.

4.2. EXPERIMENTAL SETUPS AND METHODS

4.2.1. Sampling and characterization of raw materials

Three short rotation forestry species, clones of *Eucalyptus urophila x grandis* hybrid, were used for the study. Samples of 7-year old wood were collected from a

Brazilian forestry company. These materials were selected due to the variation of their basic densities. Logs with diameters from 6 to 14 cm were selected and sawn in approximately 1.0 m height for carbonization. Six logs, representative of diameter variation, were sawn into 50-mm thick (discs), then quarter-sawn to be used in chemical and physical analysis.

Wood basic density was determined by water displacement method, according to NBR 11941 (Brazilian Association of Technical Standards, 2003). The elemental analysis of wood was determined according to the standard SS-EN ISO 16948 (European Standard, 2015). The "S element" was measured according to SS-EN ISO 16994 (European Standard, 2016). To determine macromolecular composition (lignin, extractives and holocellulose content) and ash content, the samples were crushed and sieved between 250 and 400 μm. Wood extractive content was determined according to TAPPI 204 om-88, using the total extractive method but substituting ethanol/benzene for ethanol/toluene. Lignin content was obtained by summing soluble and insoluble lignin. Insoluble lignin was determined using Klason method and soluble lignin by spectrophotometry. Holocellulose content was determined by difference, based on extractive-free wood and disregarding ash.

4.2.2. Charcoal preparation

Three types of charcoal were used in this study. The charcoals were produced in a laboratory kiln built of masonry bricks, with a diameter of 1.2 m and a height of 1.1 m, with 1.04 m^3 usable volume. 0.6 m^3 of logs were loaded into the kiln for pyrolysis. Internal heating was used to initiate pyrolysis and maintain temperatures during the process. The temperature was monitored by five thermocouples, one inserted at the dome of the kiln and the others in the wall. The temperature control of the carbonization process was according to a pre-set theoretical tracks Table 4.1. The peak temperature of carbonization was about 380 °C.

Table 4.1 - Theoretical tracks temperature for carbonization control in laboratory kiln to be measured at dome of kiln.

Steps	Temperature Range	Heating time

1	25-200 °C	16-18 h
2	200-290 °C	12-13 h
3	290-380 °C	7-8 h
4	380 °C	7-8 h

Given the heterogeneity of wood samples and, consequently, the charcoal produced, the charcoal was separated in this study in fractions to obtain greater homogeneity between samples and a better understanding of the parameters selected for evaluation.

The charcoal product was unloaded in the kiln by dividing the charge into two sections: the upper part of the charge, called charcoal from the top section, and the other from the bottom, referred to as the bottom section. The top section was unloaded first followed by the charcoal from the bottom. The charcoal in each section was weighed and a representative sample from each section was collected.

In order to separate the charcoal samples into density fractions, the charcoal was first crushed and sieved to a size fraction between 18-22 mm, then the apparent density of each lump of charcoal was measured by the hydrostatic method, in which the samples were immersed in mercury (Vital, 1984). Next, the lumps of charcoal were screened into two different fractions (denoted as high and low density). The reference density number used for classification was the mean value of density of each of the charcoals. The experiment design can be seen in Table 4.2.

Table 4.2 - Experimental design (charcoal production)

Feedstock	Run	Position in the Kiln	Density separation	Experiment identification
CL-1	2	Botton	High	1BH
CL-1	2	Botton	Low	1BL
CL-1	2	Top	High	1TH
CL-1	2	Top	Low	1TL
CL-2	3	Botton	High	2BH
CL-2	3	Botton	Low	2BL
CL-2	3	Top	High	2TH
CL-2	3	Top	Low	2TL
CL-3	1	Botton	High	3BH
CL-3	1	Botton	Low	3BL
CL-3	1	Top	High	3TH

CL-3	1	Top	Low	3TL

After carbonization, six bags of charcoal from both the top and bottom section of the kiln were randomly collected, homogenized and quartered, based on standard NBR 6923 (Brazilian Association of Technical Standards, 1981). Turn, 20L of charcoal for each experiment were acquired to determine charcoal properties.

4.2.3. Charcoal properties

Proximate analysis of the produced charcoals was performed according to procedures described in ASTM standard D1762 (American Society for Testing and Materials, 1984). The elemental analysis was determined by employing an elemental Eurovector EA 3000 CHNS-O Elemental Analyzer. The concentration of inorganic elements in the produced charcoal was measured by means of an inductively coupled plasma optical emission spectrometry (ICP-OES) according to the standard CEN/TS 15290 (European Committee for Standardization, 2006). The silicon content was determined by X-ray fluorescence technique (XRF).

The apparent density was determined by the hydrostatic method, in which the samples were immersed in mercury, according to (Vital, 1984). The absolute density was determined by the gas displacement technique using an AccuPyc 1330 Helium Pycnometer, according to the standard ISO 12154 (International Organization for Standardization, 2014). The porosity of material was obtained by:

$$Porosity = 1 - \frac{apparent\ density}{absolute\ density}\ 100\% \quad (1)$$

The pores structure of the samples was characterized by nitrogen adsorption/desorption at 196 °C. The Brunauere-Emmete-Teller (BET) method, described in DIN 66131 (Germany Committee for Stardardization, 1993) was used to measure the total surface through an automated gas adsorption analyzer (The TriSTAR 3000, Micromeritics). Prior to BET, 0.4 g of each sample, particle size of 500-200 μm, was vacuum degassed for 12 h at 250 °C in the built-in degas port of the instrument.

The friability (denoted F, expressed in %) also named “impact strength” gives an idea of the extent of breakage that will occur during loading, transportation and screening of charcoal. In this work, the drum test was used to determine the index or degree of friability of the charcoal. The samples were crushed and screened to the fraction +18-22 mm to use in the drum test. The procedure was performed according to (Noumia *et al.*, 2016).

The charcoal morphology was investigated by field-emission scanning electron microscopy (LVFESEM, Zeiss Supra 55VP). The samples were investigated before and after the SiO reactivity test. The samples after the SiO reactivity test were embedded in epoxy resin, ground and polished in order to study carbonaceous structures in relationship to silicon carbide formation. To investigate the microstructure of charcoal, measurements of the vessel diameter (μm), the frequency (vessels mm^{-2}) and vessels (%) in five images from transversal section of charcoal of each material was done. Charcoal samples was previously sanded for better visualization of the charcoal microstructure and the images were obtained using a magnifying glass coupled to an image acquisition system and were measured by software “Axio Vision 4.3”.

The measurements of fibers on charcoal tissue are rarely reported due to their small size and hence are tricky to measure. In this study, a new measurement procedure was applied using SEM microphotography followed by handling of the images obtained using the software “solution DT”. Four charcoal samples, at traversal section, were randomly evaluated for each treatment. The fiber wall area on charcoal (FWA%) was calculated by the difference between the fiber lumen area and the selected fiber area on the SEM image (Figure 1). A high contrast was used to get better differentiation between fiber lumen area and fiber wall area.

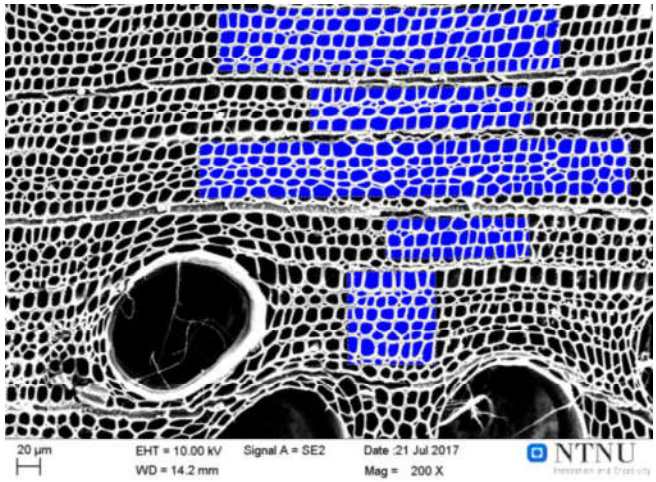

Figure 4.1 – Measurements of fiber wall fraction on charcoal surface, transverse section, by use of SEM photomicrograph with software solution DT. The squares on the image are the fiber selected areas to measure, while the blue and white color in the the selected area represent the fiber lumen and fiber wall, respectively.

4.2.4. SiO reactivity apparatus and procedures

Charcoal samples were calcined in an induction furnace to remove volatile matter, prior to SiO reactivity tests. Thereafter the samples were crushed and screened to the fraction +2-4.5 mm mesh to use in the SiO reactivity test. The SiO reactivity test was performed in an electric tube vertical furnace, using a graphite crucible (Figure 4.2).

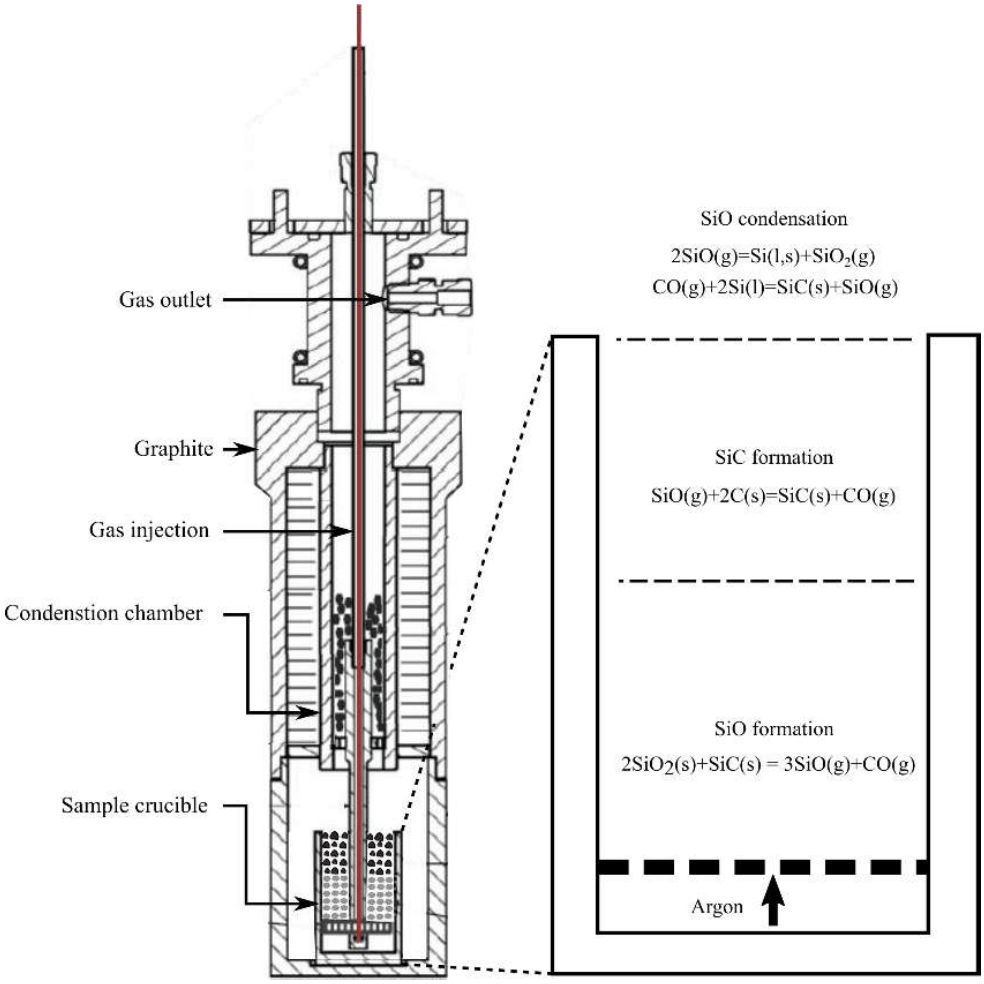

Figure 4.2 – Schematic diagram of graphite crucible used in experimental setup for SiO reactivity test (Drawings by P. Tetlie at SINTEF). The grey part in the sample crucible is SiO_2+SiC and the top part is charcoal (black).

The SiO reactivity test was carried out with use of pellets made by mixing SiC+SiO_2 powders (with molar ratios of 1:2 respectively) to generate SiO-gas, which will react with the reductant material above it. Both materials were loaded in a small graphite crucible, with a dimension of 32 mm in diameter and 60 mm in heigth. The internal surfaces of the small graphite crucible were lined with SiC coating to protect the graphite housing from being attacked by SiO gas. This crucible was placed inside the reaction chamber (Figure 1). In the experiment 15 g of pellets and 15 ml of lump charcoals were loaded, corresponding to a carbonaceous packed bed 20 mm high. This setup was defined

by the stoichiometric analysis of the pellets reaction and mass of carbon used to reach SiO-gas levels which do not restrict conversion rate of the carbon materials.

The loaded crucible was heated up to 1650 °C at a constant heating rate of 30 °C.min^{-1}, under a constant flow of argon (0,4 l.min^{-1}). Argon was used as a carrier gas, transporting SiO generated from the pellets through the packed bed of carbonaceous material. The temperature of 1650 °C and the argon gas flow through the furnace were maintained for 2 hours to complete the process. The experiment was then cooled down to room temperature. The gas analyzer ABB2020 was connected to the off-gas lance to detect the concentration of CO gas. The %CO change and temperature were recorded in the logging program where values were registered automatically every 5 seconds. The weights of charcoal, pellets and the setup crucible were measured before and after the tests. The reactivity tests in this study were carried out at a minimum of two parallel runs for each reductant material.

Figure 4.3 shows the mean curves of %CO versus time from reactivity tests of charcoals and a coke using the SiO reactivity procedure in this study.

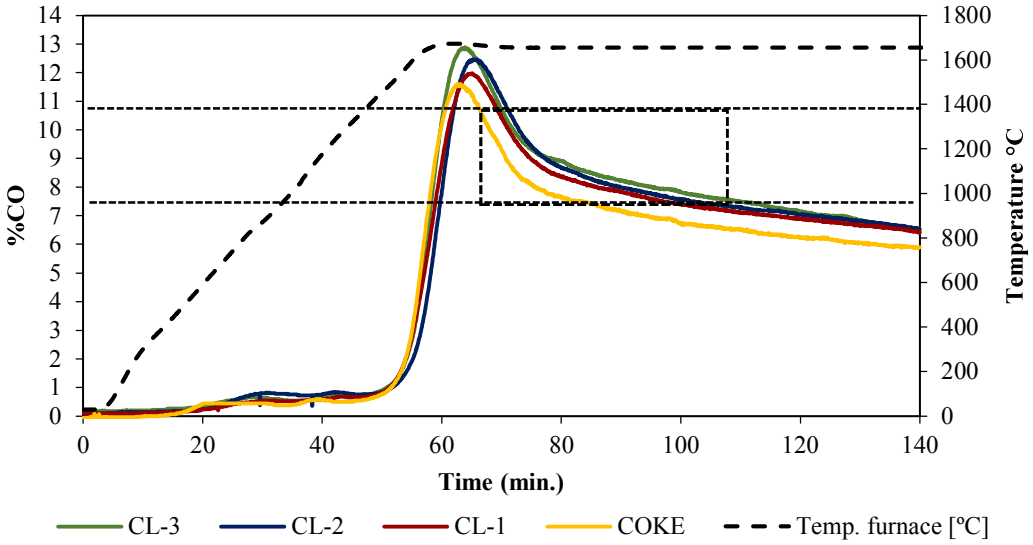

Figure 4.3 – Mean curves of %CO vs. time from reactivity tests for the charcoals and a coke as reference.

It is worth mentioning that the reactivity parameters, based on the SiO reactivity test, were calculated in different protocols, such as using the profile of CO% versus time,

weight increase, chemical analysis of free and total carbon, energy dispersive X-ray fluorescence technique and degree of conversion (X). All of these protocols showed the same behavior and trend. The degree of conversion (X) was selected in this study, due to its simplicity and feasibility to carry out and lower standard deviation. It also takes in account the carbon content of the charcoal before reaction.

The degree of conversion (X) for the particle during conversion can be expressed based on the reaction 4:

$$SiO + 2C = xSiC + xCO + (2-2x)C + (1-x)SiO \quad (4)$$

The total conversion of carbon to SiC is then expressed by the carbon reaction $SiO_{(g)} + 2C_{(s)} = SiC_{(s)} + CO_{(g)}$ when x = 1. The degree of conversion (X) base on the SiO reactivity test was calculated trough equation 5, marked as:

$$X = (m2 - m1)/[m1\,.\,C1free\left(\frac{MSiC - 2MC}{2MC}\right)] \quad (5)$$

Where "*m*" is the mass of sample, 1 and 2 refer to before and after the test, respectively. "$C1_{free}$" is free carbon content before test. The M_{SiC} and M_C are molar mass of SiC and C respectively.

The chemical analysis of free carbon was conducted by free carbon Leco Rc-412 based on EN ISO 21068:2008 with IR detection. The measurement uncertainly specified with 95pct confidence intervals is 0.1% for free C.

The feedstock properties data were subjected to analysis of variance, and, when significant differences were established, treatments (clones) were compared through the Tukey test at 5% probability. To evaluate charcoal properties, analysis of variance and adjusted linear regression models using completely randomized design (CRD) were performed. In addition, the identity model test was performed to verify the possibility of using the sole mathematical model for all clones.

A general linear model was applied and a polynomial function was developed to predict correlations between the dependent variable (degree of conversion) as a function of the independent variables (factors), as given by equation:

$$Y = \beta 0 + \sum_{i=1}^{n} \beta 1 Xi + \varepsilon \quad (6)$$

In this equation, *Y* is the predicted response (degree of conversion), β0 is the constant, Xi is the coded value of the independent variables, βi is the linear term coefficient, ε is the random error, and n is the number of factors studied.

Parameters (factor) with a p-value less than 0.05 were considered significant with 95% confidence. The coefficient of determination (R^2) was assessed as an indication of how well the model fit the data and how much variability in the data could be described by the model.

4.3. RESULTS AND DISCUSSIONS

4.3.1. Wood characterization

The characteristics of the three *Eucalyptus* feedstock are listed in Table 4.3. The clone CL-3 had the highest levels of lignin and the lowest of holocellulose, however these components did not differ significantly between clones tested. The lignin content is an important parameter to be evaluated in production and quality of charcoal, because within the molecular chemical elements of wood it is the one that presents greater resistance to thermal degradation (Raad *et al.*, 2006; Pereira *et al.*, 2013c), and, consequently, positive influence in charcoal yield (Pereira *et al.*, 2012; Protásio *et al.*, 2012). However, additionally, the quality of the lignin (syringyl/guaiacyl ratio) should be considered (Pereira *et al.*, 2013; Soares *et al.*, 2015; Santos *et al.*, 2016). According to Pereira *et al.* (2013) a minimum lignin content of 28% is required for profitable charcoal production for industrial purposes.

Table 4.3 - Mean values of holocellulose, lignin, extractives, and basic density of *Eucalyptus* clones. (N = 6)

CLONE	Lignin (%)	Holocelullose (%)	Extratives (%)	Basic density kg m^{-3}
CL-3	31.5 ±1.9 a	64.5 ±1.9 a	3.9 ±0.02 b	459.8 ±28 a
CL-2	29.4 ±0.9 a	67.2 ±1.1 a	3.3 ±0.07 a	486.5 ±41 a
CL-1	29.6 ±0.4 a	65.8 ±0.5 a	4.5 ±0.03 c	559.1 ±51 b

Means in the column followed by the same letter do not differ at 95% of probability by the Tukey Test. (±) Standard deviation. N: Number of samples.

The content of extractives of CL-1 clone was the highest, with average extractives of 4.5%, followed by 3.9% for CL-3 and 3.3% for CL-1 material. The extractives content differed between clones. The variation of extractives content is attributed to different proportions of heart and sapwood, as well as loss of extractives due to timber storage time (Silvério *et al.*, 2008; Pereira *et al.*, 2013b). According to Costa *et al.* (2017) the extractives content in wood is more concentrated in the heartwood due to the cernification process, which is characterized by death of the radial parenchymal cells, starch consumption, the increase of extractives and tyloses, oxygen consumption and the release of CO_2 (Higuchi, 1997).

As can be seen in Table 4.2 the basic density ranged from 459.8 to 559.1 kg cm^{-3} between the evaluated clones. The clone CL-1 showed highest average basic density 559.1 kg cm^{-3}, 18,2% higher than the others. The clones CL-2 and CL-3 presented average basic density of 486.5 and 459.8 kg cm^{-3}, respectively. The basic density can be considered one of the main criteria for the selection of species and clones of *Eucalyptus* for charcoal production. The wood with high basic density is usually preferred, because the use of denser woods results in higher production of charcoal for a certain volume of wood placed in the kiln (Pereira *et al.*, 2012; Carneiro *et al.*, 2014). In addition, the wood basic density is positively correlated to charcoal apparent density; denser woods produce denser charcoals, thus, higher is the carbon stock and energy densities (Assis *et al.*, 2016). If there is no detriment to other properties, the wood basic density should be as large as possible.

The elemental analysis of *Eucalyptus* clones can be seen in Table 4.4. The clones show similar values of (C, S, H and O). According to Brand (2010), by disregarding minor quantities of nitrogen and other elements such as sulfur, wood is considered to be comprised of approximately 50% carbon, 6% hydrogen, and 44% oxygen.

Table 4.4- Elemental analysis (wt %) of wood from *Eucalyptus* clones. (N=6)

Feedstock	Elemental analysis (wt %)					Mass ratio	
	C	H	S	N	O	O/C	H/C
CL-1	49.7	6.0	< 0.01	0.18	43.9	0.88	0.12
CL-2	49.4	6.0	< 0.01	< 0.10	44.2	0.89	0.12
CL-3	49.8	6.0	< 0.01	< 0.10	43.9	0.88	0.12

N: number of samples.

The content of sulfur and nitrogen in *Eucalyptus* clones were very low. The low levels of sulfur in wood and charcoal contribute environmentally to reducing SO_2 emissions in the silicon production (Monsem, *et al*., 2000). It is worth pointing out that the release of nitrogen and sulfur into the atmosphere are associated with the formation of toxic oxides - NOx and SOx (Demirbas, 2004)

4.3.3. Charcoal characterization

The parameters that characterize the chemical properties of charcoal are shown in Table 4.5.

Table 4.5 - Proximate and elemental analysis of charcoal samples (dry basis, wt%) (N=24)

Experiment	Elemental analysis (wt %)					Ratio		Proximate analysis (wt%)		
identification	C	H	S	N	O	O/C	H/C	MV	FC	Ash
1BH	71.9	3.6	<0.01	0.7	23.8	0.3	0.05	33.1±0.5	66.5±0.8	0.4±0.02
1BL	74.5	3.6	<0.01	0.8	21.0	0.3	0.05	32.4±0.1	67.2±0.1	0.4±0.04
1TH	77.0	3.4	<0.01	0.5	19.1	0.2	0.04	24.9±0.1	74.6±0.1	0.5±0.01
1TL	77.3	3.4	<0.01	0.5	18.8	0.2	0.04	24.4±0.1	75.1±0.6	0.5±0.04
2BH	73.1	3.3	<0.01	0.8	22.8	0.3	0.05	31.6±0.9	67.7±1.1	0.7±0.05
2BL	74.3	3.3	<0.01	0.9	21.4	0.3	0.04	32.4±1.1	66.9±1.3	0.7±0.02
2TH	78.3	3.1	<0.01	0.6	18.0	0.2	0.04	24.0±0.6	75.4±0.7	0.6±0.04
2TL	76.5	3.2	<0.01	0.7	18.7	0.2	0.04	24.2±1.0	75.1±1.0	0.7±0.09
3BH	75.8	3.3	<0.01	0.6	20.3	0.3	0.04	31.1±0.1	68.4±0.1	0.5±0.04
3BL	78.6	3.3	<0.01	0.7	17.3	0.2	0.04	30.1±0.7	69.3±0.6	0.6±0.03
3TH	75.4	3.4	<0.01	0.5	20.7	0.3	0.05	27.2±0.1	72.2±0.1	0.6±0.04
3TL	75.9	3.4	<0.01	0.6	20.0	0.3	0.04	27.0±0.2	72.4±0.4	0.6±0.02

(±) Standard deviation. N: number of samples; MV: Volatile matter; FC: fixed carbon.

The fixed carbon content (*FC*) and hence volatiles in charcoal showed a narrow variation between the three different clones. The average of *FC* in the CL-2, CL-1 and CL-3 wood char were 71.2, 70.5, 70.2, respectively. This is an indication that the peak carbonization temperature has been constant for all carbonizations, since there is evidence in the literature regarding the increasing trend of fixed carbon content with an increasing peak carbonization temperature (Oliveira *et al.*, 2010; Protásio *et al.*, 2014; Couto *et al.*, 2015). Regarding charcoal position in the kiln charge, there is a gradient of *FC* from the top to the bottom. The charcoal from the bottom position (3BL, 3BH, 1BL, 1BH, 2BL, 2BH) exhibited a lower *FC*, average *FC* of 67.6, whereas the charcoal from the top showed an average *FC* of 74.1 (3TL, 3TH, 1TL, 1TH, 2TL, 2TH). This is attributed to the characteristics of pyrolysis process in a batch kiln, where the charcoal from the top position are exposed to a longer hold time at the peak carbonization temperature compared to the bottom. Raad *et al.* (2006) reported that the thermal decomposition of wood (carbonization) depends on the available energy and, therefore, time and temperature.

The ash content of charcoal was less than 1% in all materials. In silicon production, the ash content in the reductant material is a source of contamination, since ash components can be transferred to the silicon metal and as a result will affect the silicon quality. The lower ash content in charcoal has potential to significantly reduce the trace elements in the silicon produced (Monsen *et al.*, 2000).

The elemental analysis, especially for the element carbon, exhibited a similar trend of fixed carbon content as mentioned early. It is noteworthy that the levels of fixed carbon content in charcoal was less than the contents of elemental carbon, because a part of carbon in the fixed carbon standard procedure is eliminated with volatile matters. Mean levels of 75.7% of carbon, 20.2% of oxygen, 3.4% of hydrogen, and 0.7% of nitrogen were observed Figure 3. All clones showed no detectable sulfur contents (less than 0,01%) in charcoal. The results found are consistent with the mean values presented by (Protásio *et al.*, 2014). It is important that the carbonization of wood aims broadly to concentrate carbon and eliminate oxygen in the solid phase - charcoal. Pereira *et al.* (2013) evaluating charcoal from *Eucalyptus* clones charred at 450 °C, observed that an average of 60.0% of the carbon from wood was stored in charcoal, while 86.8% of the oxygen content was volatilized.

The concentrations of inorganic elements in the produced charcoals are listed in Table 4.6.

Table 4.6 - Ash composition of charcoal samples. (N=24)

Samples	Chemical composition of ash (wt%)										
	AlO_3	Fe_2O_3	CaO	MgO	P_2O_5	MnO	K_2O	Na_2O	TiO_2	S	SiO_2
1BH	1.6	2.1	27.8	11.4	7.8	1.4	30.6	11.1	0.1	1.4	4.7
1BL	1.7	2.4	30.6	10.0	5.8	1.1	33.3	8.9	0.1	1.4	4.7
1TH	2.2	2.8	26.0	10.6	9.2	1.2	32.0	10.0	0.2	1.6	4.2
1TL	2.6	2.6	28.0	8.6	10.6	1.2	32.0	8.0	0.2	1.6	4.6
2BH	0.4	0.7	25.7	11.9	8.9	1.4	44.3	4.9	0.0	0.9	1.1
2BL	0.3	0.6	20.0	10.9	7.1	0.9	51.4	5.1	0.0	0.9	2.8
2TH	0.4	0.5	25.0	11.2	8.1	1.4	45.6	4.6	0.0	1.3	1.9
2TL	0.6	1.0	20.0	11.1	7.6	1.1	50.0	4.9	0.0	1.3	2.3
3BH	1.1	0.9	30.0	8.8	10.0	3.5	33.3	9.7	0.1	0.0	2.6
3BL	1.2	1.0	30.0	8.8	6.8	3.5	31.7	10.3	0.1	1.2	5.4
3TH	1.5	1.2	31.7	9.2	10.7	4.7	30.0	7.8	0.1	1.0	2.2
3TL	1.3	1.4	33.3	7.7	8.0	3.7	30.0	10.3	0.1	1.0	3.2

N = number of samples.

The dominant species are those of Ca and K in all of the charcoal samples. It is because K and Ca are essential macronutrients for plant growth which is transported from the soil to the tree in an aqueous solution (Fromm, 2010). In general, the CL-2 wood char presented the highest amount of K and lowest of Ca compared to the others. Even though some inorganics elements could be of high importance with respect to catalytic effects, the contribution of these elements to changing SiO reactivity seems to be negligible for the charcoals studied.

Figure 4.5 presents scanning electron microscope (SEM) images of *Eucalyptus* charcoals produced at atmospheric pressure. In general, it can be seen that the wood structure kept its integrity when observing the respective charcoals produced. However, the SEM analyses reveal that the CL-1 wood char appeared with fibers with thicker walls and reduced diameter. This explain the lower SiO reactivity of CL-1 charcoal comparison to the others.

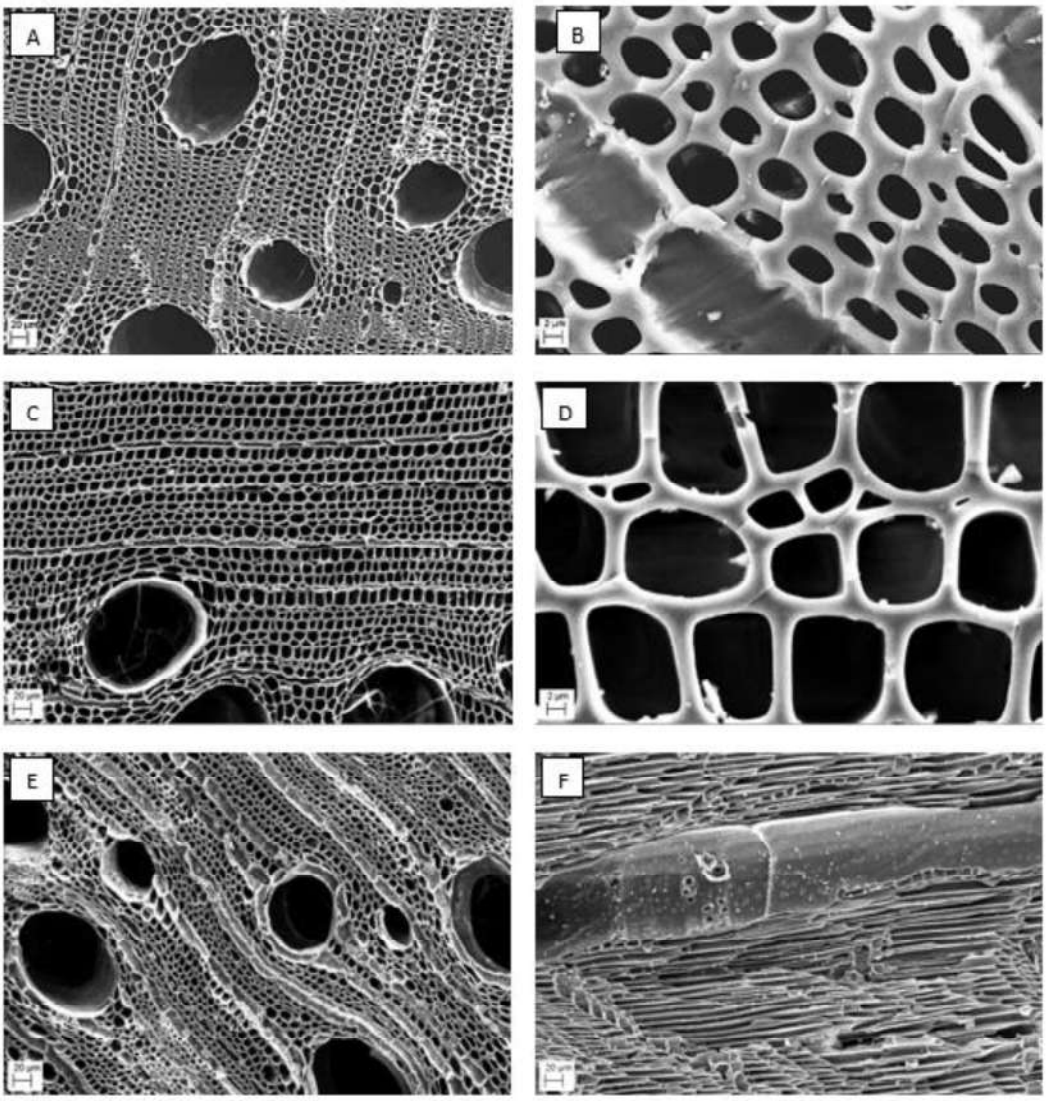

Figure 4.5 – (A) Scanning electron microscopy of the transversal section of CL-1 charcoal; (B) details of fibers and parenchyma on transversal section CL-1 charcoal; (C) scanning electron microscopy of the transversal section of CL-2 charcoal; (D) details of fibers and parenchyma on transversal section of CL-2 charcoal; (E) scanning electron microscopy of the transversal section of CL-3 charcoal;(F) scanning electron microscopy of longitudinal section of CL-3 charcoal.

4.3.4. Effect of apparent density on degree of conversion

The apparent density (AD) of charcoal presented a remarkable impact on SiO-reactivity. Figure 4.6 shows the effect of apparent density on degree of conversion (*X*). It can be clearly seen that a lower apparent density gives a higher degree of conversion (*X*).

Linear regression models best described the effect of the charcoal apparent density (*AD*), porosity and fiber wall area (*FWA*) on degree of conversion (*X*) and were verified by the F test ANOVA (Table V). The results of the ANOVA show that charcoal apparent density, porosity and fiber wall fraction are significant terms for degree of conversion (*X*) with a p-values of less than 0.05. Additionaly, the identity model test was significant to apparent density, porosity and fiber wall fraction of charcoal.

The reason to the increase in wood char SiO-reactivity by decreasing apparent density was related to the development of pores in charcoal. Qualitatively, this result is in agreement with studies by Myrhaug (2003) with charcoals from hardwood and softwood species. The formation of SiC involves the diffusion of silicon monoxide into the carbon lattice which should be facilitated by relatively higher levels of porosity, in other words, low density (Romero *et al.*, 1999).

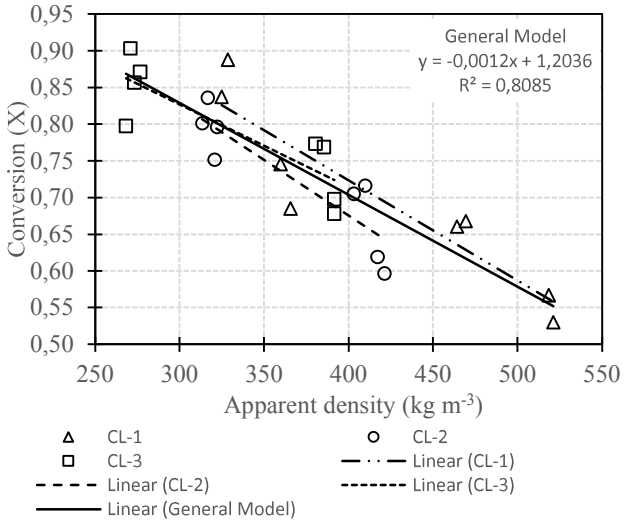

Figure 4.6 – Apparent density versus degree of conversion (X) for charcoal.

Tuset e Raaness (1976) found during their work on SiO-reactivity that this property to a large extent is related to the effective diffusivity of SiO-gas in the matrix of the reduction materials. Buø *et al.* (2000) have investigated the SiO-reactivity and petrography of several cokes. They concluded that the low density, increase of pores and thin wall thickness between the pores were beneficial for the SiO reactivity. They also

comment that the high porosity and surface area of carbon materials may be favorable to SiO diffusion.

The conversion of C to SiC is assumed to progress from the outer surface to the interior of the particle, forming a product layer around the unreacted central part (Schei *et al.*, 1998). The reaction zone may have a diffuse extension in the radial direction as can be seen in Figure 4.7, where the cross section of partially converted charcoal particle is shown. Myrhaug *et al.* (2004), studied various kinetics models to explain the reaction between charcoal and SiO gas. They showed that the shrinking core model gave the best prediction of conversion of particles versus time for the SINTEF SiO-reactivity test. In this model, the overall rate of conversion of the particle is determined by both external mass transfer through the gas film at the surface of the sphere, diffusion through the pore structure in the product layer and chemical reaction rate at the surface of the shrinking unreacted core.

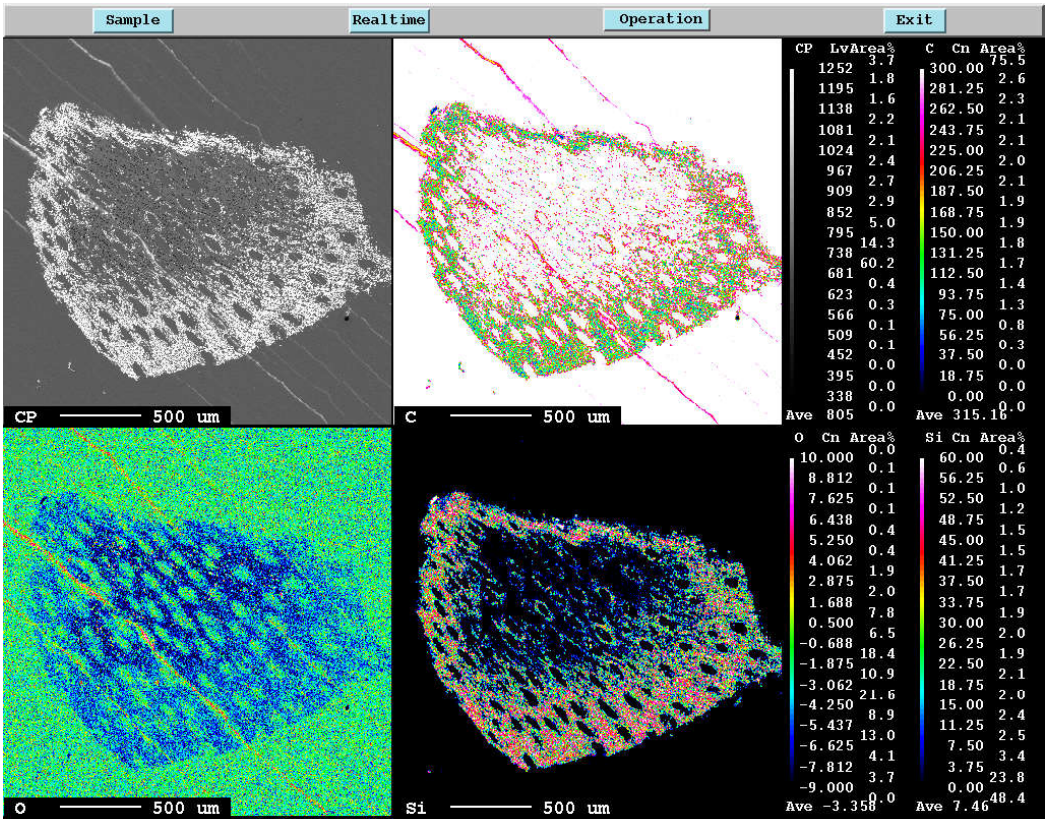

Figure 4.7- Cross section of CL-3 charcoal displaying topochemical conversion from carbon particle to SiC. Backscattering electron image (upper left corner), X-

ray maps of C (upper right corner), O (lower left corner) and Si (lower right corner).

4.3.5. Effect of porosity and surface area on degree of conversion

The porosity of charcoal is an important property in determining the charcoal SiO-reactivity. As can be seen in Figure 4.8 a higher porosity of charcoal exhibited a higher degree of conversion (*X*). The silicon carbide formation is of topochemical nature and is controlled by pore diffusion. The lump of carbon material reacts with the SiO in the gas, and the free carbon becomes covered with a layer of SiC. As the layer becomes thicker, the reaction gets slower (Schei *et al.*, 1998). Thus, higher porosity should facilitate the diffusion of silicon monoxide into the carbon matrix.

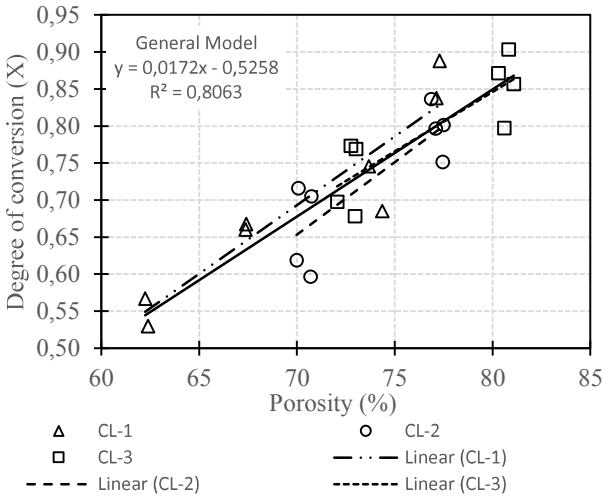

Figure 4.8 –Porosity versus degree of conversion (X).

Figure 4.9 shows the BET specific surface area (S_{BET}) vs conversion (*X*). The S_{BET} among the charcoals cannot well explain the differences in SiO-reactivity. There was a weak correlation of this parameter with the degree of conversion. This result was also verified by Morales (2003), who observed that the BET specific surface area does not seem to be closely related to SiC formation. Additionally, Zhang *et al.* (2010) reported that the pore structure obtained by the method of physical adsorption is not a clear descriptor in predicting the CO_2 gasification reactivity. It is worth pointing out that the values of BET specific surface area in all of charcoals in study was very low.

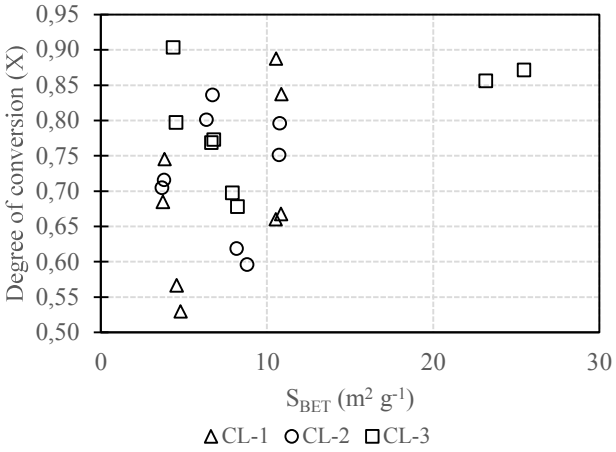

Figure 4.9 – The S_{BET} vs degree of conversion (X).

The fact that the tested charcoals have low surface area may be attributed to the low microporosity of the charcoal under the pyrolysis conditions used. As reported by Mackay e Roberts (1982), the microporosity in lignocellulosic chars is established by 500 °C. Khalil (1999) found that the very narrow microporosity and/or the presence of constrictions in the micropore entrances on lignocellulosic materials carbonized at low temperatures restricted the activated diffusion of nitrogen. He found S_{BET} values ranging from 6.1 to 16.2 $m^2\ g^{-1}$ for lignocellulosic chars produced under 550 °C in nitrogen atmosphere.

4.3.6. Effect of charcoal morphology on degree of conversion

As observed in Figure 4.10, there was a good relationship between degree of conversion and fiber wall area (*FWA*). High *FWA* on charcoal gives a lower degree of conversion (X). It is worth mentioning that *FWA* was greater correlated to apparent density and porosity of charcoal. Similar results were observed by Myrhaug (2003), where high charcoal SiO-reactivity values were related to the lower fiber wall fraction. In that case, the fiber wall fraction was presented as a fiber wall thickness parameter. It also stated that the cell wall should be as thin as possible to make the diffusion patterns of SiO short.

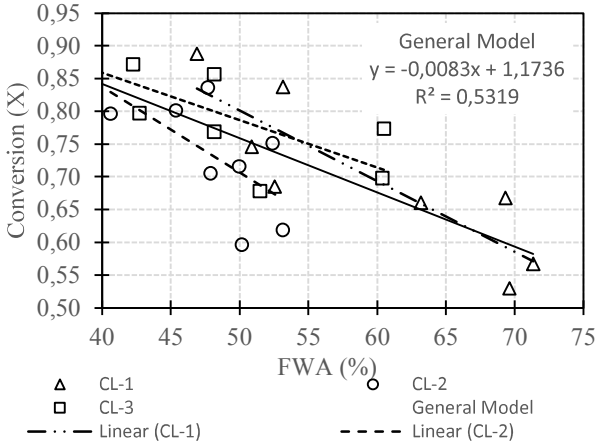

Figure 4.10 – The fiber wall area (FWA) vs degree of conversion (X).

The vessels characteristics of charcoal is shown in Table 4.7. There was no significant relationship between the vessels properties and the others properties of charcoal tested in this study, included the degree of conversion. These results are in agreement with those reported by (Pereira *et al.*, 2016).

Table 4.7 - Mean values of degree of conversion and charred vessels characteristics from *Eucalyptus* clones

Clone	Samples	Degree of conversion (*X*)	Vessels properties		
			Frequency (vessels mm^{-2})	Vessel diameter (μm)	Vessels percentage (%)
CL-1	1BH	0.55±0.02	14.9±4.7	124.5±23	24.4±3.0
CL-1	1BL	0.71±0.04	20.2±3.3	89.7±8	19.1±1.8
CL-1	1TH	0.66±0.01	21.5±5.4	111.0±6	25.6±2.1
CL-1	1TL	0,86±0.03	16.4±3.1	137.7±22	21.0±1.6
CL-2	2BH	0.71±0.01	14.7±2.5	123.9±10	21.7±2.2
CL-2	2BL	0.82±0.02	13,3±2.9	126.1±5	19.8±2.3
CL-2	2TH	0.61±0.01	15,0±2.0	121.2±13	18.8±2.0
CL-2	2TL	0.77±0.03	16.9±1.8	124.1±6	19.5±1.8
CL-3	3BH	0.77±0.01	17.6±1.7	100.8±11	23.5±1.3
CL-3	3BL	0.85±0.07	19.2±1.3	115.7±3	26.8±4.9
CL-3	3TH	0.69±0.01	18.3±1.4	104.9±15	26.5±3.3
CL-3	3TL	0.86±0.01	19.2±0.8	104.2±6	23.1±2.4

The contribution of vessels in changing the reactivities of resulting *Eucalyptus* wood chars seems to be relatively small in comparison to the effect of the fiber. It is worth pointing out that despite the large area per unit of vessel in comparison to the fiber, the average vessels percentage in charcoal was only 22.5±3, denoting that the remaining carbonized tissue (77.5%) are composed mainly by fibers from its parental wood.

The typical structure of the parent wood was practically maintained on the reacted charcoals after SiO reactivity Figure 4.11. The surface of the charcoal particles showed a SiC layer on the cell walls. In addition, the vessels and fiber lumen kept their openings. However, in 1BH charcoal, the presence of fiber lumen with reduced diameter led to small deposition of SiC on its edge. The proposal mechanism to explain these depositions is the reaction between SiO(g) and CO(g) to produce SiC(s) and SiO_2(s), which are a very fine mix particles of SiO_2(s) and SiC(s). Therefore, the $SiO_{2(s)}$ may react with C(s) and produced SiO(g) and CO(g) again, so that only SiC(s) is left. As the gas has difficulty with leaving a more thick-walled structure (diffusion resistance), this may happen more easily.

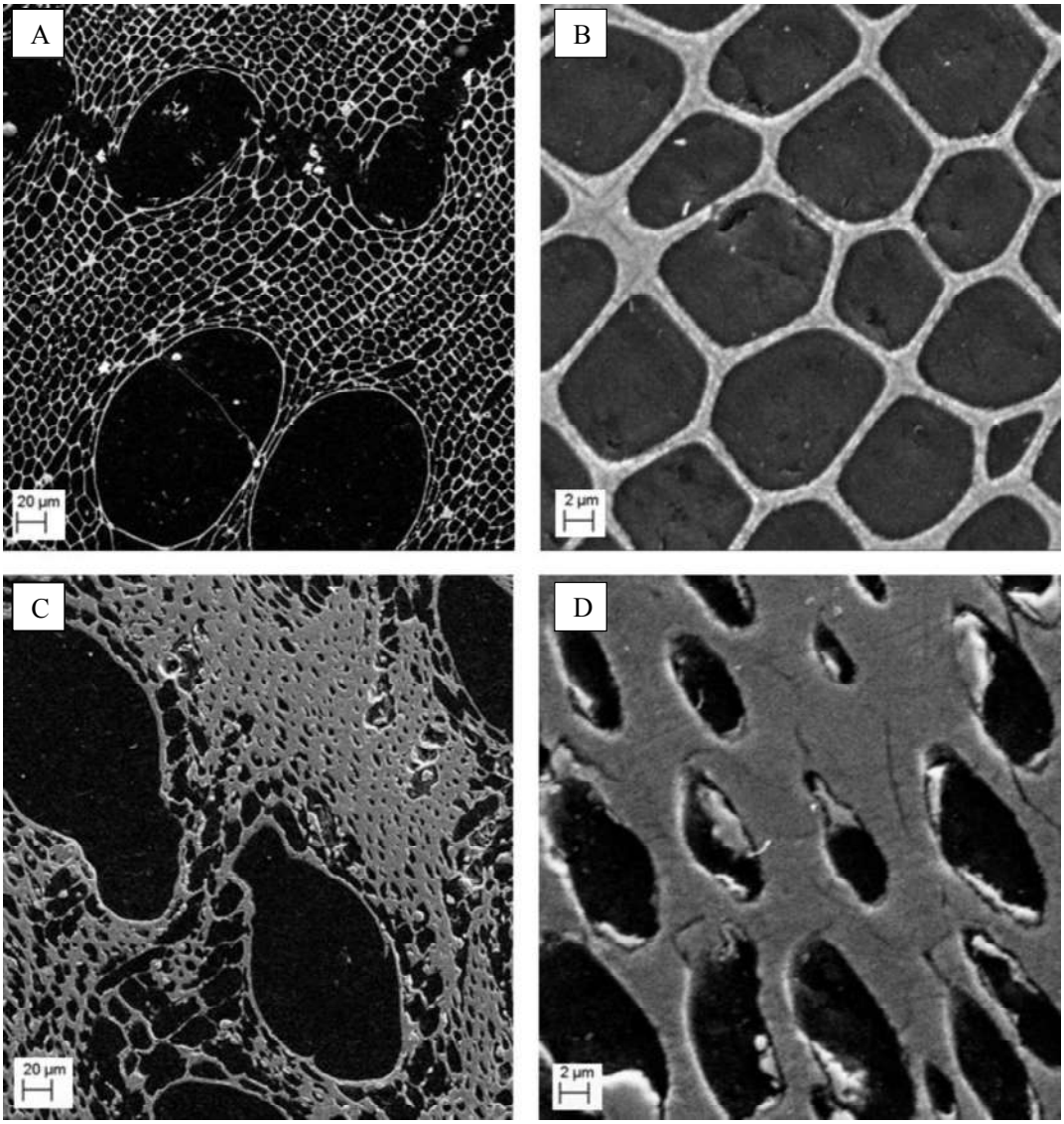

Figure 4.11 – Morphology of charcoal after SiO reactivity, image on transversal section. (A) Cross section of reacted charcoal 3BL; (B) details of fibers on 3BL charcoal; (C) cross section of reacted charcoal 1BH; (D) details of fiber on 1BH charcoal.

Regarding the morphology of charcoal and SiO reactivity, it is believed that fibers with lower wall fraction and more frequent pores promote better accessibility of the SiO(g) to the internal surface of the particle. Fibers properties in the charcoal will have the largest impact on SiO reactivity, since they are the most abundant structural units.

4.4. CONCLUSIONS

The anatomical characteristics of wood, such as shape, arrangement and organization showed little or no modification due to carbonization, including after the SiO reactivity test.

The charcoal position in the kiln had effect on charcoal properties. In general, charcoal from the top position exhibited higher fixed carbon, porosity and SiO reactivity in comparison to the charcoal from the bottom position.

The SiO-reactivity procedure test proved to be a useful tool to classify charcoal for silicon use.

The indices that are connected to pore development in charcoal, such as apparent density, porosity and fiber lumen areas played an important role in SiO reactivity, and as a result, the degree of conversion of carbon to SiC. The degree of conversion increased with the decreasing apparent density and fiber wall area, and the increasing porosity of charcoal.

4.5. REFERENCES

ASSIS, M. R. et al. Factors affecting the mechanics of carbonized wood: literature review. **Wood Sci Technol,** v. 50, p. 519-536, 2016.

BRAND, M. A. **Forest biomass energy**. Joinvile, Brazil**:** 131 p. 2010.

BUØ, T. V.; GRAY, R. J.; PATALSKY, R. M. Reactivity and petrography of cokes for ferrosilicon and silicon production. **International Journal of Coal Geology,** v. 43, n. 1-4, 243-256 2000.

CARNEIRO, A. D. C. O. et al. Potential energy of *Eucalyptus sp*. wood according to age and different genetic materials. **Revista Árvore,** v. 38, n. 2, p. 375-381, 2014.

COSTA, A. C. S. et al. Properties of heartwood and sapwood of *Eucalyptus camaldulensis*. **Brazilian Journal of Wood Science,** v. 8, n. 1, p. 10-20, 2017.

COUTO, A. M. et al. Quality of charcoal from Corymbia and *Eucalyptus* produced at different final carbonization temperatures. **Scientia Forestalis,** v. 43, n. 108, p. 817-831, 2015.

DEMIRBAS, A. Combustion characteristics of different biomass fuels. **Progress in Energy and Combustion Science,** v. 30, n. 2, p. 219-230, 2004.

FROMM, J. Wood formation of trees in relation to potassium and calcium nutrition. **Tree Physiology** v. 30, p. 1140-1147, 2010.

HIGUCHI, T. **Biochemistry and molecular biology of wood**. Berlim: 1997.

KHALIL, L. B. Porosity characteristics of chars derived from different lignocellulosic materials. **Adsorption Science & Technology** v. 17, n. 9, p. 729-739, 1999.

MACKAY, D. M.; ROBERTS, P. V. The influence of pyrolysis conditions on yield and microporosity of lignocellulosic chars **Carbon,** v. 20, n. 2, p. 95-104, 1982.

MONSEN, B. et al. The use of biocarbon in norwegian ferroalloy production. INFACON IX, 2000, Quebec City, Canada. June 3-6

MORALES, R. C. **Study of silicon and silicon carbide processing cycle by use of sugar cane bagasse charcoal in plasma reactor**. 2003. 127 (Ph.D). Mechanic Engineering, UNICAMP, Campinas.

MYRHAUG, E. H. **Non-fossil reduction materials in the silicon process - properties and behaviour**. 2003. 242 (Ph.D). Department of Materials Technology, Norwegian University of Science and Technology, Trondheim.

MYRHAUG, E. H.; TUSET, J. K.; TVEIT, H. Reaction mechanisms of charcoal and coke in the silicon process. INFACON X, 2004, Cape Town, South Africa. 1-4 February. p.108-121.

MYRVÅGNES, V.; LINDSTAD, T. The importance of coal and coke properties in the production of high silicon alloys. INFACON XI, 2007, New Delhi, India. 18-21 February. p.402-413.

NOUMIA, S. et al. Upgrading of carbon-based reductants from biomass pyrolysis underpressure. **Journal of Analytical and Applied Pyrolysis,** v. 118, p. 278-285, 2016.

OLIVEIRA, A. C. et al. Quality parameters of *Eucalyptus pellita* F. Muell. mood and charcoal. **Scientia Forestalis,** v. 38, n. 87, p. 431-439, 2010.

PEREIRA, B. L. C. et al. Influence of chemical composition of *Eucalyptus* wood on gravimetric yield and charcoal properties. **bioresources,** v. 8, n. 3, p. 4574-4592, 2013.

PEREIRA, B. L. C. et al. Study of thermal degradation of *Eucalyptus* wood by thermogravimetry and calorimetry. **Revista Árvore,** v. 37, n. 3, p. 567-576, 2013c. ISSN 0100-6762.

PEREIRA, B. L. C. et al. Effect of wood carbonization in the anatomical structure and density of charcoal from *Eucalyptus*. **Ciência Florestal,** v. 26, n. 2, p. 545-557, 2016.

PEREIRA, B. L. C. et al. Quality of wood and charcoal from *Eucalyptus* clones for ironmaster use. **International Journal of Forestry Research,** v. 2012, p. 1-8, 2012.

PEREIRA, B. L. C. et al. Correlations among the heart/sapwood ratio of *Eucalyptus* wood, yield and charcoal properties. **Scientia Forestalis,** v. 41, n. 98, p. 217-225, 2013b.

PROTÁSIO, T. D. P. et al. Mass and energy balance of the carbonization of babassu nutshell as affected by temperature. **Pesquisa Agropecuária Brasileira,** v. 49, n. 3, p. 189-196, 2014.

PROTÁSIO, T. D. P. et al. Canonical correlation analysis between characteristics of *Eucalyptus* wood and charcoal. **Scientia Forestalis,** v. 40, n. 95, p. 317-326, 2012.

RAAD, T. J.; PINHEIRO, P. C. D. C.; YOSHIDA, M. I. General equations of carbonization of *Eucalyptus spp* kinetic mechanisms. **CERNE,** v. 12, n. 2, p. 93-106, 2006. ISSN 0104-7760.

RAANESS, O.; GRAY, R. Coal in the production of silicon rich alloys. INFACON XII, 1995, Trondheim, Norway. 11-14 June. p.201-220.

ROMERO, F. J. N.; REINOSOA, F. R.; DÍEZB, M. A. Influence of the carbon material on the synthesis of silicon carbide. **Carbon,** v. 37, p. 1771-1778, 1999.

SANTOS, R. C. D. et al. INFLUÊNCIA DAS PROPRIEDADES QUÍMICAS E DA RELAÇÃO SIRINGIL/GUAIACIL DA MADEIRA DE EUCALIPTO NA PRODUÇÃO DE CARVÃO VEGETAL. **Ciência Florestal,** v. 26, p. 657-669, 2016. ISSN 1980-5098.

SCHEI, A.; TUSET, J. K.; TVEIT, H. **Production of High Silicon Alloys**. Trondheim, Norway: 1998.

SILVÉRIO, F. O. et al. Effect of storage time on the composition and content of wood extractives in *Eucalyptus* cultivated in Brazil. **Bioresource Technology,** v. 99, n. 11, p. 4878-4886, 2008.

SOARES, V. C. et al. Properties of *Eucalyptus* wood hybrids and charcoal at three ages. **CERNE,** v. 21, n. 2, p. 191-197, 2015.

SZEKELY, J.; EVANS, J. W.; SOHN, H. Y. **Gas-Solid Reactions**. New York: 1976.

TUSET, J. K.; RAANESS, O. Reactivity of reduction materials in the production of silicon, silicon-rich ferroalloys and silicon carbide. 34th Electric Furnace Conference, 1976, St.Louis. December 7-10

VITAL, B. R. **Methods for wood density determination**. SIF, Universidade Federal de Viçosa. Viçosa, Brazil, p.21. 1984

ZHANG, Y. et al. Modeling of catalytic gasification kinetics of coal char and carbon. **Fuel,** v. 89, n. 1, p. 152-157, 2010.

5. OVERALL CONCLUSIONS

This thesis discusses critical properties of charcoal and their significance in dictating reductant performance in the silicon process. Main considerations include the methods suitable for examinations of charcoal reactivity towards SiO gas. The performance of a coke was also investigated for comparison purpose. The results showed that the developed procedure to measure the reaction between carbon and silicon monoxide to silicon carbide was a useful tool to classify charcoal for use in the silicon production process. It was found that all the parallel protocols used to express SiO reactivity can be used to evaluate the ability of charcoal to react with SiO(g). Nevertheless, the degree of conversion (*X2*), which expresses the conversion rate of the free carbon in charcoal, was the most suitable parameter tested to evaluate charcoal SiO reactivity due to its smaller deviation and simplicity.

Results from the reactivity test showed that coke was less reactive than charcoal. The main reason for the observed behavior of coke is due to its low porosity. By analyzing charcoal charred at the same peak temperature of carbonization, an increasing trend of charcoal SiO-reactivity was found with a reduction of apparent density and the fiber wall area of charcoal. These indices are connected to pore development in charcoal. The ash composition and specific surface area of charcoal samples did not in fact conclude with SiO reactivity changing.

The effects of the charcoal position in the kiln on the reactivity to SiO gas was also investigated. The results revealed that the charcoal from the top position exhibited higher fixed carbon, porosity and SiO reactivity in comparison to the charcoal from the bottom position.

It was found that the peak temperature of carbonization and holding time affected the degree of conversion, hence SiO reactivity. There was an increasing trend of degree of conversion with increasing holding time from 2 hours up to 8 hours at 380 °C. However, it decreased for charcoal produced at 460 °C. This behavior was attributed to an increase of aromatic C on charcoal that is accompanied by loss of active carbon sites. Based on the parameters investigated and under the given experimental conditions, the charcoal produced at 380 °C peak temperature and 8h holding with fixed carbon around 75% appears to be the most promising candidate for industrial use in Si production.